Titre: Title:	Étude thermo-hydraulique de l'écoulement du modérateur dans le réacteur CANDU-6
Auteur: Author:	Foad Mehdi Zadeh
Date:	2016
Type:	Mémoire ou thèse / Dissertation or Thesis
Référence: Citation:	Mehdi Zadeh, F. (2016). Étude thermo-hydraulique de l'écoulement du modérateur dans le réacteur CANDU-6 [Ph.D. thesis, École Polytechnique de Montréal]. PolyPublie. https://publications.polymtl.ca/2167/

URL de PolyPublie: PolyPublie URL:	https://publications.polymtl.ca/2167/
Directeurs de recherche: Advisors:	Alberto Teyssedou, & Stéphane Étienne
Programme: Program:	Génie nucléaire

UNIVERSITÉ DE MONTRÉAL

ÉTUDE THERMO-HYDRAULIQUE DE L'ÉCOULEMENT DU MODÉRATEUR DANS LE RÉACTEUR CANDU-6

FOAD MEHDI ZADEH
DÉPARTEMENT DE GÉNIE PHYSIQUE
ÉCOLE POLYTECHNIQUE DE MONTRÉAL

THÈSE PRÉSENTÉE EN VUE DE L'OBTENTION
DU DIPLÔME DE PHILOSOPHIÆ DOCTOR
(GÉNIE NUCLÉAIRE)
JUIN 2016

UNIVERSITÉ DE MONTRÉAL

ÉCOLE POLYTECHNIQUE DE MONTRÉAL

Cette thèse intitulée :

ÉTUDE THERMO-HYDRAULIQUE DE L'ÉCOULEMENT DU MODÉRATEUR DANS LE RÉACTEUR CANDU-6

présentée par : MEHDI ZADEH Foad
en vue de l'obtention du diplôme de : Philosophiæ Doctor
a été dûment acceptée par le jury d'examen constitué de :

M. KOCLAS Jean, Ph. D., président
M. TEYSSEDOU Alberto, Ph. D., membre et directeur de recherche
M. ÉTIENNE Stéphane, Doctorat, membre et codirecteur de recherche
M. LAKIS Aouni A., Ph. D., membre
M. DAHMANI Mohamed, Ph. D., membre externe

REMERCIEMENTS

Je tiens tout d'abord à vivement remercier mes directeurs de recherche Pr. Alberto Teyssedou et Pr. Stéphane Etienne qui m'ont donné la chance de pouvoir réaliser ce projet de thèse. Je les remercie pour l'encadrement qu'ils m'ont offert, pour leur soutien précieux, pour leurs conseils et pour les idées qu'ils ont partagées avec moi tout au long de ce travail de recherche.

Je remercie les membres de jury, Pr. Jean Koclas, Pr. Aouni Lakis et Dr. Mohamed Dahmani pour avoir accepté l'évaluation de cette thèse.

Je voudrais aussi remercier M. Sébastien Paquette, M. Benoît Malouin et M. Eddy Petro, pour leurs conseils avisés pendant mon doctorat qui ont été efficaces.

Je tiens aussi à remercier M. Daniel Stubbs pour ces assistances lors de l'installation du Code_Saturne sur les serveurs du Calcul_Québec.

Je tiens à remercier M. Yvan Fournier de l'Électricité de France (EDF) pour ces conseils avisés liés à l'installation et l'utilisation du Code_Saturne.

Je remercie le Calcul_Canada pour l'attribution de ressources informatiques utilisées pour ce projet.

Je remercie également le Fonds de recherche du Québec (FRQNT) pour la bourse d'études doctorales qu'on m'a accordé.

Finalement, je remercie mes parents qui m'ont toujous soutenu et encouragé de près et de loin. Je vous aime de tout mon cœur.

RÉSUMÉ

Étant donné la taille (6,0 m×7,6 m) ainsi que le domaine multiplement connexe qui caractérisent la cuve des réacteurs CANDU-6 (380 canaux dans la cuve), la physique qui gouverne le comportement du fluide modérateur est encore mal connue de nos jours. L'échantillonnage de données dans un réacteur en fonction nécessite d'apporter des changements à la configuration de la cuve du réacteur afin d'y insérer des sondes. De plus, la présence d'une zone intense de radiations empêche l'utilisation des capteurs courants d'échantillonnage. En conséquence, l'écoulement du modérateur doit nécessairement être étudié à l'aide d'un modèle expérimental ou d'un modèle numérique. Pour ce qui est du modèle expérimental, la fabrication et la mise en fonction de telles installations coûtent très cher. De plus, les paramètres de la mise à l'échelle du système pour fabriquer un modèle expérimental à l'échelle réduite sont en contradiction. En conséquence, la modélisation numérique reste une alternative importante.

Actuellement, l'industrie nucléaire utilise une approche numérique, dite de milieu poreux, qui approxime le domaine par un milieu continu où le réseau des tubes est remplacé par des résistances hydrauliques distribuées. Ce modèle est capable de décrire les phénomènes macroscopiques de l'écoulement, mais ne tient pas compte des effets locaux ayant un impact sur l'écoulement global, tel que les distributions de températures et de vitesses à proximité des tubes ainsi que des instabilités hydrodynamiques. Dans le contexte de la sûreté nucléaire, on s'intéresse aux effets locaux autour des tubes de calandre. En effet, des simulations faites par cette approche prédisent que l'écoulement peut prendre plusieurs configurations hydrodynamiques dont, pour certaines, l'écoulement montre un comportement asymétrique au sein de la cuve. Ceci peut provoquer une ébullition du modérateur sur la paroi des canaux. Dans de telles conditions, le coefficient de réactivité peut varier de manière importante, se traduisant par l'accroissement de la puissance du réacteur. Ceci peut avoir des conséquences majeures pour la sûreté nucléaire. Une modélisation CFD (Computational Fluid Dynamics) détaillée tenant compte des effets locaux s'avère donc nécessaire. Le but de ce travail de recherche est de modéliser le comportement complexe de l'écoulement du modérateur au sein de la cuve d'un réacteur nucléaire CANDU-6, notamment à proximité des tubes de calandre. Ces simulations servent à identifier les configurations possibles de l'écoulement dans la calandre. Cette étude consiste ainsi à formuler des bases théoriques à l'origine des instabilités macroscopiques du modérateur, c.-à-d. des mouvements asymétriques qui peuvent provoquer l'ébullition du modérateur. Le défi du projet est de déterminer l'impact de ces configurations de l'écoulement sur la réactivité du réacteur CANDU-6.

La grande taille de la cuve et la variation de densité due à la chaleur rendent ces modélisations difficiles. Les analyses CFD déjà effectuées ne coïncident pas avec les données expérimentales disponibles, très probablement à cause de la sous-résolution des simulations et l'utilisation de modèles physiques non valides pour cette étude. Les simulations effectuées dans le cadre de cette recherche indiquent des instabilités propres aux conditions de l'écoulement. Cette étude numérique identifie des instabilités hydrodynamiques qui aboutissent à des oscillations dans le système. C'est la première fois que ce type d'oscillations est prédit dans l'écoulement du modérateur. Par conséquent, elles pourraient être considérées dans les analyses de la sûreté nucléaire.

Les simulations de ce projet ont été réalisées à l'aide de méthodes numériques de calcul par volumes finis en utilisant le logiciel Code_Saturne [1] développé chez Électricité de France. Dans ce contexte, ce code a été validé avec des données expérimentales disponibles. La première contribution de cette thèse est le développement d'une carte de configurations pour le fonctionnement du modérateur dans la cuve du réacteur CANDU-6. Le modèle transitoire nous a permis d'identifier les fréquences des oscillations reliées à chacune des configurations possibles de l'écoulement. La nature et les raisons de présence des oscillations ont été analysées du point de vue de la dynamique des fluides. Les prédictions thermohydrauliques de ce code ont ensuite été importées dans le code de calcul de la physique des réacteurs DONJON [2], développé à l'École Polytechnique de Montréal. Ce travail nous a permis de prédire également un effet de couplage entre les distributions du modérateur et la réactivité du réacteur CANDU-6.

Veuillez noter que cette thèse est basée sur trois articles scientifiques. L'organisation de ce document est donnée dans le chapitre 3.

ABSTRACT

Considering the size (6 m×7.6 m) and the quite complex hydrodynamic domain of CANDU reactors (i.e. 380 fuel channels embded in the vessel), the motion of the the moderator flow in the calandria is still not perfectly understood until today. Data sampling process from a reactor in operation necessitates several modifications on the calandria vessel to get access to the core. Furthermore, the intense radiation area in the reactor core requires the use of quite particular measurement instruments. Consequently, the moderator flow must necessarily be studied through experimental and/or numerical models. Concerning experimental tests, fabrication and operation of such a huge facility is very expensive. Moreover, the scaling groups of CANDU reactors are in contradiction. Consequently, numerical simulations constitute an appealing.

Because of the aforementioned constraints (i.e. complexity of the domain), the porous medium method has been used to study the moderator flow by the nuclear industry. This approach approximates the hydraulic domain as a continuous medium where, the tube bundle is replaced by hydraulic resistances. This model has the ability to predict macroscopic characteristics of the flow motion. However, it can not simulate the local effects such as temperature and velocity distributions near the calandria tubes. In the framework of nuclear safety, local effects around the calandria tubes are a point of high interest.

Predictions of porous medium method previously showed that the moderator flow can develop several hydrodynamic configurations. For some, an asymmetric behaviour in calandria vessel was observed. This can result in boiling of the moderator flow at proximity of fuel channels. In such conditions, the reactivity coefficient can change significantly, resulting in variation of the reactor power. For this reason, a CFD model that takes into account the local effects is therefore necessary to study the motion of the moderator in the calandria.

The purpose of this research is to model the complex behaviour of the flow moderator in CANDU-6 calandria, especially at proximity of calandria tubes. These simulations are used to identify possible flow configurations. This study is thus to formulate theoretical bases on behalf of macroscopic instabilities in the moderator, i.e. asymmetric motions which may cause boiling. The project's challenge was to determine the impact of these flow configurations on the reactivity of CANDU reactor.

The reactor vessel's huge dimensions in conjunction with density variations make the simulations pretty tricky and costly. The previous CFD analyses do not coincide with the experimental data available in the literature, most likely due to not-converged results and/or

use of inappropriate physical models which are not valid for this modelling. The presented numerical study identifies hydrodynamic instabilities that lead to oscillations in the system. This is the first time that this type of motion is predicted in the moderator flow. Indeed, such an asymmetry must be considered in the nuclear safety analysis.

Simulations of this project were carried out using Code_Saturne finite volume solver, developed by Électricité de France. At first, this code has been validated with experimental data. An important contribution of this thesis is the development of a moderator flow operating map. The predictions obtained from a transient model have allowed us to identify the oscillations frequencies related to each of the possible configurations of the moderator flow. In the next step, the predictions of the thermal hydraulic simulations were coupled with DONJON reactor physics solver. The coupling study revealed important features for reactor's reactivity by taking into account the moderator flow distributions.

TABLE DES MATIÈRES

LISTE DES TABLEAUX

LISTE DES FIGURES

LISTE DES SIGLES ET ABRÉVIATIONS

AECL	Atomic Energy of Canada Limited
AHWR	Advanced Heavy-Water Reactor
CANDU	CANada Deuterium Uranium
CFD	Computational Fluid Dynamics
DES	Dettached Eddy Simulation
EACL	Energie Atomique du Canada Limited
EDF	Electricité de France
KAERI	Korea Atomic Enery Research Institute
LES	Large Eddy Simulation
LOCA	Loss-of-Coolant Accident
MODTURC	Moderator Turbulent Circulation
MTC	Moderator Test Circulation
MTF	Moderator Test Facility
NPD	Nuclear Power Demonstration
PHWR	Pressurized Heavy-Water Reactor
RANS	Reynolds Averaged Navier-Stokes
SPEL	Sheridan Park Experimental Laboratory
TEACH	Teaching Elliptic Axisymmetry Characteristics Heuristically

LISTE DES ANNEXES

CHAPITRE 1 INTRODUCTION

1.1 Contexte

Les centrales nucléaires ont fourni 13% de la production mondiale d'électricité en 2012. Aujourd'hui, 31 pays dans le monde possèdent 437 réacteurs fonctionnels, dont 29 sont de type CANDU (Canada Deutérium Uranium). CANDU est un réacteur nucléaire à l'uranium naturel refroidi à l'eau lourde pressurisée à 10 MPa [3]. La technologie des tubes de force utilisée dans ces réacteurs sépare le combustible nucléaire du fluide modérateur. Alors que l'eau lourde est utilisée à la fois comme liquide de refroidissement (appelé caloporteur) et modérateur dans ces réacteurs, les circuits fournissant ces deux écoulements fonctionnent séparément. Le fluide modérateur est légèrement pressurisé, alors que le caloporteur est hautement pressurisé. Le schéma représentatif d'une centrale nucléaire de type CANDU est présenté à la figure 1.1.

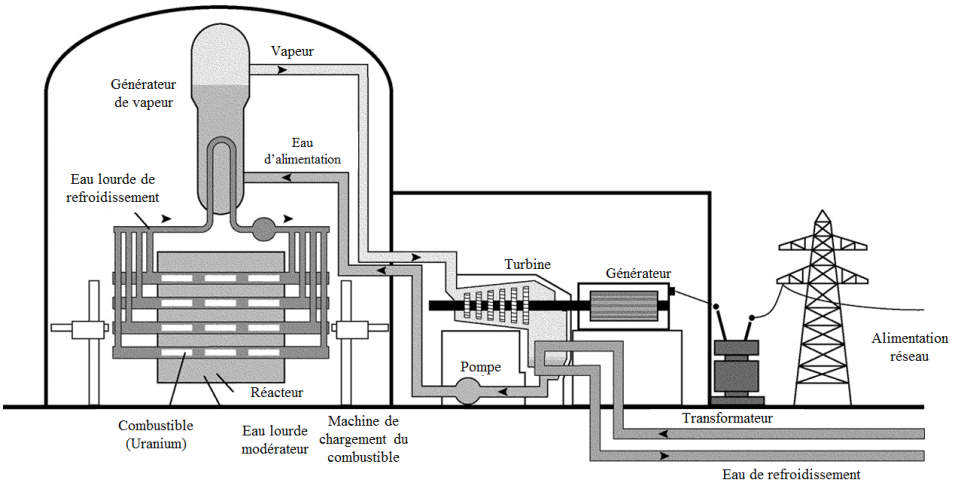

Figure 1.1 Schéma d'une centrale nucléaire de type CANDU (Source : Site web nuceng.ca).

1.1.1 Présentation générale du réacteur CANDU

Dans un réacteur de type CANDU-6, l'uranium naturel sous forme de pastilles de combustible est inséré dans des crayons de zirconium. Ces grappes se logent à l'intérieur des tubes de force où le liquide de refroidissement s'écoule dans le but d'absorber et transporter la chaleur. Le caloporteur passe ensuite à travers les échangeurs de chaleur, c.-à-d. les générateurs de vapeur, pour produire de la vapeur acheminée vers un circuit secondaire d'eau légère.

Les tubes de pression sont placés à l'intérieur de tubes externes appelés tubes de calandre.

Ces deux tubes sont séparés par un gaz isolant. Les tubes de calandre sont immergés dans la cuve du réacteur appelée calandre (en anglais : Calandria). L'ensemble du réacteur se situe dans une enceinte de confinement de béton armé. Chaque tube de force (ou tube de pression) d'un réacteur CANDU-6 contient 12 grappes de combustible. Le positionnement horizontal des canaux permet de remplacer les grappes de combustible lorsque le réacteur est en marche. La configuration schématique de la section transversale du réacteur CANDU-6 est présentée à la figure 1.2.

Le modérateur est injecté dans la cuve du réacteur au moyen de huit injecteurs logés approximativement sur le plan médian horizontal de la cuve. Les dimensions des injecteurs du CANDU-6 sont présentées à la figure 1.3.

1.1.2 Fission nucléaire et rôle du modérateur dans le réacteur

La fission nucléaire a lieu suite à l'absorption des neutrons par des noyaux lourds. Une réaction de fission nucléaire en chaîne libère généralement des neutrons de haute énergie. Afin de maintenir le processus de réaction en chaîne, il faut permettre aux neutrons d'interagir avec les atomes d'uranium 235 (ou en général les matériaux fissibles) dans le combustible. Ceci exige que l'énergie des neutrons soit réduite avant d'être absorbée par les noyaux fissiles. Le rôle principal du modérateur dans un réacteur nucléaire est de ralentir les neutrons à la gamme de 0,025 eV [4]. Le combustible fissible principal présent dans l'uranium naturel utilisé pour les CANDU-6 est l'isotpoe-235.

Près de 5% de la chaleur produite dans un réacteur CANDU-6 est transmise au modérateur. Cette quantité de chaleur exige d'être évacuée de façon permanente afin d'assurer la stabilité du réacteur. Un circuit thermique, composé d'une pompe et des échangeurs, fait circuler le modérateur dans la cuve du réacteur. Près de 70 à 80% de la chaleur transmise provient du ralentissement des neutrons et de l'absorption du rayonnement γ par le modérateur. La désintégration des résidus contribue jusqu'à 25% de cette quantité. Le reste (environ 3 à 5%) de la chaleur est liée au transfert thermique entre le tube de force et le tube de calandre. Étant donné que le ralentissement des neutrons est la principale source de chaleur transmise au modérateur, une brève introduction à ce processus sera présentée ici.

Le ralentissement est une réaction physique entre les neutrons et les noyaux du modérateur visant à l'échange de l'énergie cinétique. À la suite des collisions avec les noyaux du modérateur, les neutrons perdent leur énergie et en conséquence, dans les conditions d'équilibre l'énergie des neutrons ne dépendra que de la température du modérateur. Pour cette raison on les appelle neutrons thermiques. Un modérateur optimal ne doit pas absorber les neutrons pendant ce processus désigné de thermalisation. Pour cette raison, l'absorption minimale des

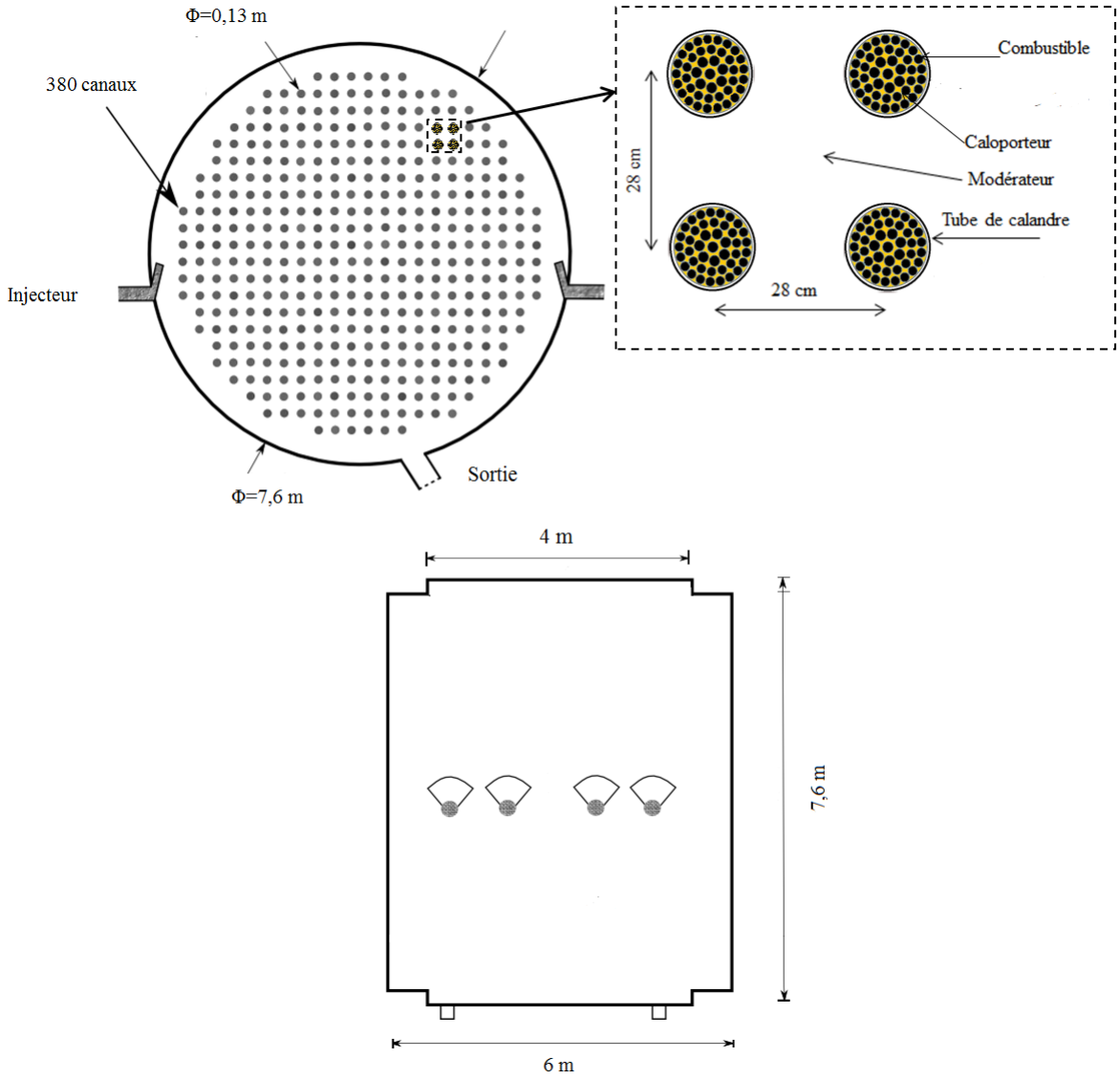

Figure 1.2 Schéma simplifié d'un réacteur CANDU-6.

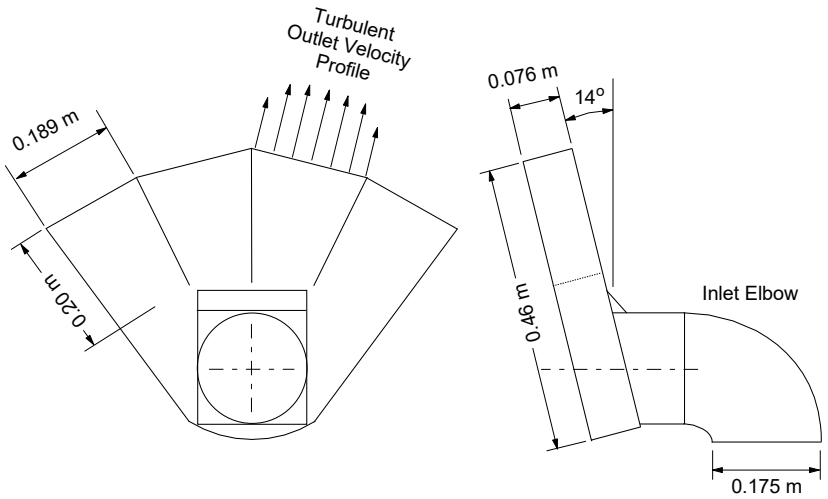

Figure 1.3 Les injecteurs du réacteur CANDU-6.

neutrons est un atout principal de l'eau lourde par rapport à l'eau légère. En revanche, la production industrielle de l'eau lourde est coûteuse et compliquée.

Dans un réacteur nucléaire, lorsque le nombre de neutrons reste constant d'une génération à l'autre, et que le système est capable de compenser les pertes de neutrons, l'état du réacteur est considéré comme critique. On définit la réactivité du réacteur comme une valeur déterminant l'écart du système par rapport à l'état critique. Par cette définition, un réacteur est appelé sous-critique lorsque la réactivité est négative et super-critique lorsque la réactivité est positive. Les variations de la réactivité du réacteur CANDU-6 en fonction de la température du modérateur sont présentées à la figure 1.4 [5]. On peut observer que la réactivité du réacteur à l'état d'équilibre du combustible s'accroît lorsque la température du modérateur augmente. Il est évident que la température de l'écoulement du modérateur au sein d'une cuve d'environ 7 mètres de diamètre et 6 mètres de longueur adopte des distributions non-uniformes avec des écarts qui, dans certaines conditions, peuvent être importants. Aux parois des tubes, des effets hydrodynamiques locaux comme les sillages et stagnations peuvent encore faire remonter la température locale du modérateur. Ces derniers peuvent mener le modérateur à l'ébullition à la paroi et l'assèchement partiel. Dans ce contexte, la connaissance de la distribution de température du modérateur est indispensable pour garantir la sûreté nucléaire.

Le rôle du liquide modérateur du système CANDU-6 ne se limite pas à l'état de fonctionnement normal du réacteur. Ceci devient un puits thermique lors d'un contact éventuel des tubes de force et de calandre. Cet événement a lieu lors d'accidents nucléaires sévères comme celui de la perte du caloporteur (In-core LOCA). Le contact thermique entre le tube de force

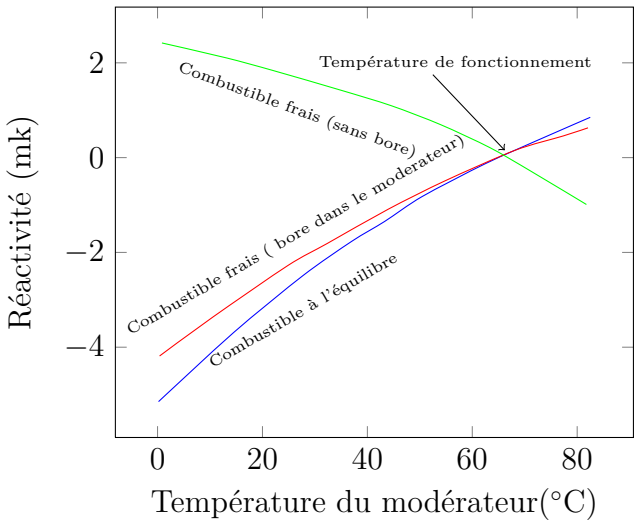

Figure 1.4 Variations de la réactivité avec la température du modérateur [5].

et le tube de calandre crée un point chaud. Dans cette situation, l'écoulement du modérateur doit refroidir les canaux, il fonctionne alors comme un puits de chaleur. La capacité d'absorption de la chaleur dépend des températures initiales et locales du modérateur. Il est donc important de connaître la répartition de la température du modérateur au sein de la cuve du réacteur et en particulier au voisinage des canaux.

1.2 Cadre théorique de l'étude

Il convient dans cette section de préciser le cadre théorique du problème ainsi que les équations et les critères de la mise à l'échelle de la cuve du réacteur CANDU-6. Selon une étude réalisée par Khartabil et al. [6], l'écoulement du modérateur dans la calandre d'un réacteur CANDU-6 peut s'écrire pour la conservation de la masse, de la quantité de mouvement et de l'énergie par les équations suivantes :

$$\begin{aligned} \nabla.\vec{V} &= 0 \\ \frac{\partial \vec{V}}{\partial t} + \left(\vec{V}.\nabla\right)\vec{V} &= -\frac{1}{\rho_{\text{ref}}}\nabla P + \frac{\mu}{\rho_{\text{ref}}}(\nabla)^2\vec{V} + \vec{g}\left(\frac{\rho-\rho_{\text{ref}}}{\rho_{\text{ref}}}\right) \\ \frac{\partial T}{\partial t} + \left(\vec{V}.\nabla\right)T &= \frac{k}{\rho_{\text{ref}}C_p}(\nabla)^2 T + \frac{q'''}{\rho_{\text{ref}}C_p} \end{aligned} \tag{1.1}$$

Avec $\vec{V}$ le vecteur de vitesse de l'écoulement (m/s), ρ la masse volumique (kg/m^3), ρ_{ref}

la masse volumique de référence (kg/m^3), P la pression (Pa), T la température (°C), t le temps (s), $\vec{g}$ le vecteur de l'accélération due à la gravité (m/s^2), μ la viscosité dynamique de l'écoulement (kg/ms), k la conductivité thermique (W/m°C), C_p la capacité thermique (J/kg°C) et q''' source volumique de chaleur (W/m^3).

Afin de dériver les paramètres de la similitude dynamique de la cuve du réacteur CANDU-6, les équations (1.1) sont adimensionnées en utilisant les paramètres suivants :

– U_i : La norme de la vitesse à l'entrée,

– ρ_{ref} : La densité de référence de l'écoulement,

– D : Le diamètre de la cuve,

– T_o : La température à la sortie,

– ΔT : La différence de la température entre l'entrée et la sortie.

On obtient finalement les équations adimensionnelles suivantes :

$$\begin{aligned} \nabla^* V^* &= 0 \\ \frac{\partial V^*}{\partial t^*} + \left(V^*.\nabla^*\right) V^* &= -\nabla^* P^* + \frac{1}{\text{Re}} \left(\nabla^*\right)^2 V^* - \text{Ar} \frac{g}{|g|} T^* \\ \frac{\partial T^*}{\partial t^*} + \left(V^*.\nabla^*\right) T^* &= \frac{1}{\text{RePr}} \left(\nabla^*\right)^2 T^* + q^* \end{aligned} \tag{1.2}$$

Les variables et les nombres adimensionnels dans ces équations sont donnés ci-dessous.

$$\begin{gathered} V^* = \frac{V}{U_i}\,,\; T^* = \frac{T - T_0}{\Delta T}\,,\; P^* = \frac{P}{\rho_{\text{ref}} U_i^2}\,,\; t^* = \frac{t U_i}{D}\,,\; \nabla^* = D\nabla \\ \text{Pr} = \frac{\mu C_p}{k}\,,\; \text{Re} = \frac{\rho_{\text{ref}} U_i D}{\mu}\,,\; \text{Ar} = \frac{g \beta_{\text{ref}} \Delta T D}{U_i^2}\,,\; q^* = \frac{qD}{\rho_{\text{ref}} C_p U_i \Delta T} \end{gathered} \tag{1.3}$$

L'écoulement du modérateur ainsi que les distributions de température sont déterminés par les paramètres adimensionnels dans l'équation (1.2) dont les définitions sont présentées au tableau 1.1. Conserver ces groupes adimensionnels conjointement avec la similarité géométrique assure la similitude dynamique entre un modèle et le prototype CANDU-6.

Afin de maintenir les groupes adimensionnels de l'équation (1.3) pour un modèle à l'échelle réduite d'une calandre de CANDU-6, trois variables indépendantes doivent être considérées : 1- le diamètre de la cuve, 2- la différence de température de l'écoulement entre l'entrée et la sortie et 3- la vitesse de l'écoulement à l'entrée de la cuve du réacteur.

Quant au nombre de Prandtle (Pr), il peut être considéré quasi-uniforme en utilisant le même type de fluide autant dans le modèle que dans le prototype. En utilisant les définitions d'Archimède et de Reynolds introduites dans les équations (1.3), on peut établir les relations suivantes entre le modèle et le prototype :

$$\frac{U_{i,M}}{U_{i,C}} = \left(\frac{D_C}{D_M}\right)\left(\frac{\rho_C \mu_M}{\rho_M \mu_C}\right) \tag{1.4}$$

$$\frac{\Delta T_M}{\Delta T_C} = \left(\frac{U_{i,M}}{U_{i,C}}\right)^2 \left(\frac{D_C \beta_C}{D_M \beta_M}\right) \tag{1.5}$$

où C et M sont respectivement des acronymes correspondants au CANDU-6 et au modèle expérimental. En substituant l'équation (1.4) dans l'équation (1.5), on obtient :

$$\frac{\Delta T_M}{\Delta T_C} = \left(\frac{D_C}{D_M}\right)^3 \left(\frac{\rho_C \mu_M}{\rho_M \mu_C}\right)^2 \left(\frac{\beta_C}{\beta_M}\right) \tag{1.6}$$

Cette équation montre que le rapport de la différence de température va nécessairement accroître à la troisième puissance si le rapport du diamètre de la calandre et du modèle est plus grand que un (ce qui est toujours le cas). Ceci est une condition qui peut ne pas être assurée alors maintenir à la fois Re et Ar pour fabriquer les modèles à l'échelle réduite est impossible. Selon Khartabil et al. [6], en ayant une valeur de Reynolds suffisamment grande et étant capable de maintenir l'écoulement turbulent dans la cuve, le nombre d'Archimède sera d'une grandeur suffisante pour respecter la similitude dynamique de la cuve. D'après Khartabil et al., l'impact de l'abandon de l'effet de Re se limite à la contribution des termes de diffusion moléculaire et énergétique dans l'équation (1.2). Ceci peut être considéré négligeable à condition que l'écoulement reste turbulent dans le modèle à l'échelle réduite.

Il faut mentionner qu'une grande partie de la chaleur déposée dans le modérateur provient du ralentissement des neutrons, ceci se traduit comme termes sources dans l'équation de la

Tableau 1.1 Groupes adimensionnels gouvernant l'écoulement du modérateur dans le CANDU-6.

Symbole	Nom	Description
Pr	Nombre de Prandtl	Le rapport entre la diffusivité de la quantité de mouvement (ou viscosité cinématique) et la diffusivité thermique.
Re	Nombre de Reynolds	Le rapport entre les forces d'inertie et les forces visqueuses.
Ar	Nombre d'Archimède	Le rapport entre l'énergie potentielle gravitationnelle et l'énergie cinétique.
q^*	-	Source de chaleur volumétrique adimensionnelle.

chaleur (c-à.d. q^* dans l'équation (1.2)). Néanmoins, il est impossible de réaliser une réaction neutronique lors des essais en laboratoire. Ainsi, ces termes sources volumiques sont remplacés par une génération de chaleur de type conducto-convective produite par des tubes chauffants encastrés dans la cuve du modèle expérimental.

1.3 Cadre numérique de l'étude

En ayant une géométrie complexe et volumineuse, ainsi qu'une physique compliquée qui est quasiment inconnue de nos jours, réaliser une étude numérique de l'écoulement du modérateur nécessite certaines validations et évaluations au préalable. Ceci est l'objectif principal de l'un de nos articles présenté à l'annexe A de cette thèse. Dans cet article, des études numériques sur des maillages, des algorithmes de calcul et des modèles de turbulences ont été effectuées sur des géométries simplifiées, mais similaires à celles du CANDU-6. Afin de spécifier une plateforme numérique optimale à l'étude, les résultats présentés dans cet article ont été comparés avec des résultats expérimentaux. Dans ce travail, il est observé que la décomposition de RANS (Reynolds-Averaged Navier Stokes equations) en conjonction avec les modèles de turbulence à deux équations sont capables de reproduire les vitesses dans les faisceaux de tubes décalés. Plus précisément, cette étude recommande le modèle $k-\epsilon$ standard dans le but d'effectuer ce genre de simulations. Toutefois, les modèles de $k-\epsilon$ modifiés ne conduisent pas à de meilleurs résultats. Quant au modèle $k-\omega$, en dépit de prédictions

excellentes autour des rangées de tubes, il n'a pas été capable de prédire l'écoulement en aval du domaine.

Plusieurs topologies de maillages ont été testées dans les simulations présentées dans cet article. Ces résultats ont été comparés avec des données expérimentales afin de trouver la forme optimale de maille autour des tubes. En outre, l'étude de la convergence présentée dans ce travail aide à déterminer le nombre de cellules requis pour une simulation de l'écoulement au sein de la cuve complète. Selon cette recherche, afin d'atteindre une bonne précision de calcul, la simulation de calandre nécessitera au moins 3,5 millions de cellules en 2-D.

1.4 Objectifs et problématiques du travail de recherche présentés dans la thèse

Le premier objectif de cette thèse est d'établir la meilleure stratégie numérique possible pour simuler l'écoulement du modérateur. La littérature montre de grandes disparités dans les méthodes et les conditions utilisées pour la simulation du modérateur. L'utilisation de modèles physiques inappropriés (par exemple l'utilisation de l'approximation de Boussinesq, le choix du modèle de turbulence, etc.) pour simplifier les simulations sans avoir évalué leur validité induit des erreurs importantes dans les résultats. De plus, une analyse numérique rigoureuse exige une étude de raffinement de maillage au préalable.

Le deuxième objectif de la thèse est de choisir, investiguer et valider un code de calcul de mécanique des fluides numérique parallèle qui soit capable de simuler l'écoulement du modérateur. Ceci doit être validé avec des données provenant des essais expérimentaux effectués avec les modèles à l'échelle réduite de la calandre d'un réacteur de type CANDU-6. Les données disponibles sont celles des expériences de Paul et al. [7], le laboratoire STERN [8] et le laboratoire MCT [9].

Dans le même contexte, Sarchami et al. [10] ont investigué les effets du type d'échauffement de l'écoulement par le transfert de chaleur surfacique à la paroi des canaux (c.-à-d. de type conducto-convectif utilisé en laboratoire) et l'échauffement volumique similaire à une réaction nucléaire ayant lieu dans le réacteur CANDU-6. Étant donné que la recherche de Sarchami et al. a montré des variations de distributions de chaleur remarquables dues au type de chauffage, le troisième objectif sera de calculer la puissance générée par toutes les grappes de combustible (c.-à-d. pour un total de 4560 grappes) et ensuite l'implémenter dans le domaine hydraulique de la calandre. Ce travail est fait à l'aide du logiciel DONJON [2], développé à Polytechnique Montréal.

Le quatrième objectif est de développer une carte de fonctionnement capable de prédire les configurations de l'écoulement du modérateur en fonction des paramètres caractéristiques.

Cette carte doit être comparée et analysée avec la carte proposée précédemment par Carlucci et Cheung [11].

Des données disponibles des essais expérimentaux de la MTF [12] montrent que les fluctuations de la température ont une amplitude allant jusqu'à 30°C à des fréquences très faibles. Dans ce contexte, le cinquième objectif est d'effectuer des simulations transitoires afin de pouvoir déterminer de possibles mouvements périodiques ayant lieu dans l'écoulement du modérateur. Ces instabilités seront analysées afin de déterminer leurs natures physiques et les raisons de leur production au sein de la calandre.

Étant donné que la distribution de l'écoulement du modérateur d'un réacteur CANDU-6 a toujours été considérée uniforme lors des calculs de la cinétique des neutrons, investiguer l'effet des distributions du modérateur sur la réactivité du réacteur est le dernier objectif de cette thèse. Ainsi, cette étude consiste en un travail de couplage entre les mouvements du modérateur et le transport de neutrons c.-à-d. la physique des réacteurs. Cette partie du travail de recherche est réalisée à l'aide du code de calcul neutronique DONJON [2] en utilisant les propriétés clefs du fluide modérateur (c.-à-d. la température et la masse volumique ainsi que la librairie des sections efficaces).

1.5 Plan de la thèse

Cette thèse comprend sept chapitres et deux annexes. Le chapitre 1 présente une introduction aux technologies reliées aux réacteurs CANDU-6. Les objectifs ainsi que les problématiques de la thèse sont détaillés dans ce chapitre. Une revue critique de la littérature est également présentée au chapitre 2. Le chapitre 3 présente la mise en contexte du sujet et la cohérence des articles publiés. Les chapitres 4, 5 et 6 comprennent les articles soumis et/ou publiés dans le cadre de ce travail de recherche. Le chapitre 7 présente ensuite une discussion générale sur les objectifs de la thèse et nos contributions les plus importantes. Finalement, les conclusions et recommandations sont présentées au chapitre 8 de la thèse.

CHAPITRE 2 REVUE DE LITTÉRATURE

Comme indiqué au chapitre précédent, la cuve des réacteurs CANDU-6 possède une géométrie complexe, remplie avec de centaines de canaux de combustible. Autour de chacun de ces tubes, l'écoulement se développe et produit des zones de sillages et de stagnation. En plus, la présence des sources de chaleur crée un écoulement secondaire ascendant dans la cuve contre l'écoulement inertiel régi par l'injection forcé du modérateur. Ainsi, à l'intérieur de la cuve, l'écoulement du modérateur s'écoule avec une physique complexe due à la compétition entre les forces inertielles et les forces gravitationnelles. La configuration adoptée par l'écoulement ainsi que les distributions de température jouent un rôle important pour la sûreté nucléaire.

Compte tenu de la complexité du problème, il n'existe que peu d'études effectuées sur la thermohydraulique de l'écoulement du modérateur, accessibles au public, dans la littérature. Effectuer une analyse basée sur le comportement réel de l'écoulement du modérateur au sein d'un réacteur fonctionnel est pratiquement impossible, surtout à cause des difficultés d'accès au cœur du réacteur pour l'échantillonnage des données. Ainsi, insérer des capteurs dans le cœur peut fragiliser les critères de sûreté dans le fonctionnement normal du réacteur. En outre, le rayonnement nucléaire existant au sein du réacteur peut ainsi induire des erreurs remarquables sur les données collectées par les instruments de mesure.

Quant aux études empiriques, fabriquer un modèle expérimental, même à l'échelle réduite, est coûteux. De plus, comme il a été mentionné au chapitre précédent, assurer la similitude dynamique entre modèle et prototype relève de la gageure. Par conséquent, afin de construire un modèle, au moins l'un des paramètres doit être négligé en faveur des autres. Puisque la physique de cet écoulement est inconnue, cette simplification pourrait grandement affecter les résultats finaux.

La modélisation numérique reste une approche alternative. Cependant, elle nécessite des ressources de calcul disponibles uniquement grâce à l'évolution récente du calcul à haute performance sur les superordinateurs. Ces simulations permettent l'utilisation de modèles physiques précis ainsi qu'une discrétisation relativement fine en trois dimensions.

Dans ce chapitre, les travaux de recherche portant sur les mouvements du modérateur des réacteurs CANDU-6 sont présentés. Ces études se groupent en deux parties, c.-à-d. numériques et expérimentales.

2.1 Études numériques portant sur l'écoulement du modérateur

Les approches numériques de la mécanique des fluides (par exemple volumes finis, éléments finis et différences finies, etc.) visent à résoudre les équations aux dérivées partielles du mouvement des fluides. Actuellement, la majorité des codes de calculs de la mécanique des fluides utilisent la méthode des volumes finis grâce à sa stabilité et sa simplicité. Cette méthode, en utilisant des approximations d'intégrales, divise le domaine d'étude en des volumes finis (appelé la technique de maillage). Les équations du mouvement sont ensuite résolues pour ces volumes. Par l'approche des volumes finis, les intégrales de volume existant dans les équations se transforment sous forme d'intégrales de surface, appelé flux. Ces flux sont ensuite évalués sur l'interface des mailles, donnant les équations de conservation.

La méthode des volumes finis a été largement utilisée afin d'étudier l'écoulement du modérateur, mais en employant des techniques variées pour modéliser le domaine. Un résumé de ces études sera présenté dans cette section.

2.1.1 Méthode des milieux poreux

La majorité des codes de calcul développés visant à étudier l'écoulement du modérateur utilisent l'approche de milieux poreux. Ainsi, une brève introduction de cette méthode semble indispensable.

La méthode des milieux poreux représente le faisceau de tubes comme une résistance dans un domaine continu. Bien que cette approche rende les simulations moins coûteuses, elle est incapable de prédire les phénomènes locaux pouvant avoir lieu au voisinage des tubes.

Les données pour la résistance distribuée, utilisées dans la plupart des codes se basant sur la méthode des milieux poreux dans le but d'étudier les mouvements du modérateur de CANDU-6 (par exemple MODTURC CLAS et les codes développés à l'institut de la recherche sur l'énergie atomique de Corée du Sud [13]) ont été obtenues par Hadaler et Fortman [14].

L'ensemble de la trainée de forme et de frottement compose la résistance hydraulique. Puisqu'aucune trainée de forme ne se produit pour l'écoulement axial dans la cuve, les corrélations conventionnelles de la perte de pression par frottement sont suffisantes afin de prédire la perte de charge axiale du modérateur.

Quant à la direction latérale de l'écoulement dans la cuve d'un réacteur CANDU-6, Hadaler et al. [14] ont proposé le coefficient de perte de pression suivant :

$$\text{PLC} \equiv \frac{\Delta P}{N_r \rho \frac{V_m^2}{2}} = 4.54 Re^{-.0172} \tag{2.1}$$

avec P la pression, N_r le nombre de rangées de tubes et V_m la vitesse moyenne en amont du faisceau de tubes. Les résistances hydrauliques implémentées dans l'équation de la quantité de mouvement comme termes sources sont les pertes de pression par unité de longueur comme suit :

$$\frac{\Delta P}{\Delta L} = N_r \rho \frac{V_m^2}{2\Delta L} 4.54 Re^{-.0172} \tag{2.2}$$

En définissant le terme de porosité (γ) comme une quantité d'espace vide entre les tubes, la vitesse en amont est liée à la vitesse locale de l'écoulement selon la relation suivante :

$$V_m = \gamma V_c \tag{2.3}$$

On peut décomposer le gradient de pression dans les directions horizontale et verticale comme :

$$\left(\frac{\Delta P}{\Delta L}\right)_x \equiv \frac{\Delta P}{\Delta L} \cos\theta = \frac{\Delta P}{\Delta L} \frac{u_x}{V_c} \tag{2.4}$$

$$\left(\frac{\Delta P}{\Delta L}\right)_y \equiv \frac{\Delta P}{\Delta L} \sin\theta = \frac{\Delta P}{\Delta L} \frac{u_y}{V_c} \tag{2.5}$$

avec θ l'angle entre le vecteur de vitesse et l'axe horizontal.

Finalement, l'équation (2.2) peut s'écrire comme suit :

$$\left(\frac{\Delta P}{\Delta L}\right)_i = \frac{N_r}{\Delta L} 4.54 Re^{-.0172} \rho \frac{(\gamma^2 V_c)}{2} u_i \tag{2.6}$$

avec i correspondant à la composante x ou y de l'écoulement. Cette équation est implémentée en tant que terme source dans l'équation de la quantité de mouvement afin de représenter

l'effet de la résistance hydraulique du faisceau de tubes.

La plus ancienne recherche portant sur l'écoulement du modérateur disponible dans la littérature a été réalisée par Carlucci [15] en utilisant le code TEACH (Teaching Elliptic Axisymmetry Characteristics Heuristically) [16]. Ce code, comme tous les résoluteurs développés à l'EACL (Énergie Atomique du Canada Limitée), utilise l'approche de milieu poreux pour modéliser le faisceau de tubes. Puisque les ressources informatiques dans les années 80 étaient extrêmement limitées par rapport à nos jours, les développeurs étaient obligés d'alléger la complexité des simulations numériques. Pour ce faire, plusieurs modèles physiques ont été utilisés dans le développement des codes de calcul, sans suffisamment vérifier leur validité selon les conditions de l'écoulement. Les modèles de turbulence à deux équations et l'hypothèse de Boussinesq pour le terme de la gravité sont parmi les modèles utilisés dans la majorité des codes de calcul. D'ailleurs, la modélisation géométrique de la cuve a été extensivement simplifiée. La plupart des simulations ont été effectuées en deux dimensions en considérant la moitié de la cuve. Bien que la géométrie de la cuve du réacteur CANDU-6 soit presque symétrique, certaines études ultérieures ont montré que la nature de l'écoulement du modérateur n'est pas symétrique sous toutes les conditions de fonctionnement. En conséquence, l'utilisation des conditions aux frontières symétriques pour simplifier le domaine de calcul affecte les résultats des simulations numériques.

Selon les conditions de fonctionnement, les simulations réalisées par le code TEACH ont prédit deux configurations pour l'écoulement. Dans la première configuration (appelée dominée par l'inertie), les écoulements de jets se rencontrent dans la zone supérieure de la cuve. Ils s'écoulent ensuite entre les tubes de calandre et continuent vers la sortie se situant dans la partie inférieure du réacteur. Dans la deuxième configuration (appelée dominée par la poussée d'Archimède), l'écoulement du modérateur devient stratifié. Dans une telle configuration, la quantité de mouvement des jets n'est pas suffisante pour vaincre la forte poussée d'Archimède existant dans la cuve due à la forte variation de densité. Puisque le modérateur ne circule pas en haut de la cuve, la température de la partie supérieure devient plus grande.

Szymansky et al. [17] ont développé le code MODTURC (Moderator Turbulent Circulation) toujours utilisé dans l'industrie nucléaire. Ce code a été extensivement validé par des données expérimentales collectées en laboratoire [17]. Les premières versions de ce logiciel ne traitaient que la moitié de la cuve. Plus tard, les simulations de Carlucci et Cheung [11], qui ont été effectuées pour la cuve complète, ont prédit des asymétries dans l'écoulement autour du plan médian vertical sous certaines conditions de fonctionnement. Il a été observé que le point de rencontre de deux jets se déplace vers l'un des deux côtés de la cuve. Bien que certains chercheurs aient considéré une cause purement numérique due à l'utilisation des

mailles décalées employées dans MODTURC, des études ultérieures ont montré une nature physique pour ces asymétries.

Ainsi, une version améliorée de MODTURC, MODTURC-CLAS a été développée par Huget et al. [8]. Ce code tridimensionnel était capable d'admettre plusieurs types de mailles. D'ailleurs, l'utilisation d'une nouvelle méthode de discrétisation des équations a amélioré la précision du code par rapport à sa version précédente. Afin de valider ce code, un modèle à l'échelle réduite a été construit chez EACL. De manière générale, les résultats des simulations de MODTURC-CLAS étaient en bon accord avec les données expérimentales [18].

Yoon et al. [19] ont employé ANSYS-CFX afin de développer un modèle CFD en 3-D qui utilisent les corrélations de perte de charge de Hadaler et Fortman [14]. Ils ont validé avec succès les résultats obtenus avec les mesures expérimentales de STERN et également avec des simulations effectuées avec MODTURC et MODTURC-CLAS. Dans d'autres études [19, 20], en utilisant la même plateforme numérique, ils ont montré l'importance de la composante axiale de l'écoulement et ainsi la nécessité d'une simulation 3-D pour prédire les mouvements du modérateur CANDU-6. Yoon et al. [21] ont également investigué l'influence du choix du résoluteur numérique (couplé / décalé) sur les résultats obtenus pour des géométries complexes comme celle du CANDU-6. Selon cette étude, un résoluteur couplé produit des résultats plus précis pour l'écoulement du modérateur. Récemment, cette plateforme a été améliorée par Lee et al. [22] dans le cadre d'études sur les accidents nucléaires In-core LOCA, où le modérateur entre en régime diphasique suite aux contacts thermiques entre les tubes de calandre et les tubes de pression. De plus, Park et al. [13] ont développé le code CUPID, étant capable de faire des simulations transitoires des écoulements diphasiques lors d'accidents des réacteurs CANDU-6. Ce code est actuellement dans la phase de validation.

2.1.2 Conditions aux limites pour le profil du modérateur à la sortie des injecteurs

Une représentation schématique du diffuseur du modérateur des réacteurs CANDU-6 est présentée à la figure 1.3. La conception de l'injecteur est telle que trois lames le divisent en quatre sous-canaux. L'écoulement du modérateur devient pleinement développé dans chacun de ces sous-canaux ayant un nombre de Reynolds égal à 379000, calculé pour une longueur caractéristique d'environ 10 (cm) qui correspond au diamètre hydraulique.

Plusieurs recherches ont visé le développement d'un profil de l'injection du modérateur afin d'éliminer les injecteurs du domaine thermohydraulique de la cuve du réacteur. En effet, utiliser un tel profil en tant que conditions aux frontières réduit les coûts de calculs sans influencer la nature physique de l'écoulement au sein de la cuve. Cependant, certains comme

Sarchami et al. [10] ont maintenu les injecteurs dans le domaine hydrodynamique de la cuve.

Dans le développement du code MODTURC, Szymansky et al. [17] ont considéré le profil d'injection uniforme, ayant une vitesse moyenne constante égale à 2 m/s. Cette hypothèse a été également retenue par Carlucci et al. [23] dans le code MODTURC-CLAS utilisé pour simuler l'écoulement du modérateur des réacteurs CANDU-9. Ils ont validé leurs simulations avec des données expérimentales de l'installation de MTF [6] ; en général, les résultats étaient en très bon accord avec les données. Kim et al. [24,25] ont utilisé un profil de vitesse constant, cependant avec des valeurs presque deux fois plus grandes que la vitesse moyenne de l'injecteur de la calandre des réacteurs CANDU-6. Aucune justification n'a été fournie par les auteurs sur cette contradiction.

Yoon et al. [26] ont simulé l'écoulement au sein du diffuseur afin de prédire le profil d'injection à la sortie. Utilisant un maillage suffisamment raffiné, ils ont employé ANSYS-CFX pour faire des simulations. Le profil de vitesse prédit par ces simulations varie entre des valeurs négatives et des valeurs positives allant jusqu'à 10 m/s. Alors que les calculs semblent être précis, selon une étude de maillage, les auteurs n'ont pas correctement appliqué les conditions aux frontières. En effet, ils ont imposé une valeur constante de la pression statique égale à 1,5 atm tout de suite à la sortie de l'injecteur comme condition aux frontières. Étant donné que pour les mouvements des fluides, la pression et la vitesse sont en correspondance directe, imposer une telle condition aux frontières à l'endroit où on cherche le profil de vitesse n'est pas correct.

Choi et al. [27] ont utilisé dans leur travail de recherche le profil de vitesse susmentionné. Ce profil 2D a été extrait sur la ligne du centre traversant la sortie de l'injecteur. De plus, Choi et al. ont extrudé ce profil afin de construire une surface représentant la distribution de l'écoulement dans la section de passage. Cette manipulation semble être incorrecte puisque les vecteurs de vitesse 3D présentés dans le travail de Yoon et al. [26] montrent de fortes distributions 3D à cet endroit.

2.1.3 Études utilisant l'approche CFD

Les études numériques mentionnées ci-dessus ont été effectuées en utilisant l'approche des milieux poreux afin de modéliser l'écoulement autour des tubes de calandre. Cependant, la présence des tubes peut conduire à des écoulements secondaires dans la cuve. L'approche des milieux poreux prédit exclusivement les caractéristiques moyennes de l'écoulement comme la perte de pression et l'augmentation globale de la température dans le domaine. Ceci est avantageux pour obtenir des résultats à faible coût. Toutefois, les tubes créent des points de stagnation et des zones de sillages dans l'écoulement environnant. Ceci peut provoquer

l'augmentation de la température au voisinage des tubes et éventuellement conduire à l'assèchement local de la surface. D'autre part, récemment, Rhee et Kim [28] ont montré que certains termes moyennés et négligés dans l'approche des milieux poreux utilisés dans MODTURC peuvent considérablement induire des erreurs de calcul. De ce fait, des chercheurs ont utilisé une approche CFD afin de pouvoir modéliser les conditions locales de transfert de chaleur. Ici, à la place d'un milieu poreux, le faisceau de tubes est représenté comme conditions aux frontières de type Dirichelet (c.-à-d. de type paroi).

Kim et al. [24] ont utilisé un modèle CFD afin de simuler le modérateur en régime stationnaire à l'aide du logiciel ANSYS Fluent- 6.0. Dans ce travail, la vraie géométrie de CANDU-6 avec 380 canaux de combustible a été modélisée. De manière similaire aux prédictions du code MODTURC, cette recherche a conclu que les principaux paramètres affectant les configurations d'écoulement sont la vitesse d'entrée de l'écoulement ainsi que la chaleur transmise au liquide modérateur. Quant à la configuration nominale du réacteur CANDU-6, en raison de la combinaison des forces inertielles de l'injection et de la flottabilité de l'écoulement, il en résulte une configuration mixte. Cependant, la vitesse d'entrée présentée dans ce travail était de 5.3 (m/s). Cette vitesse est plus que deux fois plus grande que la vitesse moyenne d'entrée du modérateur ($\approx$ 2 m/s) selon le manuel [29]. Aucune explication pour ce choix n'a été fournie. De plus, les auteurs n'ont pas effectué d'étude d'évaluation de l'erreur de discrétisation du domaine. Les mailles étaient composées de 53 000 cellules en 2-D, et de 830 000 cellules en 3-D, avec à peine 5 cellules entre chacun des canaux. Le problème d'estimation d'erreur est assez commun, même dans les études plus récentes comme ceux de Sarchami et al. [30], Farhadi et al. [31], et Kim et al. [25]. Il a été mentionné au chapitre 1 qu'une étude de convergence a montré qu'au moins 3.5 millions de cellules sont nécessaires pour réaliser une simulation 2-D d'écoulement du modérateur.

La nature non stationnaire de l'écoulement du modérateur nécessite des simulations en régime transitoire. Cependant, l'approche stationnaire a été amplement utilisée dans les études portant sur l'écoulement du modérateur afin de réduire les ressources informatiques requises. Il faut noter que la convection naturelle est un phénomène transitoire pendant lequel, en raison de la gravité, le fluide plus dense se déplace vers la partie inférieure et il est remplacé par le fluide moins dense. Un modèle stationnaire de l'écoulement peut uniquement prédire une tendance générale sur les phénomènes transitoires alors qu'en réalité, l'écoulement varie en fonction du temps dans la cuve du réacteur. De l'autre côté, Sarchami et al. [30] ont effectué des simulations en régime transitoire, mais pour une durée de 150 (s) qui semble être trop courte pour prédire tous les phénomènes pouvant avoir lieu dans l'écoulement.

2.2 Études expérimentales

L'objectif principal des essais expérimentaux sur l'écoulement du modérateur était la validation des logiciels développés dans les centres de recherche pour effectuer les analyses de la sûreté nucléaire. Comme expliqué à la section 1.2, il est impossible de conserver tous les groupes adimensionnels de l'écoulement du modérateur pour construire un modèle à l'échelle réduite. En conséquence, aucune étude expérimentale visant l'écoulement du modérateur ne respecte les lois de la similitude dynamique.

Koroyannakis et al. [32] et Quraishi et al. [33] ont réalisé la première étude expérimentale en construisant le modèle SPEL (Sheridan Park Experimental Laboratory). Ce modèle n'était pas mis à l'échelle d'une cuve de CANDU-6, toutefois, il possédait certaines caractéristiques typiques du CANDU-6, comme un faisceau de tubes et deux injecteurs d'écoulement. Le modèle SPEL est composé d'une cuve cylindrique de 0.74 m de diamètre avec un faisceau de tubes contenant 52 canaux chauffants. Grâce à la simplicité de la géométrie utilisée pour cette expérience, les données ainsi collectées ont été largement utilisées lors de la validation des différents codes numériques [24, 34, 35].

Afin de valider le code MODTURC, les expériences du laboratoire STERN ont été réalisées par Huget et al. [8,36]. Ce modèle comprend une cuve mise à l'échelle un quart d'un CANDU-6 tel que présenté à la figure 2.1. Bien que les sorties de CANDU-6 soient inclinées, elles sont placées dans le modèle de STERN sur le plan médian vertical. En conséquence, toute asymétrie de géométrie est éliminée. Le faisceau de tubes se compose de 440 tubes, chacun de 33 mm de diamètre. Afin de créer un domaine bidimensionnel, les deux injecteurs couvrent toute la profondeur de la cuve. Les résultats de ces expériences ont aussi été utilisés pour la validation des codes MODTURC-CLAS [37] et CUPID [22]. Plusieurs recherches numériques ont visé l'analyse des résultats de ces tests, comme celles, présentées dans les références [28, 38, 39].

Récemment, Kim et al. [40] ont débuté des recherches expérimentales sur l'écoulement du modérateur au KAERI (Korea Atomic Energy Research Institute). Cette recherche vise la validation des codes internes développés pour des analyses d'accidents de type LOCA. Ce programme de recherche comprend la construction de deux modèles expérimentaux à l'échelle 1/40 et 1/8 de la calandre d'un réacteur CANDU-6 [40–42]. À ce moment, les modèles sont en phase préliminaire du développement. Cependant, certaines études numériques ont été effectuées ultérieurement au KAERI afin de déterminer les paramètres de la mise à l'échelle de ces modèles [43].

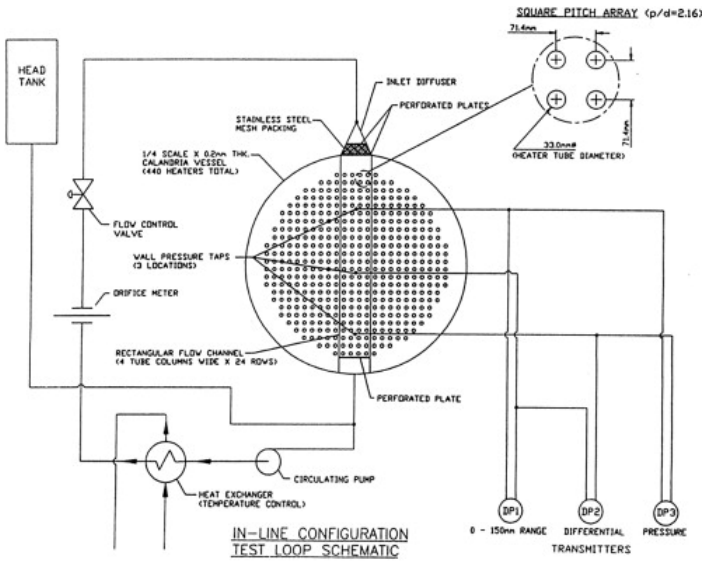

Figure 2.1 Configuration de l'installation d'essai au laboratoire STERN [38].

2.3 Études sur des concepts évolués du réacteur CANDU

La conception de CANDU à évolué au fil du temps ; de petits réacteurs de puissance de type NPD (Nuclear Power Demonstration) vers les réacteurs thermiques de 600 MWe (CANDU-6), ensuite 900 MWe (Bruce et CANDU-9) et la génération future ACR-1000 qui est actuellement dans la phase de développement. Un schéma représentatif du réacteur CANDU-9 est illustré à la figure 2.2. Ce réacteur comprend 480 canaux de combustible. Les réacteurs CANDU de BRUCE et DARLINGTON possèdent une technologie se plaçant entre celle de CANDU-6 classique et celle de CANDU-9. Le concept de ces réacteurs ressemble à celui de CANDU-6, mais avec des injecteurs supplémentaires de "By-Pass" incorporés en haut de la calandre afin d'aider la circulation du modérateur.

L'EACL a construit le MTF (the Moderator Test facility), un modèle expérimental 3-D à l'échelle 1/4 du réacteur CANDU-9 et Bruce avec 480 canaux. Il a été fabriqué essentiellement en vue de fournir des données pour valider les codes informatiques. Les données expérimentales, correspondant à la configuration CANDU-9, provenant de l'installation MTF sont disponibles dans la littérature [6,44]. Carlucci et al. [23] ont comparé ces données expérimentales avec les résultats prédits de MODTURC-CLAS. Cependant, les données correspondantes à la configuration de Bruce sont confidentielles et peu disponibles dans la littérature publique. On peut trouver certaines données dans le travail de Sarchami et al. [10,12] qui ont investigué les effets de l'utilisation de la méthode de chauffage surfacique (conducto-convective) qui est utilisée dans les expériences de MTF, en les comparant à la méthode de chauffage volumique

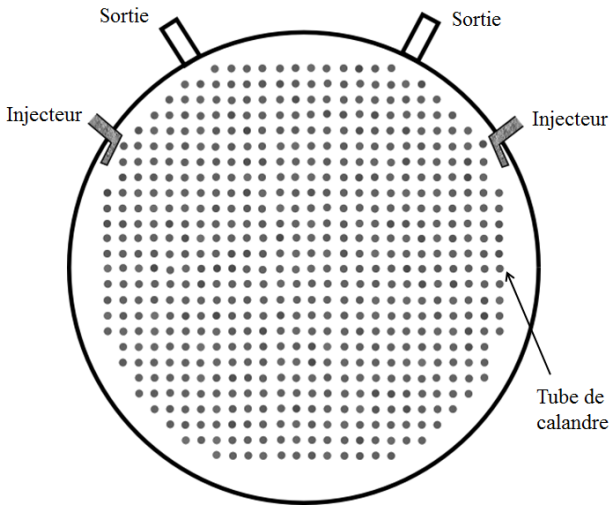

Figure 2.2 Section transversale de la cuve du réacteur CANDU-9.

d'un vrai réacteur. Il a été observé que l'asymétrie de l'écoulement existe dans la cuve, indépendamment de la méthode de chauffage. Cependant, les distributions de température ne sont pas identiques dans les deux cas. Sarchami et al. [45] ont comparé les résultats d'un modèle à l'échelle 1/4 contre un réacteur à échelle réelle [30, 46]. Bien que les travaux de Sarchami et al. dévoilent certains problèmes liés à la mise à l'échelle de la cuve, les erreurs numériques générées par la discrétisation du domaine n'ont pas été étudiées. La discrétisation utilisée dans ce travail est composée uniquement de $3{,}2\times10^6$ cellules en 3-D. D'ailleurs, la carte de puissance utilisée par Sarchami et al. (présentée à la figure 2.3.a) semble être erronée, car en réalité la puissance dans le centre du réacteur est plus élevée que dans les zones situées aux extrémités. À titre d'exemple comparatif, une carte de puissance du réacteur CANDU-6 correspondant à la centrale nucléaire Gentilly-2 est présentée à la figure 2.3.b. Cette carte à été obtenue à l'aide d'un calcul de la physique des réacteurs effectué par le code DONJON [2]. Les conditions de calcul reliées à cette carte sont présentées en détail à la section 6.8.

Suite à une entente de transfert de technologie avec le Canada, l'Inde a fabriqué les réacteurs PHWR-indien en utilisant la plateforme de CANDU. La technologie de ce réacteur ressemble beaucoup à celle du CANDU-6. Cependant, ce réacteur comprend douze injecteurs de modérateur ainsi que quatre sorties situées en bas de la cuve tel que présenté à la figure 2.4. Grâce aux changements apportés à la conception de ce réacteur, les études thermohydrauliques illustrent que l'écoulement du modérateur possède une distribution beaucoup plus uniforme dans ce réacteur par rapport à celui dans la calandre du CANDU-6 [47–49]. La génération prochaine de CANDU en Inde (les réacteurs AHWR : Advanced Heavy Water Reactor au thorium) possédera une cuve verticale [50].

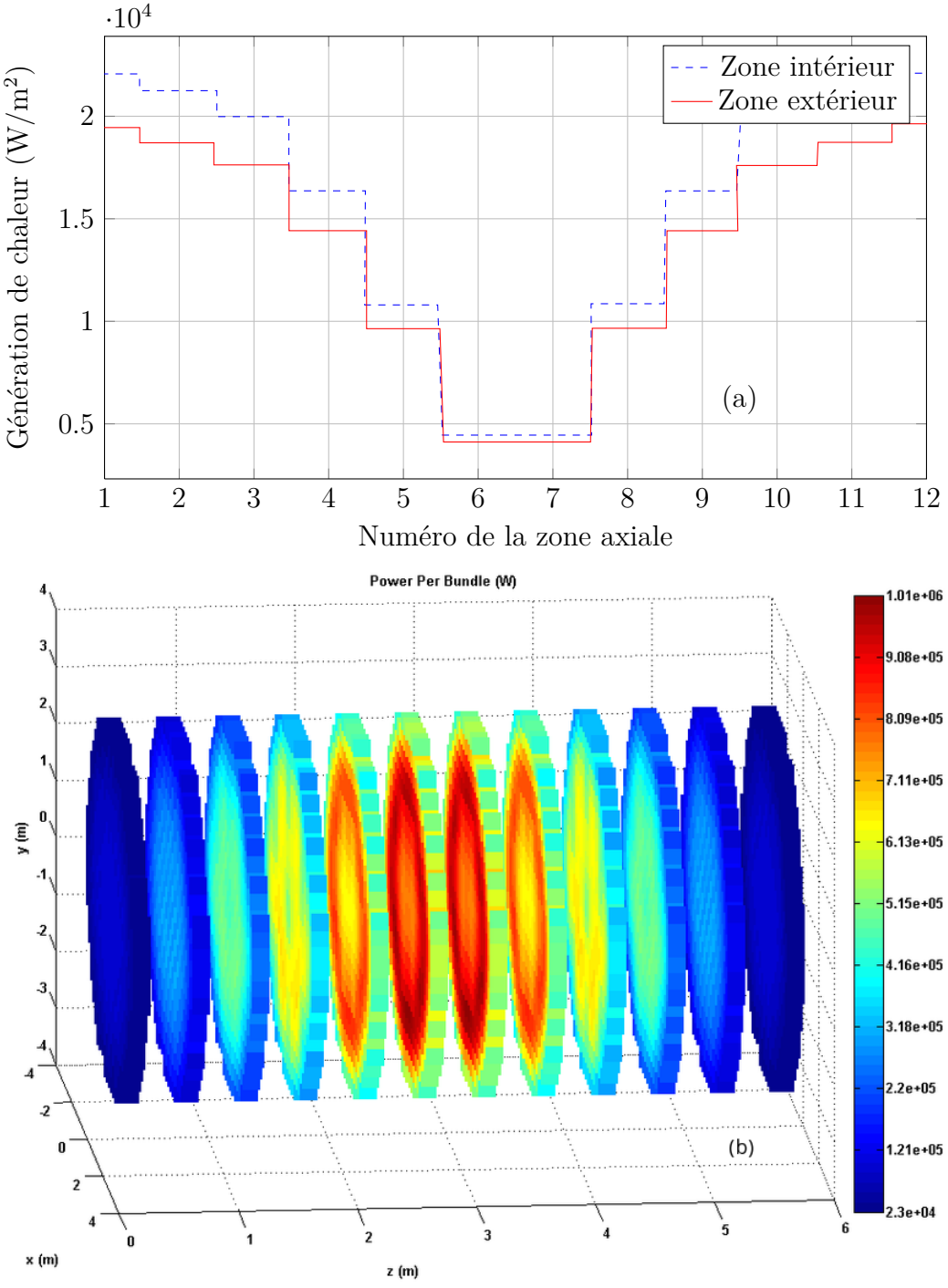

Figure 2.3 a) Carte de puissance utilisée par Sarchami et al. [12] ; b) Carte de puissance pour CANDU-6 (Gentilly-2) générée par le code DONJON.

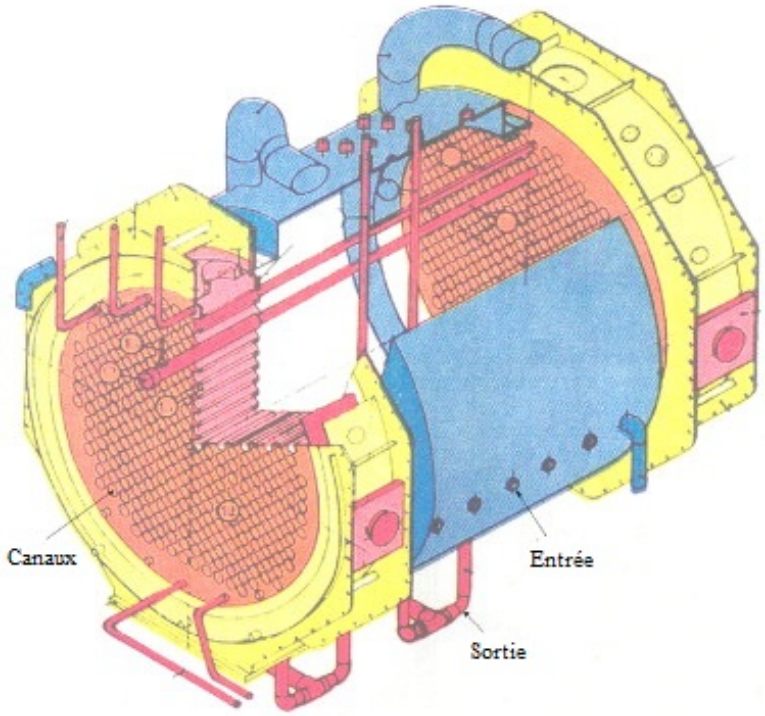

Figure 2.4 Réacteur PHWR indien avec 12 injecteurs et 4 sorties de modérateur [48].

2.4 Collecte de données d'un réacteur en fonctionnement

Il a été mentionné que la collecte de données à l'intérieur d'un réacteur nucléaire en fonctionnement est un processus très difficile en raison des difficultés d'accéder au cœur du réacteur pour installer les dispositifs de mesure. Outre cela, l'effet de rayonnement sur les instruments de mesure exige l'utilisation de capteurs particuliers et résistants. Austman et al. [51] ont utilisé un certain type de thermocouple pour pallier à la radiation intense dans le cœur du réacteur.

L'accès direct au cœur du réacteur était seulement possible à travers le mécanisme de réactivité (barres d'arrêt). Les positions des barres d'arrêt existantes du CANDU étaient loin de la zone d'intérêt. En outre, la collecte de données ponctuelles composées de 15 capteurs de mesure n'était pas suffisante pour effectuer une analyse robuste sur les configurations de l'écoulement.

2.5 Résumé et limitations des travaux antérieurs

Les limites des études numériques précédentes sont les suivantes :

– Manque d'étude de la convergence espace-temps.
– Utilisation des modèles physiques non valides pour simuler les réacteurs CANDU-6.
– Utilisation de l'approche des milieux poreux et l'impossibilité de la prédiction des effets locaux.
– Utilisation des conditions aux frontières symétriques pour réduire la taille du domaine.
– Analyses uniquement basées sur des simulations en régime stationnaire.
– Temps de simulations transitoires trop courts qui ne permettent pas d'observer les oscillations à basses fréquences.

Quant aux études expérimentales, elles sont généralement utilisées afin de fournir des résultats qui seraient utilisés pour valider les codes numériques. Toutefois, fabriquer ce type de modèle expérimental nécessite un investissement remarquable puisque plusieurs dispositifs d'échantillonnage à haute précision sont nécessaires pour l'échantillonnage de donnée. Outre cela, les études expérimentales sont limitées par les contraintes suivantes :

– Contradiction entre les paramètres de la similitude dynamique du domaine pour fabriquer un modèle à l'échelle réduite.
– Type de chauffage limité aux flux de chaleur constants de type surfacique conducto-convectif.

CHAPITRE 3 ORGANISATION DE LA THÈSE ET COHÉRENCE DES ARTICLES

3.1 Mise en contexte

L'énergie nucléaire compte pour 15% de la production de l'énergie électrique du Canada, avec 19 réacteurs en fonction produisant 13.5 GWe [52]. Dans ce contexte, l'importance de cette recherche est de mieux comprendre le comportement hydrodynamique complexe du modérateur et ainsi d'assurer le bon fonctionnement de ce système. Pour cela, l'étude de l'écoulement du modérateur dans la calandre du réacteur est nécessaire afin de prédire et prévenir les risques d'ébullition locale du fluide modérateur. Ainsi, ce travail s'inscrit dans la démarche continue d'amélioration de la sûreté des réacteurs nucléaires.

Dans le but de clarifier l'organisation de la thèse, un aperçu des chapitres sera présenté. L'objectif principal de ce travail de recherche est de simuler l'écoulement complexe du modérateur au sein de la calandre des réacteurs de type CANDU.

Cette thèse a mené à la publication de trois articles dans des revues avec comité de lecture en tant qu'auteur principal, un article dans une revue avec comité de lecture en tant que coauteur et un article publié dans le compte rendu de la conférence CSME&CFD-SC 2014, Toronto. Ces articles sont présentés dans les chapitres suivants. L'ordre de présentation ainsi que les point importants dans chacun de ces article sont illustrés à la figure 3.1.

3.2 Évaluation de la plateforme numérique, synthèse de l'article : *"Moderator flow simulation around calandria tubes of CANDU-6 nuclear reactors" (Annexe A)*

Cet article a été publié en 2014 dans la revue "Engineering Applications of Computational Fluid Mechanics Vol. 8, No. 1, pp. 178- 192". Étant donné que je ne suis pas l'auteur principal de cet article, il est présenté en annexe A. Ma contribution a pour but de réaliser une étude d'indépendance de maillage pour les calculs présentés dans ce travail de recherche. Puisque cette recherche formule la plateforme numérique utilisée dans ce projet, ma contribution dans cet article a constitué le point de départ de mon doctorat. C'est pour cette raison que cet article a été présenté dans la thèse.

Ce travail consiste à étudier l'écoulement du modérateur à travers deux configurations de faisceaux de tubes représentant les mouvements du modérateur dans la calandre. Les calculs sont effectués en utilisant le logiciel ANSYS-Fluent dans le but d'investiguer les modèles de

turbulence à deux équations ainsi que les algorithmes de calcul pour prédire les comportements du modérateur. Ces prédictions ont été évaluées en comparant les résultats avec des données expérimentales. Les études de maillages présentées dans ce travail ont été utilisées comme une pré-estimation du nombre de cellules requis pour effectuer des simulations numériques d'une cuve de réacteur contenant des tubes.

3.3 Étude cartographique du modérateur, synthèse de l'article : *"CFD simulation of the moderator flow in CANDU-6 nuclear reactors"*

Cet article a été soumis en octobre 2015 à la revue "Journal of Nuclear Engineering and Radiation Science ". Une copie est présentée au chapitre 4. Il a été accepté pour publication en février 2016.

Cette recherche présente des simulations stationnaires en deux dimensions pour un vaste ensemble de conditions de fonctionnement. La première partie consiste à évaluer la précision des approximations numériques ainsi que la validité des modèles physiques utilisés dans les études CFD dans le but de simuler le comportement du liquide modérateur. Une représentation cartographique de l'écoulement du modérateur a été développée, basée sur des simulations numériques. Cette carte prédit la configuration du modérateur en fonction des paramètres adimensionnels de l'écoulement. La distribution de température au sein de la calandre a été étudiée et analysée pour chacune des configurations. Ainsi, des prédictions déterminent les zones surchauffées du liquide modérateur. La plateforme numérique utilisée pour cette recherche a été validée en utilisant des données expérimentales ainsi que des données numériques obtenues par une approche des milieux poreux.

3.4 Analyses du comportement dépendent du temps de l'écoulement du modérateur, synthèse de l'article : *"2-D CFD Time-dependent Thermal-hydraulic Simulations of CANDU-6 Moderator Flows"*

Cet article a été soumis en janvier 2016 à la revue "Nuclear Engineering and Design". Une copie est présentée au chapitre 5.

L'étude en régime stationnaire (présentée au chapitre 4) prédit que pour certaines conditions de fonctionnement où les forces de flottabilité sont dominantes, une stratification thermique de l'écoulement du modérateur peut avoir lieu. En particulier, il s'agit des transitions entre configurations qui sont fortement dépendantes du temps. Par conséquent, réaliser une étude numérique dépendant du temps est nécessaire pour l'analyse de la sûreté nucléaire. Dans ce contexte, cette recherche porte sur les simulations numériques de l'écoulement du modérateur

en régime transitoire. Afin d'obtenir une meilleure compréhension des phénomènes physiques, les simulations ont été réalisées sur de longues périodes de temps réel. Les résultats montrent une région où l'écoulement est caractérisé par des structures cohérentes de fluctuations (c.à-d. une configuration mixte).

Suite aux commentaires des membres du jury et des examinateurs de la revue, les éléments suivants seront ajoutés à la version révisée de l'article :

- Justification pour l'utilisation d'un modèle 2-D,
- Modèle de turbulence utilisé,
- Intensité de turbulence à l'entrée,
- Type de la loi des parois,
- Équations du modèle,
- Temps de calcul,
- Coefficients utilisés dans la fonction du filtre,
- Corrélation croisée entre les valeurs de la température du modérateur dans la calandre.

Veuillez noter que ces modifications ne sont pas incluses dans la version préliminaire de cette publication présentée dans la thèse.

3.5 Étude du couplage thermohydraulique-neutronique du modérateur, synthèse de l'article : *"Effect of 3-D moderator flow configurations on the reactivity of CANDU-6 nuclear reactors"*

Cet article a été soumis en avril 2016 à la revue "Annals of Nuclear Energy". Une copie est présentée au chapitre 6.

Les études portant sur la physique des réacteurs CANDU ont toujours été effectuées en utilisant une distribution uniforme des caractéristiques thermohydrauliques du modérateur. Puisque les simulations CFD de l'écoulement du modérateur ont prédit des fluctuations assez remarquables du modérateur (dans certaines conditions, des différences de plus de 50°C ont été constatées), l'objectif de cette recherche est d'étudier les effets de ces distributions de l'écoulement sur la réactivité des réacteurs CANDU-6. Dans ce contexte, cette recherche présente des simulations CFD robustes du modérateur de CANDU-6 en 3-D couplé à des calculs de la physique des réacteurs. Ainsi, les simulations présentées permettent d'étudier non seulement les différentes configurations de l'écoulement du modérateur, mais aussi leurs effets sur le coefficient de réactivité du réacteur.

Il faut noter que les commentaires des examinateurs de la revue n'ont pas été reçus jusqu'à la date de soumission finale de cette thèse. Cependant, les éléments suivants seront ajoutés

ou modifiés dans la version révisée de l'article selon les commentaires des membres du jury.

- Précision sur la constante "n" utilisée dans l'équation (6.2) ;
- L'équation (6.5) est l'équation de la diffusion des neutrons ;
- Les valeurs de la puissance thermique présentées à la figure 6.13 sont par canal, mais pas par grappe ;
- L'utilisation du mot "obvious" sera limitée ;
- Dans la légende de la figure 8.16a, la température du modérateur lors de cette simulation sera précisée ;
- À la section 6.8.1, "Fuel temperature" sera remplacée par "Moderator temperature" ;
- À la section 6.9, "Gentilly-2" sera remplacé par "CANDU-6".

Similairement à l'article précédent, les modifications mentionnés ci-haut, ne sont pas incluses dans la version préliminaire de cette publication telle que présentée dans la thèse.

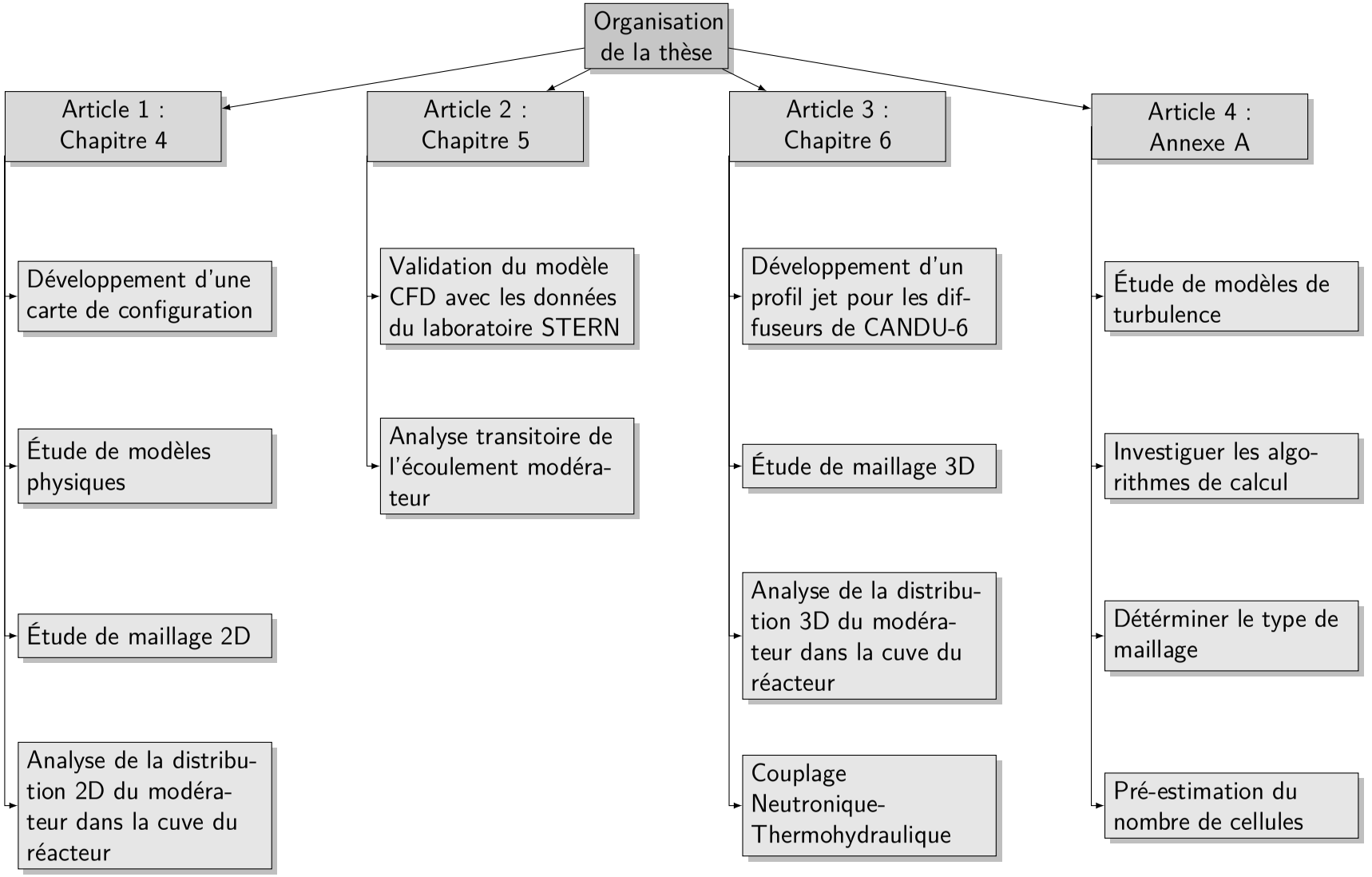

Figure 3.1 Organisation de la thèse.

CHAPITRE 4 ARTICLE 1 : CFD simulation of the moderator flow in CANDU-6 nuclear reactors

Authors : Foad Mehdi Zadeh, Stéphane Etienne and Alberto Teyssedou, submitted to the Journal of Nuclear Engineering and Radiation Science, Accepted for publication in February 2016.

4.1 abstract

For CANDU nuclear reactors, the characterization of the moderator thermal-hydraulic behavior under both normal and abnormal operating conditions constitutes an important safety issue. For normal operating conditions, the flow temperature distribution may produce changes on the heavy water mass density, which in turn may affect the neutron moderation rate. Consequently, these variations influence the thermal neutron flux distribution in the reactor core. Therefore, it is fundamental to know all possible moderator flow configurations as well as the corresponding temperature distributions. In particular, any possibility of a dry out at the external wall of the calandria tubes and consequently excessive temperature excursions must be prevented. Within this framework, this paper presents detailed 2D numerical steady-state simulations for a wide range of flow conditions. Both the accuracy of the numerical approximations as well as the validity of some physical models used in CFD codes are assessed. The numerical results are then used to construct a cartographical representation of the moderator flows in CANDU-6 reactors. To support the existence of coherent flow asymmetries and eventually flow structure oscillations, the present numerical results are also compared with previous ones obtained using a porous medium modeling approach.

Nomenclature

a, b, c, d, e, f	Coefficients used to validate the Boussiesq approximation
A_i	Total nozzle cross-sectional area, m^2
c_p	Isobar specific heat, J/kg °C
D	Vessel diameter, m
d	Tube diameter, m
g	Acceleration of gravity, m/s^2
h	Grid's characteristic size, m
$\underline{J}_a$	Vector flux, W/m^2
k	Thermal conductivity, W/m °C
Q	Heat load, W
r	Grid refinment factor
$\underline{\underline{R}}$	Reynolds' stress tensor, m^2/s^2
S	Momentum and energy source terms, N/m^3; W/m^3
T	Temperature, °C
T_0	Reference temperature, °C
$\underline{u}''$ and a''	Fluctuating flow components, m/s;° C
U_x	Axial velocity component, m/s
V_i	Inlet flow velocity, m/s
V_m	Mean flow velocity, m/s
x	Horizontal coordinate
y	Vertical coordinate

Greek letters

α	Thermal expansion coefficient, 1/K
α_0, ϵ_i	Coefficients used to validate the Boussiesq approximation
β	Compressibility coefficient, m^2/N
Γ	Mass source terms, $kg/m^3\,s$
ζ	Order of convergence
θ	Temperature difference, °C
μ	Viscosity, kg/s m
ρ	Mass density, kg/m^3
τ	Viscous stress tensor, N/m^2
ψ	Generic function

Non-Dimensional Numbers

Ar Archimedes' number ; $\left(\frac{g\alpha QD}{c_p\rho A_i V_i^3}\right)$

Gr Grashof's number ; $\left(\frac{g\alpha\Delta TD^3\rho^2}{\mu^2}\right)$

Pr Prandtl's number ; $\left(\frac{c_p\mu}{k}\right)$

Ra Rayleigh's number ; $(\mathbf{Gr}\cdot\mathbf{Pr})$

Ri Richardson's number ; $\left(\frac{g\alpha QD}{c_p\rho A_i V_i^3}\right)$

Acronyms and abbreviations widely used in text and list of references

CANDU	CANada Deuterium Uranium
CFD	Compuitaional Fluid Dynamics
EDF	Électricité de France
GCI	Grid Convergence Index
LES	Large Eddy Simulation
MODTURC	MODerator TURbulent Circulation
MODTURC-CLAS	MODerator TURbulent Circulation-Co-Located Advanced Solution
SIMPLE	Semi-Implicit Method for Pressure Linked Equations
SIMPLEC	Semi-Implicit Method for Pressure Linked Equations-Consistent
TEACH	Teaching Elliptic Axisymmetry Characteristics Heuristically

4.2 Introduction

Nuclear power plants provided 13% of the global electricity consumed in 2012 [53]. More precisely, 31 countries operate 437 reactors, 29 of which are CANDU (CANada Deuterium Uranium) types. In these reactors, natural uranium-dioxide fuel pellets are held inside a zirconium alloy cladding forming the fuel pins. They are arranged in the form of bundles that are inserted into horizontal pressure tubes where they are cooled using pressurized heavy water. Each pressure tube contains 12 fuel bundles. The pressure tubes are coaxially placed inside external shrouds called calandria tubes, separated by a thermal insulating gas. These tubes are immersed in a cylindrical vessel, *i.e.* the calandria, filled with heavy water which acts as a neutron moderator [54]. Under steady-state operating conditions, about 5% of the thermal power produced by fission is deposited into the moderator. This energy is released to the environment by a separate moderator cooling system.

The calandria of CANDU-6 reactors has a complex cylindrical geometry containing 380 horizontal tubes. Inside this vessel, due to the volumetric heat distribution and to the angularly injected fluid mediated by eight circumferential nozzles, the moderator follows intricate flow patterns. Up to now, there exist few Computational Fluid Dynamic (CFD) studies about the thermal-hydraulic behavior of the moderator. In fact, modeling the flow inside the ca-

landria requires huge computational resources. From an experimental point of view, certain works were carried out using scaled models. In fact, some of these studies have given rise to the possible existence of flow instabilities triggered by a competition between buoyancy and inertia forces.

In the 80's, Carlucci [15] used the TEACH (Teaching Elliptic Axisymmetry Characteristics Heuristically) code [16] based on the porous medium approach to simulate both steady and unsteady moderator flows. The calandria tubes were empirically modeled using isotropic porosity and flow resistance distributions. To characterize the configurations of the moderator, Carlucci proposed to use Archimedes' number as an indicator of the intensity of buoyancy required for counterbalancing the inertia forces. He has defined this number as follows :

$$Ar = \frac{g\alpha\dot{Q}D}{c_p\rho A_i V_i^3} \tag{4.1}$$

where g, α, $\dot{Q}$, D, c_p, A_i and V_i are the acceleration of gravity, the coefficient of thermal expansion, the heat generation rate, the vessel diameter, the isobar specific heat, the total nozzle cross-sectional area (in the present case the number of nozzles is two) and the inlet flow velocity, respectively. The definition given by Eq. (4.1) corresponds to the ratio of buoyancy to inertia forces generated by the water jets. It is important to mention that this number also corresponds to the ratio between the gravitational and viscous forces which seems to be different from the designation given in [15] and [55]. In turn, Eq. (4.1) indicates the importance of natural convection relative to forced convection associated to the injected flow, which corresponds to the Richardson number (Ri) and not the Archimedes one. Therefore, in order to emphasize the effects of both the thermal power and buoyancy, Eq. (4.1) will be referred to as the Richardson number for the rest of this document.

Depending on the reactor operating conditions, Carlucci [15] predicted two different possible configurations : *i*) a momentum-dominated flow and *ii*) a buoyancy-dominated one. He correlated these observed flow patterns as a function of the buoyancy to the inertia force ratio. Carlucci was able to show that the behavior of the flow is associated to buoyancy only when the aforementioned ratio is relatively high. Later, Szymansky et al. [56] developed the MODTURC (MODerator TURbulent Circulation) flow solver, very similar to the TEACH code (both softwares employ the distributed porosity approach), still used by the Canadian nuclear industry.

Subsequently, Carlucci and Cheung [11] applied MODTURC to simulate the moderator flow. The two previously mentioned flow configurations were observed from these calculations. However, for the momentum-dominated configuration some flow patterns were asymmetric,

sweeping along the circumferential direction. To elucidate the possible numerical nature of these asymmetries, Huget et al. [8] introduced the MODTURC-CLAS (Co-Located Advanced Solution) flow solver. They used the same set of equations as MODTURC but the algorithm was improved to handle structured and non-structured discretization meshes. For most of the isothermal cases they studied, the comparisons of the predictions by both solvers were in good agreement with the experimental data. However, when thermal sources were considered, they noticed that the location where the reversal of the circumferential flow velocity occurs was tilted to one side of the calandria with respect to a vertical mid-plane [18, 57].

More recently, Yoon et al. [19, 20] employed the ANSYS CFX-4.4 software to simulate CANDU-6 moderator flows. They argued that the momentum-dominated configuration becomes asymmetric, *i.e.* tilted to one side of the calandria, when inertia and buoyancy forces are of the same order of magnitude. Thus, they were able to conclude that the asymmetries of the moderator flow are real. Furthermore, these simulations have also shown that the velocity components along the axial direction of the vessel are not negligible and therefore they must be considered in CFD calculations [21].

Arsene et al. [58] compared ANSYS-CFX simulations of the moderator flow both for CANDU-6 and CANDU-9 nuclear reactors. They argue that the distributions of the moderator temperatures in the CANDU-9 are more homogeneous than those in the CANDU-6. This conclusion is due to the number and location of the nozzles in the CANDU-9 design. To validate the scaling laws of the calandria vessel, Rhee and Kim [28] performed a comparative study of simulated moderator flows for 1/4 scale and full-size models. Most of these studies were performed using the porous medium modeling approach. Nevertheless, the presence of the calandria tubes may trigger secondary flows and wakes that can only be roughly simulated by this method (it predicts the average behavior of the flow at relatively low computational costs). However, detailed flow variables are necessary, because close to the external walls of the calandria tubes, the appearance of stagnation points and wake zones can bring about local dry out conditions and consequently excessive wall temperatures. In the case of the MODTURC software, Rhee and Kim [28] claim that neglecting viscous dissipation in the energy conservation equation produces erroneous results. In particular, from a nuclear safety stand point and in order to confirm that the moderator fulfils its role everywhere within the calandria vessel, it is mandatory to correctly estimate the local flow conditions that determine the heat transfer across the calandria tubes.

To overcome some of the aforementioned difficulties, Kim et al. [24] performed 2D and 3D numerical simulations by applying a steady state CFD model in the ANSYS Fluent-6.0 software. 2D calculations were conducted with a mesh made of 53,000 nodes. This number was increased up to 830,000 when performing 3D simulations, with scarcely five cells between each

calandria tube. Even though they have shown that they are capable of properly simulating the moderator flow, the authors did not present a rigorous numerical convergence analysis. It is important to note that this is a major weakness encountered in most studies dealing with the numerical modeling of the moderator flow, amongst others in : Sarchami et al. [59], Farhadi et al. [31], and Kim and Rhee [25].

Mandal and Sonawane [55] performed steady-state simulation of a modified version of a CANDU-6, for laminar and turbulent flows by using an in-house code. The Navier-Stokes equations with an artificial compressibility [60] formulation were solved by imposing a symmetry free-slip wall condition along the vertical mid-plane of the vessel. Half of the calandria section was discretized using hybrid grids with 31,712 nodes. Just like Carlucci [15], they found that the flow configurations predicted by steady-state calculations strongly depend on the initial conditions ; both inertia-dominated and buoyancy-dominated flow patterns can be obtained depending on these conditions. For buoyancy-dominated flow, a maximum moderator temperature difference of about 117 K was predicted. In addition to the fact that the number of discretization nodes was not sufficient to completely satisfy a good numerical convergence, the effect of imposing symmetrical boundary conditions (*i.e.* free-slip wall mid-plane) implies flow constraints that produce erroneous results. Due to the nature of the convective heat transfer coupled to the geometrical asymmetry associated to the inclined off-center outlets, the use of symmetrical boundary conditions seems inappropriate. In fact, Carlucci [15], and Carlucci and Cheung [11] observed a bifurcation of the flow configuration when this kind of boundary condition is used. They argued that the simulations for the 2D full-plane of the calandria agreed better with reality.

In this paper, steady-state moderator flows of a CANDU-6 nuclear reactor are simulated for a 2D calandria full-plane. To this purpose, the Navier-Stokes equations for different reactor operating conditions are solved using the Code_Saturne [1] flow solver with temperature dependent thermo-physical fluid properties. The results are analyzed to re-examine the flow map proposed by Carlucci and Cheung [11], and to determine the transitions between different flow configurations as a function of the Richardson number.

4.3 Validity of the Boussinesq approximation in numerical studies of CANDU reactors

Most numerical simulations of the moderator reported in the literature have used the Boussinesq approximation. Indeed, the variations of the thermophysical fluid properties as a function of temperature and pressure slow down the numerical solutions of the Navier-Stokes equations. Therefore, the use of an appropriate simplification becomes appealing. In the Boussinesq approximation [61], it is assumed that the mass density of the fluid is constant except

for buoyancy forces, which are considered as linear functions of the temperature. If α is the thermal expansion coefficient and ρ_0 a reference mass density, the Boussinesq approximation yields :

$$\rho(T) - \rho_0 = -\alpha\rho_0\theta \tag{4.2}$$

with θ representing the fluid temperature difference. In this formulation the remaining thermophysical properties of the fluid are assumed to be constant and viscous dissipation is also neglected. Hence, the source term in the momentum conservation equation can be simplified as follows :

$$S_M = \rho_0(1 - \alpha\theta)g \tag{4.3}$$

The use of such a simplification for simulating the moderator in CANDU-6 nuclear reactors is, however, questionable. In fact, the Boussinesq approximation is not valid when the variation of the fluid temperature within the domain is too large. Gray et al. [62] have proposed a method to determine the interval of validity of this approximation. After linearizing and dimensionalising the Navier-Stokes equations, the following inequalities are obtained :

$$\epsilon_1 \,\text{to}\, \epsilon_{10} \text{ and } |\epsilon_{11}\frac{T_0}{\theta}| \leq 0.1 \text{ and } |\epsilon_{11}|\sqrt{\frac{Pr}{Ra}} \leq \frac{0.1}{\sqrt{PrRa}} \tag{4.4}$$

Where, Pr and Ra are the Prandtl and Rayleigh numbers, respectively. The parameters in Eq. (4.4) are defined as :

$$\begin{aligned} &\epsilon_1 = \alpha_0\theta_m, \quad \epsilon_2 = \beta_0\rho_0 g L_0, \quad \epsilon_3 = c_0\theta_m, \quad \epsilon_4 = d_0\rho_0 g L_0, \quad \epsilon_5 = a_0\theta_m, \\ &\epsilon_6 = b_0\rho_0 g L_0, \epsilon_7 = m_0\theta_m, \quad \epsilon_8 = n_0\rho_0 g L_0, \quad \epsilon_9 = e_0\theta_m, \quad \epsilon_{10} = f_0\rho_0 g L_0, \quad \epsilon_{11} = \frac{\alpha_0 g L}{c_{p0}} \end{aligned} \tag{4.5}$$

In this equation θ_m corresponds to the maximum expected temperature difference of the fluid and the coefficients are given by :

$$\alpha = -\frac{1}{\rho}\frac{\partial \rho}{\partial T}\,, \quad a = \frac{1}{c_p}\frac{\partial c_p}{\partial T}\,, \quad c = \frac{1}{\mu}\frac{\partial \mu}{\partial T}\,, \quad e = \frac{1}{\alpha}\frac{\partial \alpha}{\partial T}\,, \quad m = \frac{1}{k}\frac{\partial k}{\partial T}\,, \quad \beta = \frac{1}{\rho}\frac{\partial \rho}{\partial p}\,,$$
$$b = \frac{1}{c_p}\frac{\partial c_p}{\partial p}\,, \quad d = \frac{1}{\mu}\frac{\partial \mu}{\partial p}\,, \quad f = \frac{1}{\alpha}\frac{\partial \alpha}{\partial p}\,, \quad n = \frac{1}{k}\frac{\partial k}{\partial p}\,, \quad \theta_m = (T_{max} - T_0) \tag{4.6}$$

with ρ, c_p, μ , α and k defined as the density, the isobar thermal capacity, the viscosity, the thermal expansion and the thermal conductivity, respectively. Eq. (4.4) represents two inequalities : $p\theta_m < 0.1$ and $qL < 0.1$ which must be satisfied in order to guarantee that the approximation error is lower than 10%. Therefore, the most restrictive values of ϵ_i must be taken into account. For the CANDU-6, these values were calculated by considering a reference temperature $T_0 = 71°C$ (*i.e.* the outlet heavy water temperature) ; thus, ϵ_8 and ϵ_9 are the most restrictive parameters. They are used to determine the Boussineq validity range shown in the Fig. 4.1. It is obvious from this figure that the variations of the moderator flow temperature are outside the interval of validity of the Boussinesq approximation. In fact, the fluid temperature difference across the calandria is too high and the fluid is 1.5 times more viscous at the inlet of the calandria than at the outlet.

Preliminary simulations of the flow velocities were performed using the Boussinesq approximation and were then compared with those obtained using the temperature-dependent thermophysical properties of water. The variances of the differences of the flow velocities along the vertical and horizontal axes obtained with and without the use of the aforementioned approximation were found to be 0.06 and 0.14, respectively. Contrary to most studies encountered in the open literature, our results confirm unambiguously that such a simplification should not be used for simulating the CANDU-6 moderator flow.

4.4 Computational model, cell geometry and simulation conditions

Figure 4.2 shows a cross-sectional view of the calandria vessel of a CANDU-6 nuclear reactor having a total depth of about 6 m. Its design is such that the moderator (*i.e.* heavy water) circulates around a group of 380 horizontal tubes at a relatively low flow velocity. The principal characteristics and geometrical data of the calandria are given in Table 4.1 [3].

The simulations presented in this paper were performed with Code_Saturne V3 [1, 63] on a high performance cluster of 8064 cores. To perform the current simulations, 120 Intel Westmere EP X5650 (2.667 GHz) cores with 10 nodes containing 12 CPUs each were used. Code_Saturne is a finite-volume open-source code that has been developed by Électricité de France (EDF) for nuclear thermal-hydraulic applications. It has the capacity of solving the mass weighted time Reynolds-averaged Navier-Stokes set of equations [64] by using different

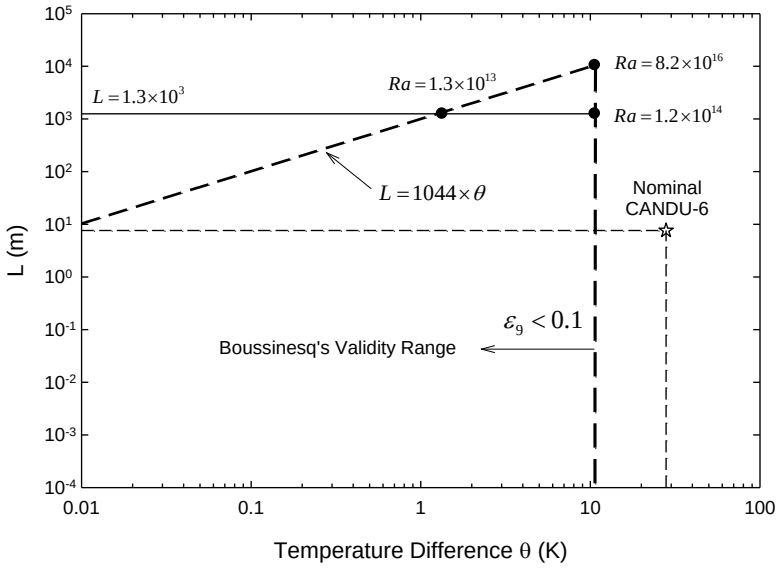

Figure 4.1 Validity of the Boussinesq approximation at T_0=344 K (Nominal CANDU-6 operating value).

solvers (*e.g.* SIMPLE, SIMPLEC, etc.) and simulation models (e.g, conventional turbulence models, LES, etc.). The governing equations can be written in a compact form as :

$$\begin{aligned}
\frac{\partial \rho}{\partial t} + \mathrm{div}\left(\rho \overline{u}\right) &= \Gamma \\
\frac{\partial \rho \underline{u}}{\partial t} + \mathrm{div}\left(\rho \underline{u} \otimes \underline{u}\right) &= -\mathrm{grad}\left(P\right) + \mathrm{div}\left(\underline{\underline{\tau}} - \rho \underline{\underline{R}}\right) + \underline{S}_{\underline{u}} \\
\frac{\partial \rho a}{\partial t} + \mathrm{div}\left(\rho \underline{u} a\right) &= \mathrm{div}\left(\underline{J}_a - \overline{\rho a'' \underline{u}''}\right) + S_a
\end{aligned} \tag{4.7}$$

where $\overline{(.)}$ represents the average operator, $\underline{\underline{(.)}}$ are tensors and $\underline{(.)}$ are vectors. In this equation, Γ indicates the mass source term, $\underline{\underline{\tau}}$ is the viscous stress tensor, $\underline{\underline{\mathrm{R}}}$ is the Reynolds stress tensor, $\underline{S}_{\underline{u}}$ represents the source terms and a is a scalar property. Moreover, $\underline{u}''$ and a'' are the fluctuating components of the Favre's decomposition method [64], and $\underline{J}_a$ is a vector flux expressed by the Fick-Fourier law, namely, $\underline{J}_a = K_a \nabla a$. This set of equations is closed by using an appropriate turbulence model. Based on our previous experience [65], we have selected the standard $k-\varepsilon$ model proposed by Launder and Spalding [66] in conjunction with the SIMPLEC algorithm [67]. In addition, to avoid using the Boussinesq approximation, we have included into the code the relationships required to evaluate the thermo-physical properties of the water as a function of its temperature.

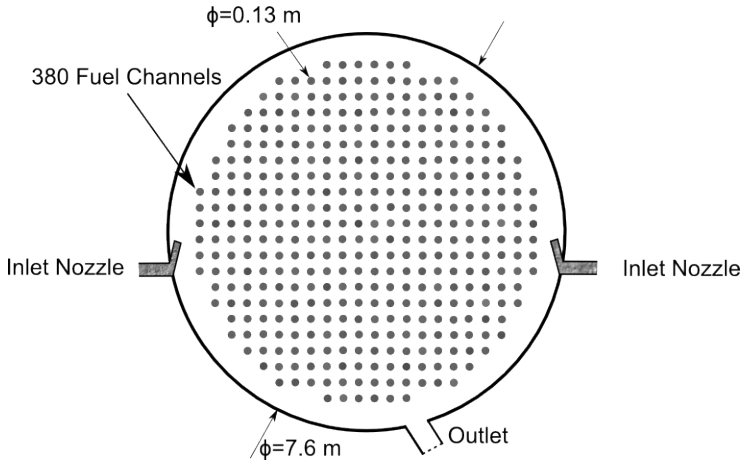

Figure 4.2 Cross-sectional view of the calandria vessel of a CANDU- 6 nuclear power reactor.

A 2D hybrid mesh made of triangles and quadrangles composed of 3.5×10^6 cells was generated using Gambit and Icem-CFD commercial softwares. The topologies of the meshes around the tubes and the injectors are shown in Fig. 4.3. The number of cells required to perform the simulations was selected based on a convergence study which is discussed in the following section. The calandria tubes, the shell and the injectors were represented by wall boundary conditions. The inlet flow velocity and the outlet of the calandria constitute two additional boundary conditions. In particular, uniform velocity distributions were imposed as outlet nozzle conditions. Afterwards, the number of discretization cells in these regions allow the appropriate jet profile to be estimated [68]. Furthermore, it was assumed that about 5% of the thermal power generated in the pressure tubes is deposited into the moderator due to neutrons slowing down. To this purpose, we have used the average channel power given in [69] and reproduced in Fig. 4.4 ; note that this profile is, for instance, more realistic than the one used by Sarchami [12]. These values were imported into the domain as imposed averaged surface-boundary conditions.

4.5 Numerical grid sensivity study

The estimation of the errors due to the discretization and the validity of the numerical results are discussed in this section. To this purpose, three computational meshes made of 0.875×10^6, 3.5×10^6 and 12×10^6 cells were generated using the same grid stretching ratio for both x and y directions. The discretization errors were then evaluated using the Richardson extrapolation method [70] as recommended by ASME standards [71]. By employing the values obtained from coarser grids, this method estimates the asymptotic value when the cell's grid size becomes relatively small. Hence, the following equation was used to determine

Table 4.1 Characteristic information of a CANDU-6 vessel.

Item	Value
Number of fuel channels	380
Input heat to the moderator [MW]	103
Calandria tube diameter [m]	0.131
Gap between channels [m]	0.286
Diameter of vessel [m]	7.6
Length of vessel [m]	5.9
Flow rate per nozzle [L/s]	117.5
Number of nozzle	8
Number of outlet	2
Inlet temprature [°C]	43

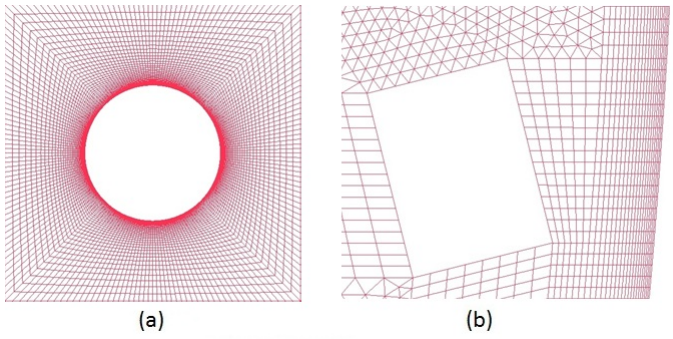

Figure 4.3 Grid topology around ; a) calandria tubes b) water injectors.

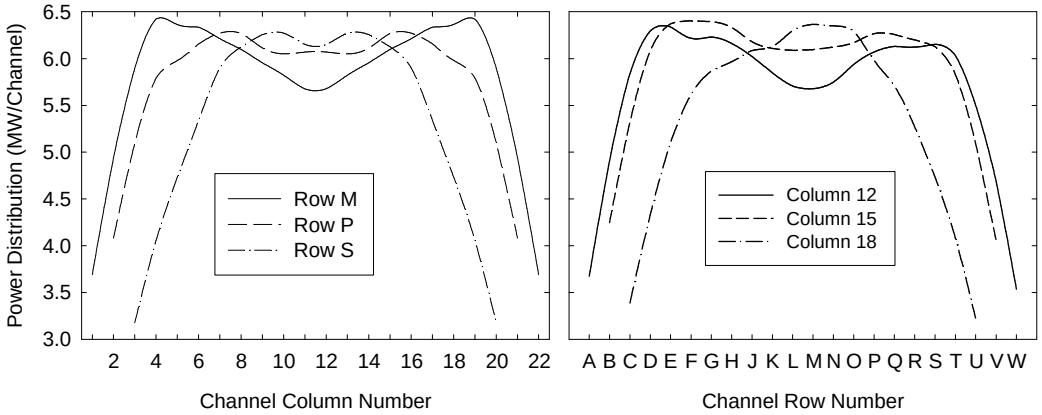

Figure 4.4 Typical averaged channel thermal power [69].

the extrapolated results :

$$f_{\text{exact}} = f_1 + \frac{(f_1 - f_2)}{r^{\zeta} - 1} \tag{4.8}$$

Where the order of convergence ζ is calculated using :

$$\begin{aligned} \zeta &= \frac{\left|\ln\left|\frac{f_3 - f_2}{f_2 - f_1}\right| + q(\zeta)\right|}{\ln(r_{21})} \\ q(\zeta) &= \ln\left[\frac{r_{21}^{\zeta} - s}{r_{32}^{\zeta} - s}\right] \\ s &= \text{sign}\left[\frac{f_3 - f_2}{f_2 - f_1}\right] \end{aligned} \tag{4.9}$$

Where r is a grid refinement factor ($r = h_{\text{coarse}}/h_{\text{fine}}$) as h defines the grid size of a representative cell in the domain $r_{ij} = r_i - r_j$. In the current study, the average velocity along a reference plane at 60° with respect to the horizontal plane was calculated for different grid sizes ($f_1, f_2, ...$) and equations (4.8) and (4.9) were solved iteratively. Finally, the (Grid Convergence Index) GCI, that provides an error estimation interval of the numerical results is calculated according to :

$$\text{GCI}_{21} = \frac{1.25|f_2 - f_1|}{|f_1|(r_{21}^{\zeta} - 1)} \tag{4.10}$$

For two computational meshes of 3.5×10^6 and 12×10^6, the GCI was lower than 5% and so we have considered the first one as an acceptable value for the present simulations. It is important to remark that this simple calculation indicates that 2D simulations of a full-size CANDU-6 nuclear reactor require at least 3.5×10^6 discretization cells as observed in our previous study [65].

4.5.1 Validation of Code_Saturne with experimental data

The objective of this section is to validate the capability of Code_Saturne to predict complex circulation flows. To this purpose, it was applied to predict the experimental data collected by Paul [72] and Paul et al. [7] using the horizontal bundle of staggered tubes schematically shown Fig. 4.5. In addition, the predictions of Code_Saturne were also compared with similar ones obtained by using the CFD software Ansys-Fluent [73]. The numerical platform applied to carry out these simulations (*i.e.* the gird size and topology, flow conditions, turbulence model, solver algorithm, etc.) were those discussed above, which have been considered as optimal in a previous work [65]. The results of these simulations are compared with the data

in Fig. 4.6.

This figure shows that both software's produce similar outcomes ; their results follow the experimental trends quite well. Nevertheless, Code_Saturne seems to better predict the overall flow behavior. In fact, close to the wall of the channel, it is able to catch the flow recirculation as indicated by the experimental data (for instance, see Fig. 4.6 (a) and Fig. 4.6 (c) for y/d close to 4). Moreover, the Fig. 4.6 (b) and Fig. 4.6 (d) also show that Code_Saturne reproduces the experimental observation within the high velocity regions as well. Consequently, the comparison of the predictions with the data confirms the robustness of the Code_Saturne to reproduce a flow behavior similar to the one that can be encountered for the circulation of the moderator across the calandria tubes. Beside this validation, the fact that this is an open-source software permited us to easily implement all the functions required to calculate the thermophysical properties of the water.

4.6 Moderator flow configurations in CANDU-6 nuclear reactors

According to previous numerical and experimental studies, three kinds of flow configurations seem to occur in the calandria vessel. As shown in Fig. 4.7, they correspond to *momentum-dominated*, *mixed* and *buoyancy-dominated* flow patterns. It is obvious that the generation of heat, *i.e.* the volumetric heat distribution and the heat transfer from the calandria tubes, may trigger transitions amongst these configurations. For isothermal flows (*i.e.* under the absence of buoyancy effects), Fig. 4.7(a) shows that inertia forces dominate. This configuration is characterized by a flow-stagnation point (*i.e.* the impingement point of the flow jets) due to the mutual interaction of the two jets. In this particular case, the given point is located at 90° with respect to the horizontal plane. However, the addition of heat provokes a flow asymmetry and therefore the location of the stagnation point shifts to one side of the calandria. This

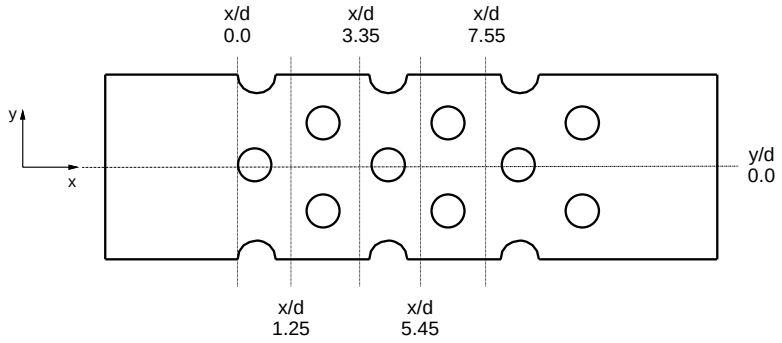

Figure 4.5 Experimental set-up and positions of the measurement planes given in : Paul [72] and Paul et al. [7].

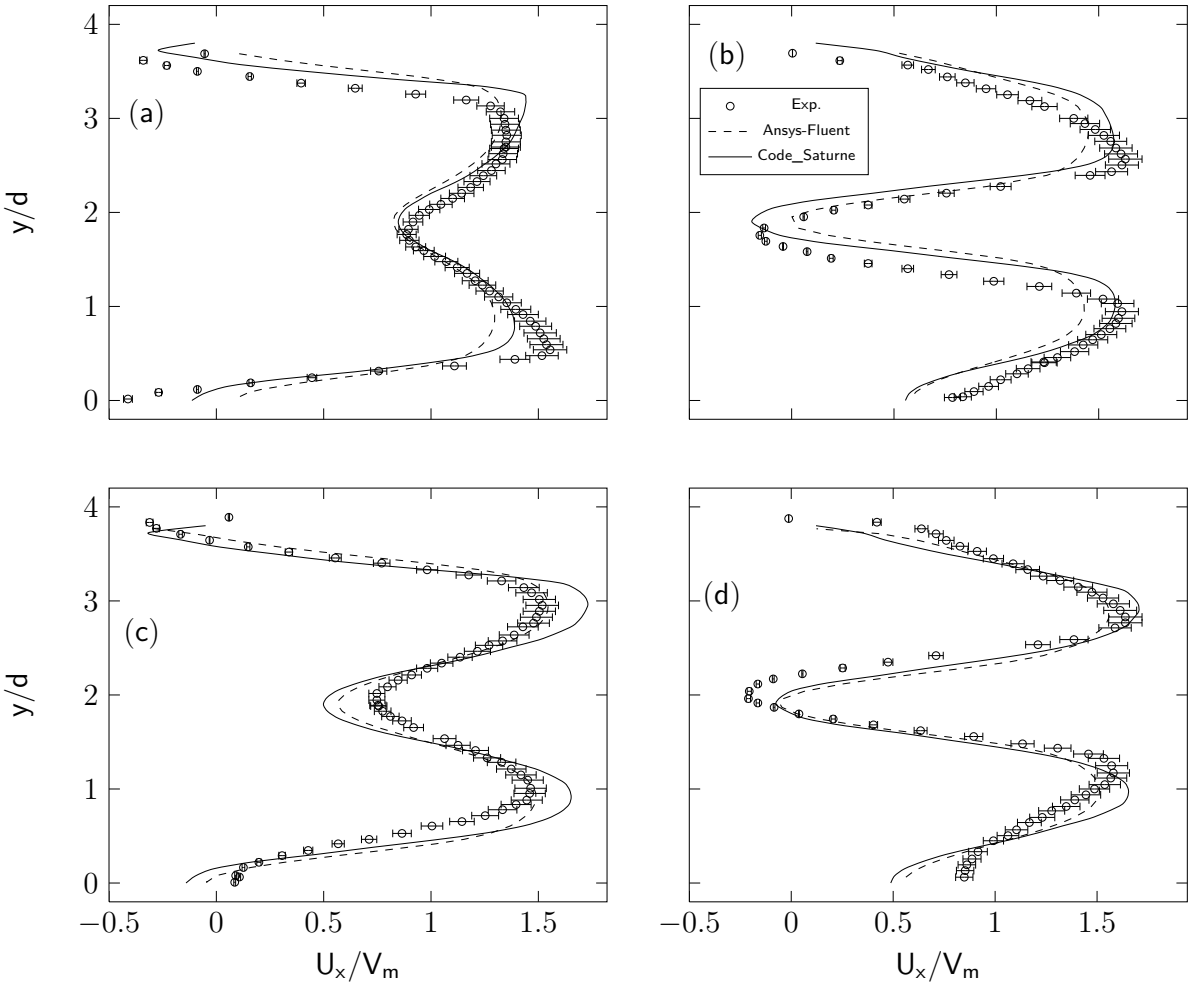

Figure 4.6 Comparasion of simulated lateral velocity profile with data of Paul et al. [7, 74]; a) $x/d = 1.25$, b) $x/d = 3.35$, c) $x/d = 5.45$ and d) $x/d = 7.55$.

behavior is mainly due to the competition between inertia and buoyancy forces, as shown in Fig. 4.7(b). Increasing the amount of heat brings about important mass density gradients which in turn triggers a secondary counter-flow motion that drives the hotter fluid towards the top of the vessel. Hence, a significant buoyancy-induced flow prevents the occurrence of a stagnation point in the upper region of the calandria, as it is schematically shown in Fig. 4.7(c). It is obvious that the buoyancy-dominated configuration should produce the highest temperature difference across the moderator. From a nuclear-safety standpoint, high moderator temperatures may lead to the local formation of steam which in turn may cause the external wall of the calandria tubes to dry-out. Such a situation can produce excessive local wall-temperature excursions which can affect the mechanical integrity of these tubes.

4.6.1 Moderator flow simulations

This section discusses the results obtained from Code_Saturne numerical simulations performed using a Richardson number ranging from $\mathrm{Ri} = 0$ to $\mathrm{Ri} = 0.35$. The entire set of simulations was carried out by applying the radial power distribution proposed by Rozon [69] for nominal operating conditions of a typical CANDU-6 nuclear reactor, *i.e.* a total power of 103 MW within the moderator (see Fig. 4.4). To perform 2D calculations, the time and bundle-averaged thermal power were normalized along the axial length of two bundles (*i.e.* about 1 m). To cover the proposed range of Richardson's number, the inlet water velocity per nozzle was varied from 1.5 m/s to 9.1 m/s. Therewith, it is important to mention that the nominal value of this velocity is about 2 m/s [29].

Instead of presenting the velocity and temperature fields in a continuous color map and in order to provide a clear explanation of the phenomena at hand, the components of the velocity and the temperature were sampled along six reference planes. These planes were arbitrarily selected and intersect the calandria vessel in half and in quarter sections along both horizontal and vertical directions (*i.e.* $x = -1.43,\ 0,\ +1.43\,\mathrm{m}$ and $y = -1.43,\ 0,\ +1.43\,\mathrm{m}$). Furthermore, to clearly show the effect the ratio between the thermal power and volumetric flow rate has on the temperature distribution, data was collected from simulations performed by applying three different values of the Richardson number 0.008, 0.07 and 0.23.

Fig. 4.8 shows the results obtained for a Richardson number equal to 0.008. The vertical velocity components are positive and stronger at the proximity of the calandria's wall (see Fig. 4.8(a)). Moreover, these components are very small and become much more uniform towards the center of the vessel. The relatively low fluctuations observed in the figure are caused by the wakes generated behind the calandria tubes. Also, as shown in Fig. 4.8(b), the vertical velocity components become negative close to the outlet. Furthermore, for this value of Richardson's number, the lateral velocity components shown in Fig. 4.8(c) and 4.8(d)

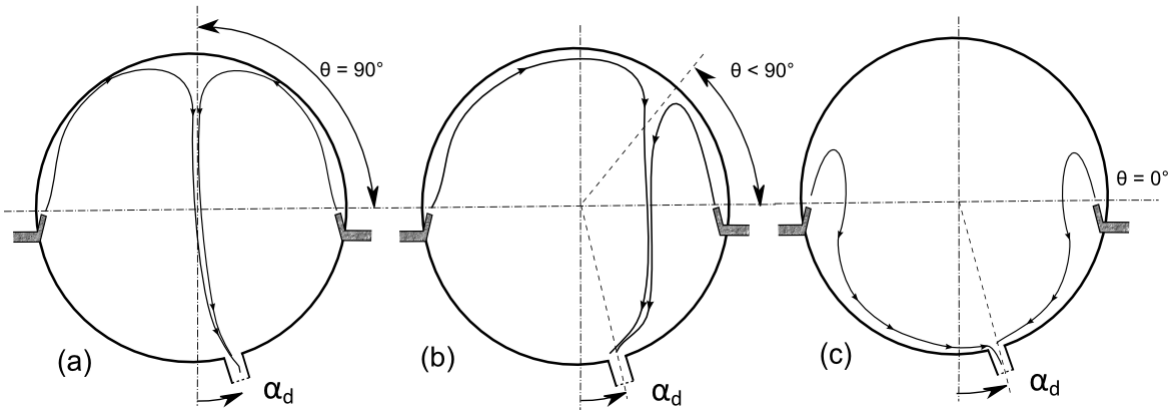

Figure 4.7 Expected moderator flow configurations. a) Momentum-dominated b) Mixed-type c) Buoyancy-dominated.

indicate that the flow configuration is similar to that of Fig. 4.7(a), *i.e.* it is dominated by inertia. In fact, their values are relatively important and positive on the left side of the calandria, while the opposite occurs on the right side. In particular, along the y direction, the strong flow reversal indicates the presence of a stagnation or impingement point near the mid-plane of the vessel (*i.e.* at 90° with respect to the horizontal mid-plane, $y > +2.5$ m). From a thermal perspective, Fig. 4.8(e) indicates a near-uniform radial temperature distribution on the upper regions of the vessel, with the highest values taking place at the bottom and towards the periphery of the calandria. The asymmetry with respect to the vertical mid-plane (*i.e.* the difference between the temperatures for $x = \pm 1.43$ m as well as for $y = \pm 1.43$ m) is made possible by the effect of the off-center position of the flow discharge (see Fig. 4.2). It is interesting to remark the consequence that the descending jets have on the flow temperature at the center of the calandria where, in general, the neutron flux peaks. The data points in the y direction confirm the aforementioned temperature trends, *i.e.* for this flow configuration the temperatures are higher at the bottom than at the top of the vessel.

Fig. 4.9 shows the results obtained for a Richardson number Ri $= 0.07$. The maximum values of the vertical velocity components occurring close to the wall of the calandria (*i.e.* for $y > 0$ m) decrease with increasing values of Richardson's number (*e.g.* compare Fig. 4.8(a) with Fig. 4.9(a)). Furthermore, the flow fluctuations due to the wakes are more important on the right side of the vessel. In the vertical direction (Fig. 4.8(b)), these velocity components generally become more uniform. Also, even though the lateral components along the x axis follow a similar behavior than those explored in the previous case (*i.e.* Ri $= 0.008$), the intensity is reduced by 50%. In turn, the lateral velocity components indicate the presence of a flow reversal region (Fig. 4.9(c)) ; this flow behavior is more apparent in the y

direction. In fact, within the upper-most portion of the vessel, a remarkable flow reversal occurs (compare Fig. 4.9(d) with Fig. 4.8(d) for $y = +1.43$). This provides an indication that the impingement point of the two jets has shifted to the right, generating a large recirculation zone on the left-side region of the calandria. In this zone, the flow is clearly affected by the presence of calandria tubes (note the periodic local velocity fluctuations). Thus, for $\mathrm{Ri} = 0.07$, the overall trends of the sampled velocity components follow a behavior similar to the flow distribution schematized in Fig. 4.7(b). It is obvious that, for this particular value of the Richardson number, the observed flow seems to represent a mixed configuration. From a thermal standpoint, this flow distribution increases the moderator temperature at the upper region and on the left side of the calandria as shown on Fig. 4.9(e) and 4.9(f). Even though for the present case these temperatures are far away from saturation (the maximum temperature difference is about 20 K and the moderator pressure is slightly higher than that of the atmosphere) they tend to reduce the mass density of the heavy water which in turn can affect the reactor's reactivity. It is obvious that studying the effect that these temperature variations have on the entire reactor core behavior necessitates neutronic-thermal-hydraulic coupled calculations.

Increasing the Richardson number from 0.09 (not shown in these figures) to 0.35 restores almost completely the symmetry on the vertical components of the velocity (see Fig. 4.10(a)). In fact, along the y direction they are very uniform (Fig. 4.10(b)). They become slightly negative towards the bottom of the calandria, which corresponds to the effect induced by the angular position of the discharge. A similar symmetry characterizes the lateral velocity components (Fig. 4.10(c) and 4.10(d)). It is important to note the lack of an impingement point caused by the negligible values of these components at the upper portion of the vessel (Fig. 4.10(d)). Nevertheless, the former figure also shows the flow reversal imposed by the asymmetric location of the outlet. It is apparent that the flow distribution shown in Fig. 4.10 follows the pattern schematically illustrated in Fig. 4.7(c). Hence, for a Richardson number higher than 0.09, the flow distribution evolves from mixed to buoyancy-dominated. To this aim, it is important to observe the effect of the velocity distribution on the temperature profiles ; the moderator becomes significantly hotter almost everywhere along the center of the calandria (Fig. 4.10(e)). In fact, for all sampled radial positions the moderator temperature increases almost linearly in the y direction with a maximum temperature difference of about 28 K (*i.e.* the flow becomes thermally stratified). It is obvious that this flow configuration can be critical because it can bring about boiling or dry out conditions of the moderator around the external walls of the upper calandria tubes. In addition, just like it is the case for the mixed-flow configuration, the change in the temperature could certainly affect the reactor's reactivity coefficient.

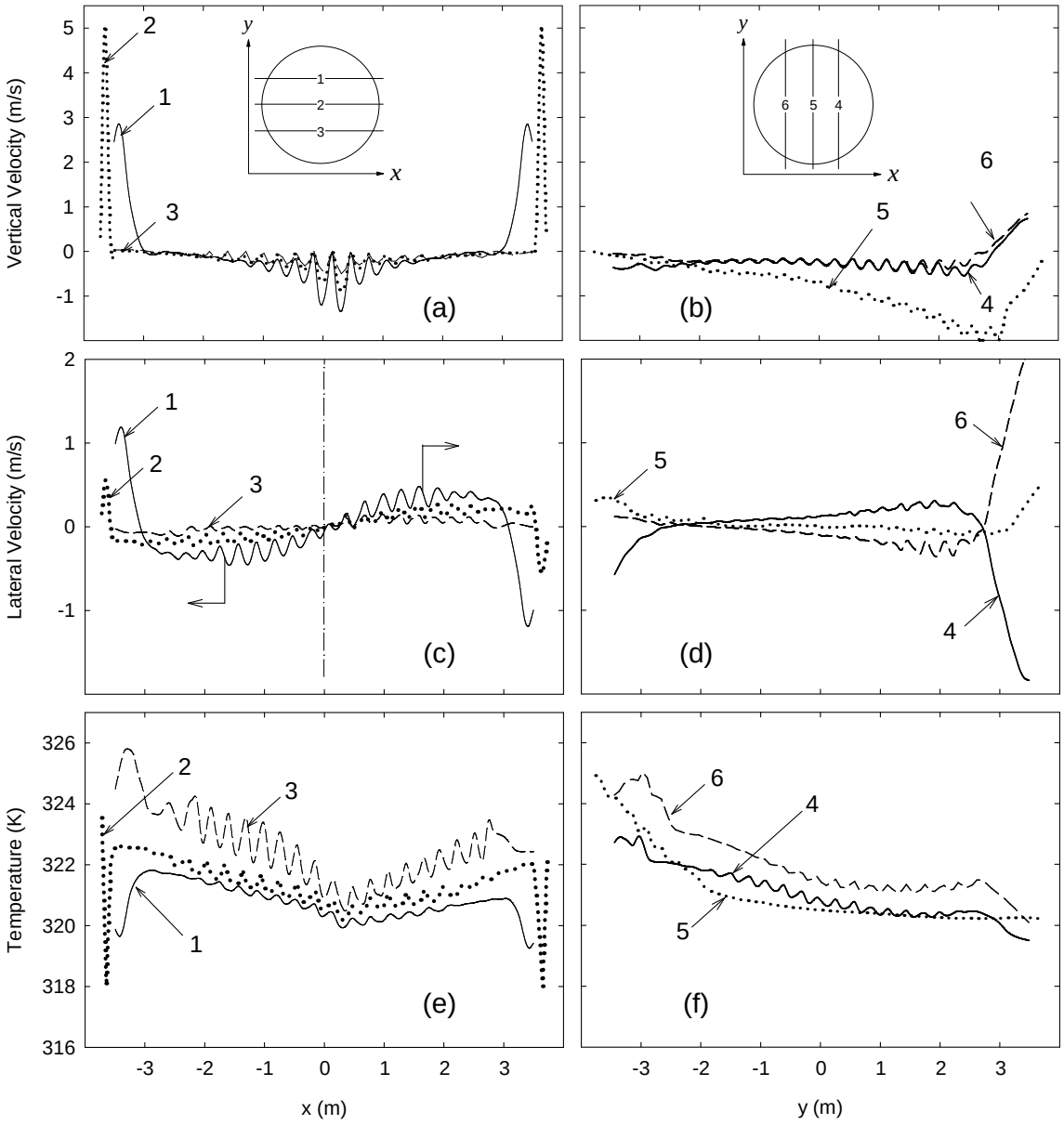

Figure 4.8 Sampled values for the inertia-dominated configuration (Ri=0.008). 1 : $y = +1.43$ m, 2 : $y = 0$ m, 3 : $y =$ -1.43 m. 4 : $x = +1.43$ m, 5 : $x = 0$ m, 6 : $x =$ -1.43 m.

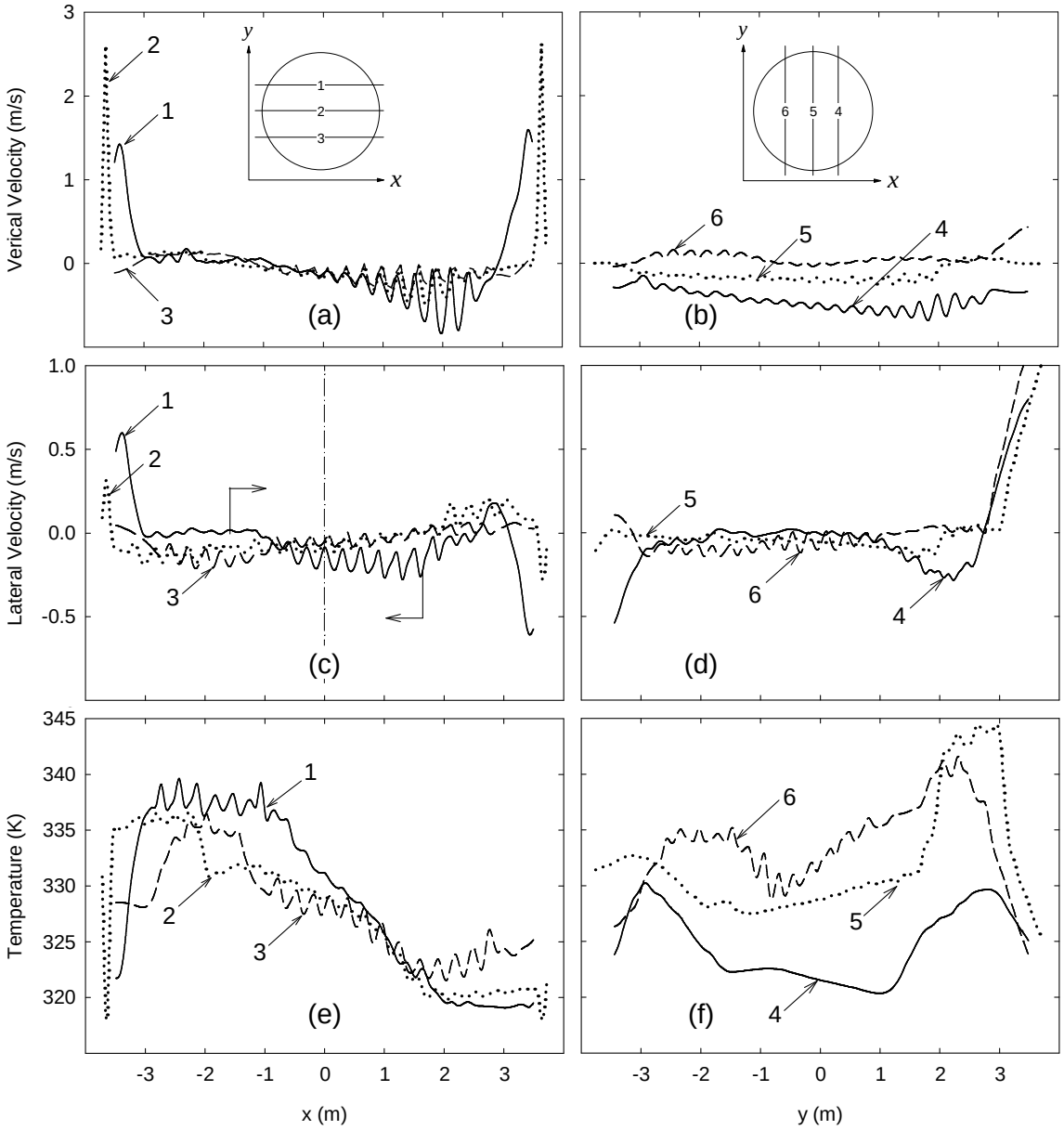

Figure 4.9 Sampled values for mixed-type configuration (Ri=0.07). 1 : $y = +1.43$ m, 2 : $y = 0$ m, 3 : $y =$-1.43 m. 4 : $x = +1.43$ m, 5 : $x = 0$ m, 6 : $x =$-1.43 m.

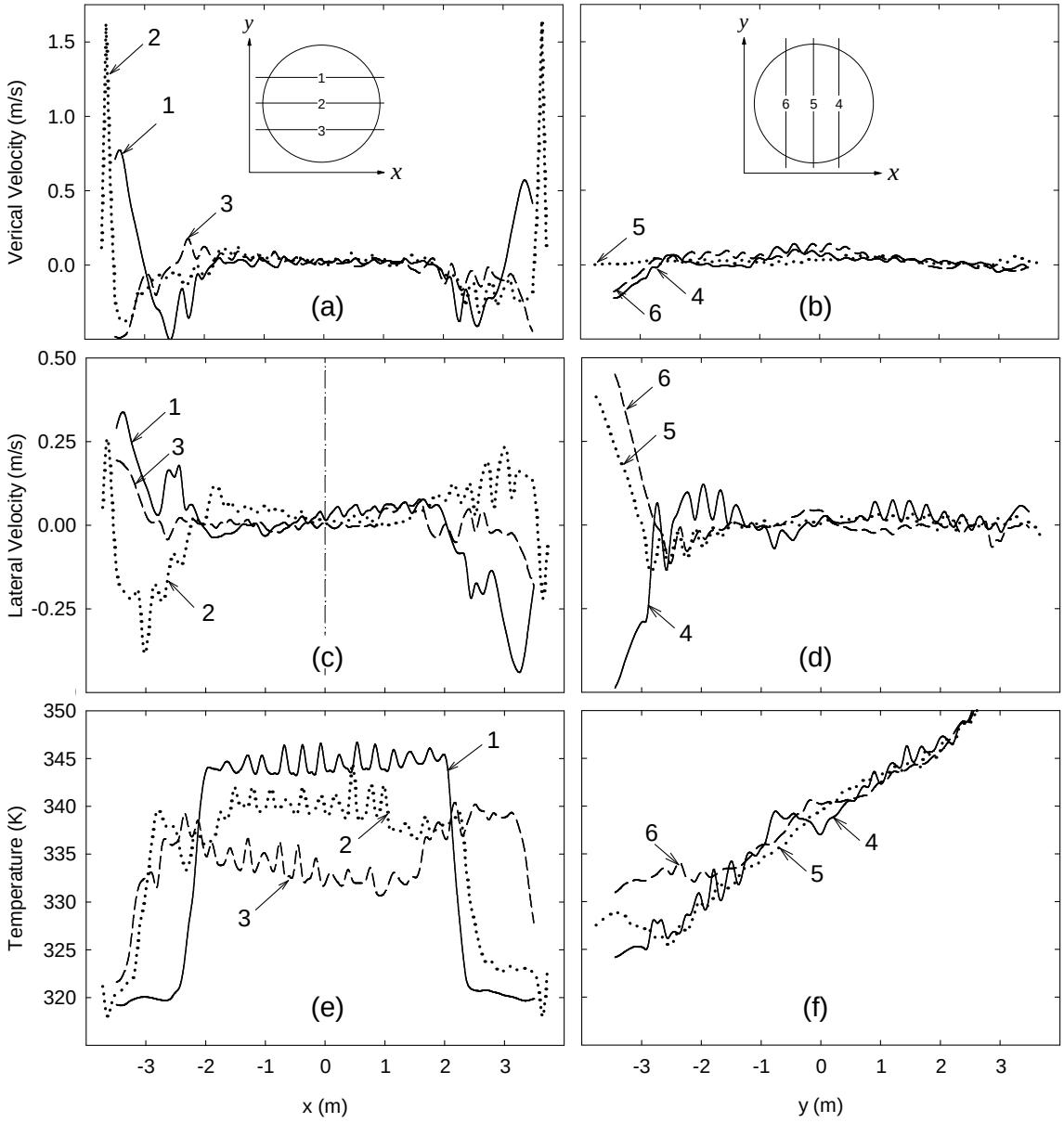

Figure 4.10 Sampled values for buoyancy-dominated configuration (Ri=0.23). 1 : $y = +1.43$ m, 2 : $y = 0$ m, 3 : $y =$ -1.43 m. 4 : $x = +1.43$ m, 5 : $x = 0$ m, 6 : $x =$ -1.43 m.

Even though the present results are similar to those given by Carlucci and Cheung [11], a qualitative comparison of the velocity vectors (predicted by MODTURC [11] and Code_Saturne for Ri $=$ 0.05 and illustrated in the Fig. (4.11), shows some differences. The flow skewness are very similar and both calculations indicate the presence of two recirculation zones (Fig. 4.11(a)). However, the extent of the flow structures given by Code_Saturne seems to be smaller than those predicted by MODTURC (Fig. 4.11(b)). In addition, MODTURC also predicts a strong recirculation at the center of the vessel. This gives the impression that it corresponds to an incorrect numerical result which does not appear in our simulations (Fig. 4.11(a)). It must be pointed out that this singularity has also been discussed by other authors [56]. For these reasons, it is difficult to accept the legitimacy of the temperature distribution given in [11] for which, towards the center region of the calandria, cold fluid streams seems to shift upward.

4.7 Cartographical representation of the moderator flow

Carlucci and Cheung [11] characterized the flow as a function of the variation of an angle with respect to a horizontal median plane where *"the near-wall circumferential velocity of the jet becomes negative"*. They have correlated this angle using a wrong definition of the Archimedes number ; identified in the present work with the Richardson number (see Section 4.2). Carlucci and Cheung conducted several 2D numerical simulations for a half-plane (*i.e.* a free-slip wall boundary condition applied at the calandria's vertical mid-plane) and for the full-plane of a typical calandria vessel. They established that the flow is fully dominated by inertia when the angle is equal to 90°. Within the range of $0.125 < \mathrm{Ri} < 0.275$ and for half-plane simulations, they observed that depending on the initial flow conditions, the flow may present either buoyancy-dominant or inertia-dominant behaviors. Instead, in the 2D full-plane simulations for which the flow patterns were systematically not symmetrical about the vertical mid-plane, the reversal angle was defined as the average of the angles formed by the two jets. Therefore they represented these conditions by a series of data points at 90° as shown in Fig. 4.12(a). For $\mathrm{Ri} > 0.125$, they observed that the flow adopts a buoyancy-dominated configuration independent of the initial flow conditions. However, for the half-plane cases, the inertia effect seems to control the configuration only if the flow is initially dominated by inertia. These results are presented in the Fig. 4.12(a) by an angle of 90° for inertia-controlled cases and by smaller angles for the buoyancy cases. Carlucci and Cheung have argued that the principal reasons for these two contradictory results are merely due to the effect of using free-slip wall boundary conditions along the vertical mid-plane.

Similar studies performed by Yoon et al. [19], Kim et al. [24], Sarchami et al. [59] and Kim and Rhee [25] have shown that for the nominal value of the inlet flow velocity, the

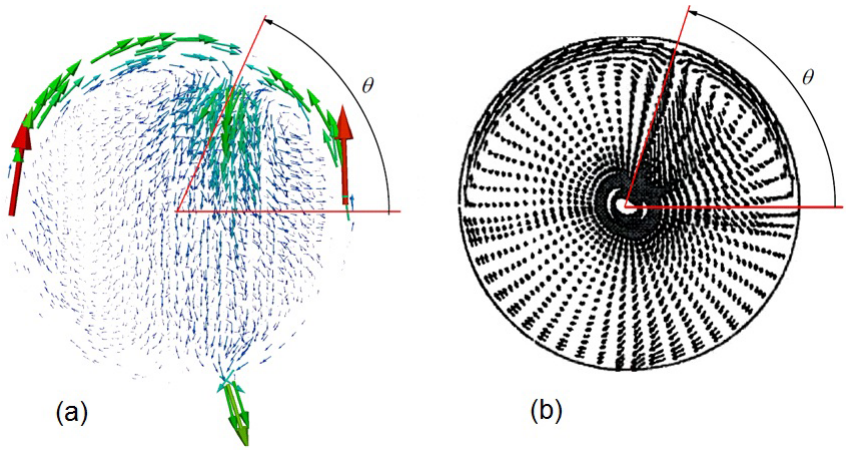

Figure 4.11 A qualitative comparison of velocity vectors for Ri=0.05 ; a) predicted by Code_Saturne, b) predicted by MODTURC [11].

moderator follows a mixed-type configuration similar to the ones schematically shown in Fig. 4.7(b). Nevertheless, it must be pointed out that Kim et al. [24], and Kim and Rhee [25] performed their simulations by assuming twice the nominal CANDU-6 inlet flow velocity, while Sarchami [12] used a thermal power distribution corresponding to 50% of the nominal power and strongly depleted at the center of the reactor core, which does not correspond to a real case [69].

Up to now, there is a huge discrepancy associated not only to the methodology used but also to the numerical predictions of the moderator flow in CANDU-6 nuclear reactors. Therefore, in order to analyze our calculation data, the following paragraphs will present a cartographical representation similar to the one proposed by Carlucci and Cheung. Nonetheless, instead of using the near-wall velocity reversal proposed by these authors, we have determined the location of the impingement point between the two jets (when present in the simulations) by examining the local behavior of the components of the flow velocity vectors. In fact, while the determination of the reversal of the near-wall velocity can be obtained from simulations performed using a porous medium approach, it was nearly impossible to be achieved for the entire set of simulations carried out in the present work. In fact, Code_Saturne provides the fine structure of the flow which is strongly affected by the presence of the external walls of the calandria tubes. The important fluctuations induced by these tubes make it very difficult to establish, without ambiguity, a unique criterion based on the reversal of the circumferential velocity as suggested by Carlucci and Cheung. Thus, it becomes clear that this is only possible when the effects of the tubes are treated using a distributed flow resistance correlation (*i.e.* the porous medium approach). Furthermore, to cover a wide range of Richardson numbers

($0 \leq \text{Ri} < 0.35$), we performed more than a dozen 2D full-plane steady-state numerical simulations using Code_Saturne and the discretization scheme discussed in Section 4.4.
The Fig. 4.12(b) shows the estimated location of the impingement point of the two jets. For Richardson numbers below 0.125, Carlucci and Cheung [11] predicted that the flow is always asymmetric and tilted (skewed) to either sides of the calandria with an average value equal to 90°. They argued that the degree of skewness decreases with a decreasing value of the Richardson number. They noted that this tilt vanishes only when Ri tends to zero. In turn, within the same range of Richardson numbers, our simulations show a lower threshold above which the beginning of the skewness occurs (see Fig. 4.12(b)). In fact, only for Richardson numbers below 0.04 does the flow always becomes symmetric without any shift of the impingement point. It is quite possible that Carlucci and Cheung did not perform simulations for $0 < \text{Ri} < 0.04$. Indeed, only when the buoyancy forces start competing with the inertia, a flow asymmetry should take place and the flow starts developing a mixed-type configuration. Moreover, for this type of configuration, we do not have enough arguments that could confirm the equiprobable skewness of the flow with respect to the vertical mid-plane since the present results concern steady-state calculations. Thus, we judge that for steady state calculations the preferential tilting angle should be conditioned by the asymmetrical location of the discharge. In fact, there are no apparent physical reasons that could permit one to conclude that repeating the same calculations under the same flow conditions would lead to a switch in the flow from one side to the other of the calandria vessel. Our results also show that the mixed configuration is divided into two distinct recirculation zones of different extent. In particular, in the largest region, the flow is driven by buoyancy forces with an upward flow in the smallest zone, the downward flow is driven by inertia forces. It is obvious that this configuration generates an important non-uniform temperature distribution, which from a nuclear safety standpoint can be of major concern. In fact, the shift of the flow to either side of the vessel's mid-plane should affect the moderator recirculation rate and consequently the amount of heat that each particle constituting the fluid can remove from the calandria. This is an important aspect that should be considered for scaling down the real calandria vessel, which seems to be impossible without changing not only the geometry and the thermal power but also the properties of the working fluid (*i.e.* to achieve equivalent fluid recirculation rates). Furthermore, heat transfer conditions across calandria tubes are also strongly influenced by the flow distribution which can trigger excessive fluid temperature differences across the moderator.
For the range of Richardson numbers $0.04 < \text{Ri} < 0.09$, the simulations performed with Code_Saturne are generally, in agreement with the map proposed by Carlucci and Cheung [11]. Nevertheless, for $0.1 < \text{Ri} < 0.275$, the flow patterns do not exhibit the bifurcation ob-

served by Carlucci and Cheung. In fact, for a half-plane domain with free-slip wall conditions applied at the vertical mid-plane and depending on the initial flow conditions, Carlucci and Cheung have observed that either inertia- or buoyancy-dominated flow configurations can occur. However, they have not observed such a bifurcation for their full-plane calculations (see Fig. 4.12(a)). Within the same range of Richardson numbers, our simulations indicate the existence of only a buoyancy dominant configuration which starts at a Richardson number lower than the one observed by Carlucci and Cheung (see Fig. 4.12(b)). Between the mixed and buoyancy configurations, a flow-transition region appears and therefore the angular location of the impingement point cannot be obtained from steady-state calculations. After this region, the flow becomes completely thermally stratified and the physical definition of such an angle seems to be meaningful. These results give the impression that the use of a mid-plane symmetrical boundary is not appropriate for studying such a complex flow behavior (which is very sensitive against the thermal power to the flow velocity ratio). Furthermore, for the buoyancy-dominated region, the temperature of the moderator in the vicinity of the upper calandria tubes is much higher than the overall average fluid temperature. Although in the present simulations this temperature does not reach boiling conditions, it should be considered for further nuclear safety analyses. Notwithstanding possible local boiling flow conditions, the higher the fluid temperature is the lower the water's mass density becomes. Such an effect may also influence the macroscopic nuclear cross-section of the heavy water and thus perturb the local density distribution of thermal neutrons.

4.7.1 Sensitivity analysis

According to the Eq. (4.1), the correct estimation of the transitions between different flow configurations depends on the ratio of the thermal power to the inlet flow velocity. Therefore, the determination of the moderator flow configuration at nominal operating conditions should be obtained by applying the appropriate figures of these two key variables. Nevertheless, there exist huge discrepancies amongst the nominal value of the inlet flow velocity applied to the numerical simulations presented in the literature. In most cases, the authors argue that this velocity is almost twice the value proposed by AECL in the CANDU-6 design manual [29] and/or the geometry of the nozzles does not have the correct dimensions. Consequently, we have examined the sensitivity of CANDU-6 moderator system to the variations of the inlet water flow rate and this, by maintaining the same thermal power distribution. From a simple energy balance and for the same overall temperature difference, the thermal power removed from the moderator varies linearly with the flow velocity. Therefore, the inlet flow rate affects Eq. (4.1) and in turn the configuration of the flow. To determine this effect, we have considered a constant inlet flow rate ($= \rho_i V_i A_i$) and we have increased the inlet

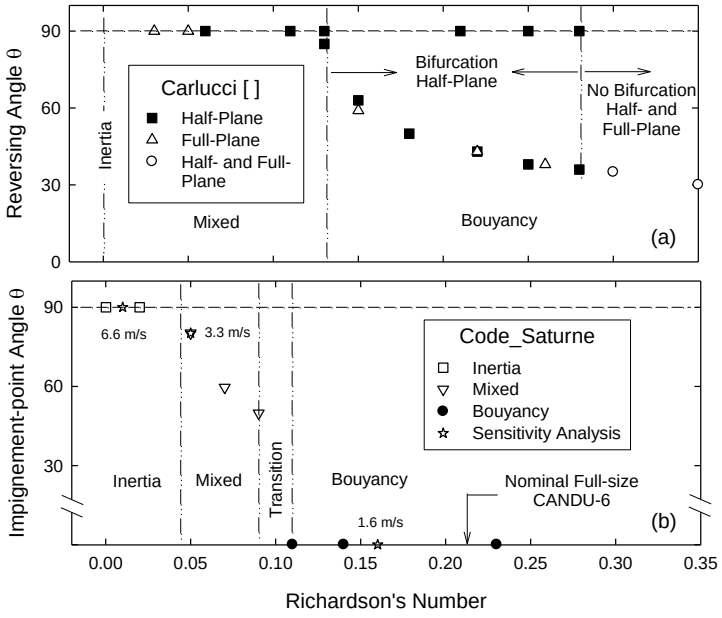

Figure 4.12 Moderator flow configuration map. a) Proposed by Carlucci and Cheung [11]. b) Present work using Code_Saturne.

flow velocity by changing the cross-sectional area of the nozzles; the results are shown by $\star$ in the Fig. 4.12(b). By changing sequentially the inlet flow velocity by a factor of 2, the configuration shifts from inertia-dominated to mixed and then to buoyancy-dominated. Thus, it is very clear that there exists a discrepancy between the results given in the literature and those predicted by Code_Saturne. Consequently, in order to correctly estimate the behavior of the moderator flow, it is mandatory to apply the thermal-hydraulic values given in the CANDU-6 design manual [3, 29].

4.8 Conclusion

In general, the open literature shows huge discrepancies amongst the methods and conditions used for simulating the moderator flow in CANDU nuclear reactors. For instance, most researchers have made an inappropriate use of Boussinesq's approximation and/or have oversimplified the implemented numerical models by reducing the number of discretization elements. Furthermore, in some cited works, neither the nominal thermal power distribution nor the inlet water velocities seem to be correctly addressed, these are some of the reasons that motivated the work presented in this paper. To this purpose, the numerical simulations of full-plane and full-scale moderator flows in a CANDU-6 nuclear power reactor have been presented. The calculations were carried out using an open-source nuclear thermal-hydraulic code (Code_Saturne [1]). Before performing the simulations, a rigorous analysis of common

approximations encountered in the open literature was performed. It has been determined that Boussinesq's approximation should not be used for these types of numerical simulations. Furthermore, a convergence study has shown that this type of 2D calculation requires at least 3.5×10^6 cells in order to guarantee a satisfactory numerical convergence.

The simulations presented in this paper confirm the existence of three moderator flow configurations : inertia-controlled, mixed and buoyancy-controlled. In fact, the transitions between these states are functions of the ratio between the thermal power and the inlet flow velocity. In particular, we observed that both the mixed and buoyancy-controlled configurations can trigger high moderator temperature differences and therefore are of concern for nuclear safety analyses pertaining to this type of nuclear reactor. In fact excessive fluid temperature differences across the moderator can provoke local fluid mass density changes, boiling and eventual wall dry out conditions which in turn may affect the mechanical integrity of the calandria tubes and the reactor‘s reactivity coefficient.

To better analyze the flow behavior, the components of the simulated flow velocities as well as the fluid temperature were sampled at strategic locations inside the moderator. The behavior of both the velocity and temperature profiles collected along the x and y axes for different values of the Richardson (Ri) number, confirms the existence of the aforementioned three configurations. Afterwards, these flow configurations were compared with those proposed by Carlucci [15] and Carlucci and Cheung [11] based on the analysis of the predictions given by a porosity medium model. We have presented the data in a cartographical representation similar to the one proposed by Carlucci. Nevertheless, due to a more detailed flow structure generated by Code_Saturne, instead of determining the point where the reversal of the circumferential velocity occurs (as suggested by Carlucci) we have correlated the position of two jet impingement point as a function of the Richardson number. Even though the configurations presented in this paper are similar to those suggested among others by Carlucci [15], Carlucci and Cheung [11], Kim et al. [24], we must point out the following relevant aspects :

– Only for $\mathrm{Ri} < 0.04$ does the flow seem to be controlled by the inertia. In fact, under these conditions, the differences in the fluid mass density are not high enough to counterbalance the inertia forces.
– For $0.04 < \mathrm{Ri} < 0.09$ the flow is submitted to a competition between inertia and buoyancy forces ; thus, the configuration becomes mixed. Under these conditions the flow distribution starts switching to one side of the calandria, bringing about important temperature differences across the moderator. Nevertheless, our calculations cannot confirm the existence of a symmetric flow tilting about the vertical mid-plane as suggested by Carlucci and Carlucci and Cheung.

– For $0.09 < \mathrm{Ri} < 0.12$ there is a transition region that cannot be analyzed from steady-state calculations. In fact, to elucidate the effect of buoyancy on the flow distribution and due to the large dimensions of the calandria, long periods of real-time transient simulations should be performed.
– For $\mathrm{Ri} > 0.12$ the buoyancy forces happen to be dominant and therefore the flow becomes thermally stratified and the determination of the impingement point becomes meaningful. This configuration produces the highest temperature difference across the moderator ; hence, it must be considered for further nuclear safety analyses. In this region, we have not obtained the bifurcation as cited in the work given by [11] for 2D half-plane simulations. We can thus confirm that imposing symmetrical boundary conditions at the calandria's vertical mid-plane is not appropriate for this kind of flow calculation.
– A sensitivity analysis has shown that the configuration of the moderator depends strongly on the ratio between the thermal power and the inlet water velocity. In particular, for a full CANDU-6 operating at the nominal inlet heavy water velocity of 2 m/s, we have shown that the moderator is completely controlled by buoyancy.

However, the transition between different flow configurations as well as the existence of possible moderator flow oscillations necessitates long real-time transient flow simulations coupled to time-dependent thermal power distributions. To this aim, the CFD calculations should be coupled with reactor physics codes in order to model the spatial variations of the thermal neutron fluxes as a function of the local moderator temperatures.

Acknowledgments

The authors would like to thank the Fonds de recherche du Québec-Nature et technologies (FRQNT B-2 PhD excellence research fellowship) for their financial support, Compute Canada for the allocation of computational resources and the development group of Code_Saturne at EDF for their technical assistances. We are very grateful to Professor Guy Marleau for his valuable suggestions. This work was funded by a discovery grant (RGPIN 41929) of the National Sciences and Engineering Research Council of Canada (NSERC).

CHAPITRE 5 ARTICLE 2 : 2-D CFD Time-dependent Thermal-hydraulic Simulations of CANDU-6 Moderator Flows

.

Authors : Foad Mehdi Zadeh, Stéphane Etienne and Alberto Teyssedou, submitted to Nuclear Engineering and Design.

5.1 abstract

The distribution of the fluid temperature and mass density of the moderator flow in CANDU-6 nuclear power reactors may affect the reactivity coefficient. For this reason, any possible moderator flow configuration and consequently the corresponding temperature distributions must be studied. In particular, the variations of the reactivity may result in major safety issues. For instance, excessive temperature excursions in the vicinity of the calandria tubes nearby local flow stagnation zones, may bring about partial boiling. To this aim, steady-state simulations have shown that for operating condition, intense buoyancy forces may be dominant, which can trigger a thermal stratification. Therefore, the numerical study of the time-dependent flow transition to such a condition, is of fundamental safety concern. Within this framework, this paper presents detailed time-dependent numerical simulations of CANDU-6 moderator flow for a wide range of flow conditions. To get a better insight of the thermal-hydraulic phenomena, the simulations were performed by covering long physical-time periods. The results show not only a region where the flow is characterized by coherent structures of flow fluctuations but also the existence of two limit cases where fluid oscillations disappear almost completely.

Keywords : CANDU-6, Moderator flow, Nuclear reactor thermohydraulics, CFD, Numerical simulations.

5.2 Introduction

Currently, CANDU nuclear power reactors are in operation in several countries. In particular, CANDU-6 reactors uses 0.5 m long fuel bundles formed by 37 pins which contain pellets of unenriched natural uranium. Twelve of these bundles are inserted within each of the 380 horizontal fuel channels (i.e. the pressure tubes). Each fuel channel is mechanically and thermally (coaxially) separated from the moderator by external shrouds, i.e. the calandria tubes. In order to minimize heat transfer from the coolant to the moderator, the gap between pressure and calandria tubes is filled with gas. The calandria tubes are considered as constituents of the calandria vessel which contains heavy water, i.e. the moderator,

at almost atmospheric pressure [54]. The scattering of neutrons by light deuterium nucleus permits an efficient thermalization to be achieved at very low absorption cost. Thus, the release of inelastic neutron collision energy is dissipated as a non-negligible amount of heat which has spatial and temporal distributions tightly correlated to the neutron flux prevailing in the reactor core. At normal operating conditions, the thermal energy dissipated in the moderator corresponds roughly to 5% of the total amount produced by fission. Therefore, a separate thermal-hydraulic circuit is used to cool the moderator and keep its overall temperature below saturation. Nevertheless, the non-uniform heat distribution coupled to the intricate geometry of the vessel (i.e. the calandria), yields spatial- and time-dependent flow temperature variations which can trigger non-negligible heavy water density gradients. These differences may provoke buoyancy forces which can largely compete with inertia, bringing about complex moderator flow distributions (i.e. flow configurations). Furthermore, the inherent unsteady hydrodynamic behavior within a very large and quite complex geometry, closely interrelated to the neutron flux distribution, makes both numerical and experimental studies to be extremely cumbersome and very costly. To this purpose, a particular effort has been deployed to correlate moderator flow distributions as a function of nondimensional numbers [6, 11, 15].

From dimensional analysis of the Navier-Stokes equations, Khartabil, et al. [6] have determined that the Richardson number can be used as a key correlation parameter to represent CANDU moderator flows ; this number is given as :

$$Ri = \frac{g\alpha\dot{Q}D}{C_p\rho A_i V_i^3} \tag{5.1}$$

where g, α, $\dot{Q}$, D, C_p, A_i and V_i are the gravity, the thermal expansion coefficient, the volumetric heat generation rate, the diameter of the calandria vessel, the specific heat at constant pressure, the total nozzle cross-sectional area and the inlet flow velocity, respectively. It is obvious that Eq. (5.1) represents the ratio between buoyancy and inertia forces produced by the water jets in the calandria. It is important to mention that the same dimensionless number was also used in the past by several researchers. In particular, Carlucci [15] and Carlucci & Cheung [11] proposed a similar number to correlate the configurations of moderator flows as a function of the angle with respect to a horizontal plane at which, due to the mutual interaction between opposite jets, the peripheral flow velocity becomes equal to zero (i.e. the location of an impingement point). In particular, based on his numerical simulations performed by using a porous medium modeling approach, Carlucci observed that for high values of the Richardson number, the flow distribution was driven by buoyancy forces. He argued that strong buoyancy effects cancel out the formation of the flow impingement

point and thus, triggering a prematurely flow reversal close to the water injectors without permitting the jets to penetrate a thermal stratified region formed on the top of the vessel. From numerical calculations performed at relatively low values of the Richardson number and using the same modeling approach Carlucci [15] and Carlucci & Cheung [11] observed that the flow distributions were always asymmetric, characterized by the location of the impingement point systematically tilted to one side of the calandria. Since buoyancy decreases with decreasing Richardson's number, they concluded that the asymmetry should disappear only when the volumetric heat generation goes to zero (i.e. Ri = 0). The numerical model used by Carlucci [15] and Carlucci & Cheung [11] was able to provide overall flow values for the pressure losses and mean temperature distributions at a reasonable cost, but was unable to correctly predict local flow effects. Undeniably, local flow fluctuations generated by the wakes and stagnation regions strongly affect the temperature distribution and consequently the heavy-water density. In turn, both neutron thermalization and absorption rates are very sensitive to moderator density. Moreover, local flow conditions must be determined with the highest precision possible to predict heat transfer across the calandria tubes and thus, confirm that the moderator fulfills its role under normal and off-normal reactor operation conditions. Despite the aforementioned weakness of the porous medium approach, some softwares based on this methodology are still used by the nuclear industry, e.g. MODTURC [17] and MODTURC-CLAS [8]. In other cases, commercial software were adapted to handle the experimental values of porosity and flow resistance distributions. For instance, to perform 3D simulations of moderator flows Yoon et al. [19,20] employed ANSYS CFX-4.4 with the aforementioned porosity distribution implemented as a source term in the momentum conservation equation. They concluded that the asymmetry previously observed by Carlucci [15] and Carlucci & Cheung [11], are not the product of numerical artifacts but physical (i.e. they observed similar axial flow asymmetries). An analogous simulation approach based on ANSYS-CFX was used by Arsene et al. [58] to study the moderator flow behavior in both CANDU-6 and CANDU-9 nuclear power reactors. Due to the use of a different water injector system, the flow seems to be better distributed within the CANDU-9 vessel. It must be pointed out that up to now, complete CFD simulations of this kind of flow are very limited. Furthermore, the existing ones were performed using a limited number of discretization cells and consequently the assessment of numerical convergence was not necessarily satisfied [24, 25, 30, 31, 59]. To this purpose, Teyssedou et al. [65] used ANSYS-Fluent to show that 2D simulations of the moderator of a CANDU-6 reactor requires a minimum of 3.5 million grid cells. The time-dependent nature of the moderator flow is an almost ignored important subject of study. For instance, by considering only natural convection effects, a time-dependent phenomenon along which globs of denser fluid start moving downwardly while they are replaced by upwardly

moving less dense ones, should be observed. In such a case, steady state calculations can only predict general trends, whereas in the real case, the flow distribution varies continuously with time. The CFD model developed by Farhadi et al. [31] is probably the first time-dependent numerical approach intended to study the moderator flow which does not use the porous medium approach. This work shows that within the calandria the flow is quite unstable, presenting large low and high frequency fluctuations. In fact according to Sarchami et al. [46] who analyzed some experimental data collected at AECL (Atomic Energy of Canada Limited), the moderator flow never reaches steady state conditions. Within this framework, Sarchami [75] and Sarchami et al., [46] performed a transient simulation of the moderator flow using Ansys-Fluent, by covering 150 s of physical time. They argued that only after the first 20 to 40 s, the numerical simulations become fully developed and thus, the data can be considered for analyses. It is obvious that the rest of about 100 s of physical time are not sufficient enough to completely represent the real moderator flow behavior. Unfortunately, the quite short time window they used, in conjunction with a lack of a previous numerical convergence and validation study, constitute some weakness of this work. Mandal & Sonawane [55] simulated the CANDU-6 moderator flow using an in house code that included an artificial compressibility [60] formulation of the Navier-Stokes equations. The numerical CFD model was solved by imposing a symmetrical free-slip wall condition along the vertical mid-plane of the vessel. Nevertheless, due to the transient nature of convective heat transfer conditioned by geometrical asymmetries of the calandria, the use of symmetrical boundary conditions does not seem suitable for performing these types of CFD simulations. In fact, Carlucci [15] and Carlucci & Cheung [11] argued that the application of such a boundary condition produces a bifurcation on the flow configuration. Recently, Choi et al. [27] developed the CUIPD two-phase numerical software, intended to simulate the moderator flow during a postulated Loss-of-Coolant Accident (LOCA). Although their calculations covered 3000 s of physical-time, which seems to be appropriate, they presented and analyzed the numerical results only after the solutions converged to steady-state conditions. Hence, they essentially studied the moderator flow behavior at the end of the simulations, without considering its time-dependent behavior. To partially fulfill the apparent lack of information about the moderator flow dynamics, this paper presents full-plane, two-dimensional time-dependent CFD simulations of a CANDU-6 nuclear power reactor. To this purpose, the Navier-Stokes equations for different reactor operating conditions were solved using a nuclear thermal-hydraulics code. The time-dependent numerical results, covering up to 5000 s of physical-time, by using a time step of 0.01 s and 3.5×10^6 cells (i.e. around 7×10^6 vertex) are analyzed in both time and frequency domains.

5.3 Numerical model and computation platform

Figure 5.1 shows a cross-sectional view of the calandria vessel of a CANDU-6 nuclear reactor ; its total depth is about 6 m. Its design is such that the moderator (i.e. heavy water) circulates around a bank of 380 horizontal tubes with a relatively low flow velocity. The principal characteristics and geometry of the calandria are given in the CANDU-6 Design Manual [29]. The simulations presented in this paper were performed using the version 3 of Code_Saturne [1,63] running on a high performance cluster of 8064 Intel Westmere EP X5650 (2.667 GHz) cores. This code is a finite volume open-source software that has been developed by Électricité de France (EDF) for nuclear thermal hydraulic applications. Hybrid meshes (tetra and quad) composed of 3.5×10^6 cells were generated using Gambit and ICEM-CFD commercial software. To perform the transient flow simulations, the same topology and number of grids discussed in our previous work were used [65]. The calandria tubes, the calandria shell and water injector sheaths were represented as wall boundary conditions. The inlet flow velocity and the outlet atmospheric pressure were two additional boundary conditions applied during the simulations. Furthermore, it was assumed that about 5% of the thermal power produced in a CANDU-6 reactor is dissipated in the moderator as a heat load due to the neutron thermalization. To this purpose, we have applied the averaged channel power distribution given in [69] and reproduced in Fig. 5.2. The total value of the power per unit of vessel's length ($= 17.17$ MW/m) was imported into the domain as space-dependent volumetric thermal source terms, which follow the channel power distribution shown in Fig. 5.2.

5.3.1 Validation of the simulation method against experimental data

Before performing time-dependent simulations of the moderator, the CFD model was validated against available experimental data. However, it is important to mention that the number of controlled experiments in this field is very limited. Therefore, the data collected at the STERN laboratory using a 1/4 calandria model containing 440 horizontal channels [8] was selected to fulfill this purpose. The details on the geometry as well as the flow conditions applied to perform the experiments are also given in [13] and [38]. In particular, they measured vertical and tangential flow velocity components using the PIV technique with an estimated accuracy of 3% of the readings. The vertical values were collected along the vessel mid plane, while the tangential ones were obtained along a 60° diagonal plane.
A grid containing 4×10^6 cells based on a square topology [65] was used to perform the present validation. The comparisons between predictions and experimental data are shown in Fig. 5.3. Along the vertical mid plane, the calculations follow the experimental trends quite well (Fig. 5.3a). In particular, the predictions clearly show the effect of the outlet (i.e. strong negative velocity at a height of -1 m) as well as the increase of this velocity component approaching

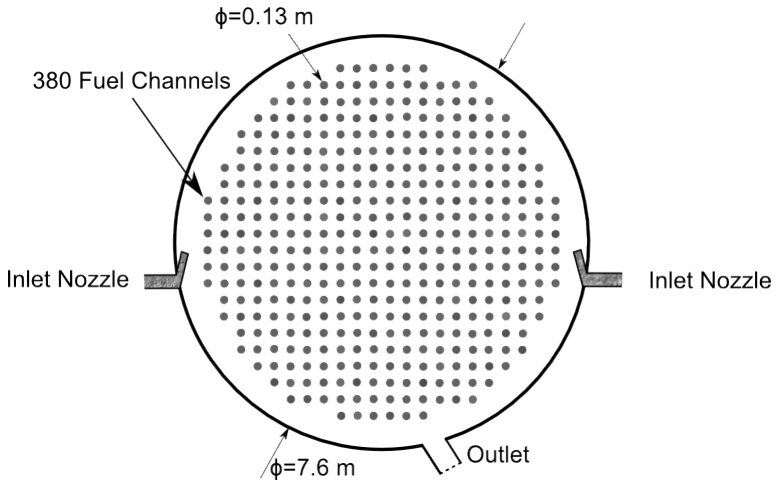

Figure 5.1 Cross-sectional view of the calandria vessel of a CANDU- 6 nuclear power reactor.

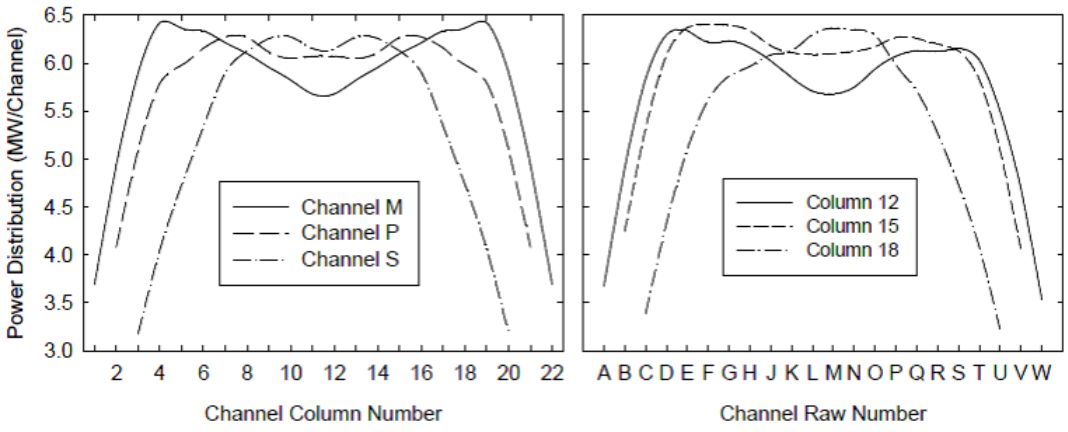

Figure 5.2 Typical plane-power distribution of CANDU-6 nuclear reactors [69].

the place where the two water jets mutually interact. Furthermore, the oscillations appearing in the simulations are produced by the presence of the horizontal channels inside the vessel (see Fig. 5.2). Even though along a 60° inclined plane (Fig. 5.3 b) the difference between the predictions of the tangential velocity with the data is more pronounced, the calculated values pass across the experimental ones. Herewith, the tangential velocity predicted by Code_Saturne clearly shows the effect of the wall, i.e. change of the slope starting at a radial distance of about 0.98 m. Note that this particular behavior does not appear in the data. Based on these results, we consider that Code_Saturne seems to be appropriate for simulating complex moderator flow distributions.

5.4 Moderator flow configurations in CANDU-6 nuclear reactors

There is consensus amongst researchers, including ourselves [11, 12, 15, 19, 20, 76] that depending on the reactor operating condition, (i.e. the inlet flow velocity and the thermal power dissipated within the moderator) in the CANDU-6 three different flow moderator configurations may occur. They are schematically shown in Fig. 5.4 and they are classified as : momentum-dominated (Fig. 5.4a), mixed-type (Fig. 5.4b) and buoyancy-dominated (Fig. 5.4c). The transitions between these configurations can be characterized as a function of the Richardson number given by Eq. (5.1) (i.e. the ratio between buoyancy to inertial forces). Hence, the flow adopts an inertia-dominated configuration for relatively small values of this number, which typically occurs for relatively high flow injection rates or relatively low heat generation rates.

Thus, for this type of flow configuration (Fig. 5.4a), the action of strong inertia forces or low heat addition, overwhelms any possible buoyancy effect. Therefore, the two jets of water impinge at about 90° with respect to the horizontal plane. The addition of heat, however, or a decrease in the injection flow rate can generate buoyancy effects which can counterbalance the inertia forces. Under such flow conditions, the competition between inertia and buoyancy forces may triger an asymmetry in the flow distribution. Consequently a new moderator flow configuration is developed, where the location of the impingement point of the two water-jets is tilted to one side of the calandria vessel. This mixed-type of flow configuration is schematically shown in Fig. 5.4b. It is obvious that the effect of buoyancy increases with increasing the amount of heat or with decreasing the injection flow rate. Therefore a transition from the mixed-type flow pattern shown in Fig. 5.4b, toward the buoyancy-dominated flow distribution shown in Fig. 5.4c may occur. For this type of flow configuration, the increase on the density gradient provoked by the important vertical temperature difference, triggers an upward flow in the vessel and consequently, the moderator may become thermally stratified. As shown in Fig. 5.4c, the buoyancy-dominated flow prevents the occurrence of any impingement point

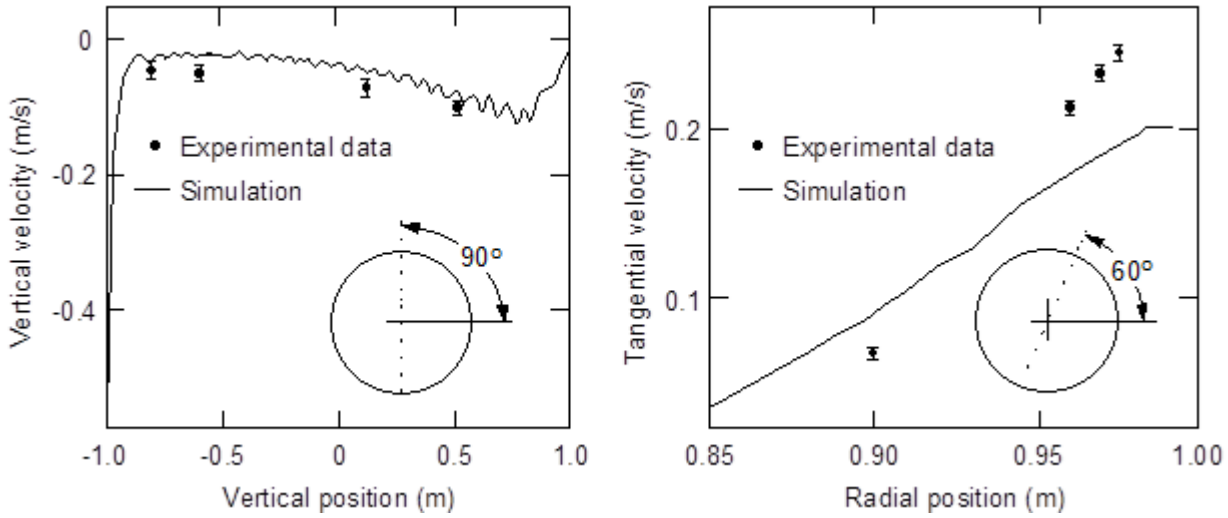

Figure 5.3 Comparison of simulated velocity profiles with Stern Laboratory experiments [8]. a) Vertical velocity distribution along a vessel mid-plane ; b) Tangential velocity along a plane at 60° with respect to the horizontal one.

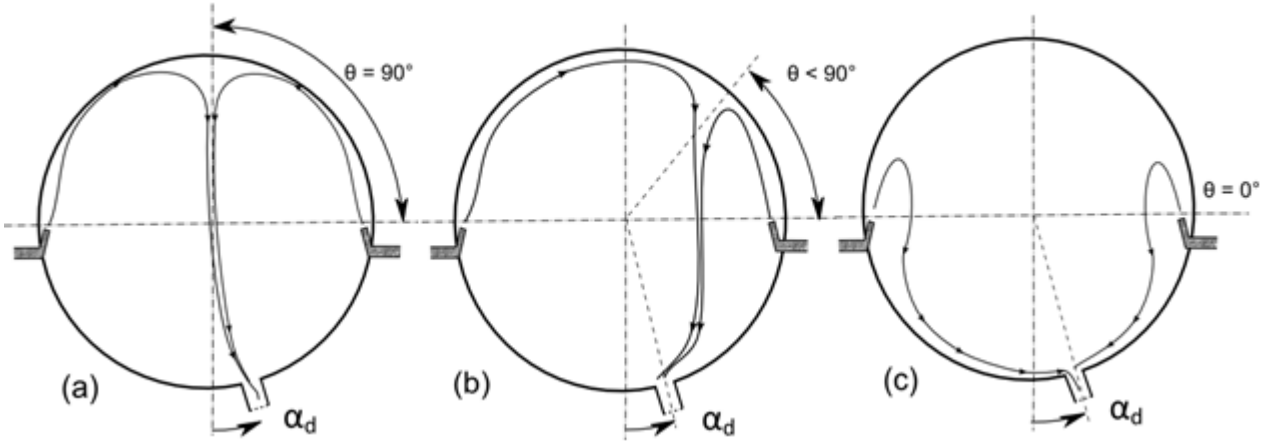

Figure 5.4 Moderator flow configurations within the calandria. a) Momentum-dominated ; b) Mixed and c) Buoyancy-dominated.

between the jets. It must be pointed out that, these types of flow configurations have been largely studied both experimentally and numerically under steady state conditions, amongst others by Carlucci [15], Carlucci & Cheung [11], Huget et al. [8], Khartabil et al. [6] , Yoon et al. [19, 20],Kim & Chang [38] and Mehdi Zadeh et al. [76], nevertheless up to now, only few works were performed to characterize the time-dependent behavior of these types of flows.

5.5 Time-dependent moderator flows : motivation of the present work

The motion of a fluid driven by density gradients (i.e. natural convection) is essentially time-dependent. Consequently, the transition between the flow configurations illustrated in Fig. 5.4 cannot be predicted by performing steady-state numerical calculations. For a big cylindrical vessel such as a CANDU-6 nuclear reactor, the variations of the fluid density due to the internal heat released by neutrons can bring about a quite complex unstable flow behavior. There exists few works that provide evidences of moderator flow instabilities observed both experimentally and numerically, [12, 13, 39, 59]. In particular, from transient numerical simulations, Sarchami [12] observed that moderator flow instabilities are triggered locally in the vessel and after a certain period of time they spread out and consequently modify the overall flow configuration. He also predicted flow fluctuations that seems to be more significant in the upper region of the calandria, where higher moderator temperatures prevail. Even though Sarchami and Sarchami et al. carried out a quite complete and interesting work, we consider that their results should be taken with some care. For instance, according to other works [39, 65, 76], we conclude that the number of discretization cells they used to discretize the entire 3-D domain (i.e. 3.2 million) is not appropriate to ensure a correct numerical convergence. The geometry of the entrance pipe to the injector does not corresponds to the real case, the applied heat flux distribution does not represent the common value encountered in CANDU-6 reactors [69] and the simulations covered only a very short period of physical-time (i.e. 150 s). Besides these facts, Sarchami [12] also presented experimental time-dependent temperature data collected in a 1/4 Moderator Test Facility (MTF) containing 480 horizontal channels. The principal characteristics of this facility, intended to study the moderator flow behavior in the Bruce B power nuclear reactor, are summarized in Table 1. For completeness of the present work, this MTF temperature record is reproduced in Fig. 5.5, where the existence of important temperature fluctuations with apparent coherent structures that repeat with time-intervals much longer than the simulation time presented by Sarchami [12] and Sarchami et al. [59] can be observed. In particular, we consider the amplitudes as well as the repetition rate of this data, do not correspond to the characteristic random signals generated by any type of temperature measurement device ; thus, they contain the fingerprints of a very interesting phenomenon.

In order to emphasize the time-dependent structure of these fluid temperatures, the same data was digitized and filtered using the following algorithm :

$$\tilde{S}_i = \sum_{i=1}^{3} a_i S_i - \sum_{i=1}^{2} b_i \tilde{S}_{i-1} \tag{5.2}$$

Where S_i, $\tilde{S}_i$ are the original and filtered temperatures respectively, with a_i, b_i appropriate coefficients determined as a function of both the signal sampling time and an appropriate low-frequency corner cutoff. The results obtained by applying the aforementioned numerical algorithm to the original temperature signal is shown in Fig. 5.6 ; the lags between the most relevant variations of the temperature are also indicated in the same figure. They have been determined by selecting the minimum value within each of the most representative temperature regions (i.e. coherent flow structures).

From this temperature record, it is apparent that the flow fluctuates with a characteristic mean relaxation time of about 60 min. Therefore, to correctly study the unsteady flow behavior of this complex thermal-hydraulic system, the numerical simulations must be able to cover a very long period of physical-time, otherwise the coherent flow structures shown in Figs. 5.5 and 5.6 cannot be observed. For this reason, we consider that the results presented by Sarchami [12] and Sarchami et al. [59] do not necessarily reflect a complete physical picture of the problem, and consequently do not represent the real-time thermal-hydraulic behavior of such a complex system.

Even though the temperature record reproduced in Fig. 5.5 does not correspond to a real CANDU-6 nuclear reactor, this previous analysis motivated us to carry out 2D time-dependent moderator flow simulations of a full-size calandria vessel, by covering more than 5000 s of physical-time. Though, before presenting and discussing the results, we performed a CFD numerical convergence study which is discussed in the following section.

5.5.1 Convergence study for moderator CFD simulations

Based on previous works [39, 65, 76], the current numerical simulations were carried out using the same number of cells and topology discussed in Section 5.3. Nevertheless, to perform time-dependent CFD calculations, the time step must be selected as a compromise between numerical stability, accuracy and the available computational power necessary to fulfill the maximum anticipated physical-time interval of the problem. Within this framework, a previous knowledge of the dependence of the calculations with respect to the time step is mandatory. It is obvious that in order to guarantee the temporal accuracy required to correctly analyze the flow behavior (i.e. the propagation of coherent flow structures, the determination of predominant frequency components, etc.), the selection of this key variable

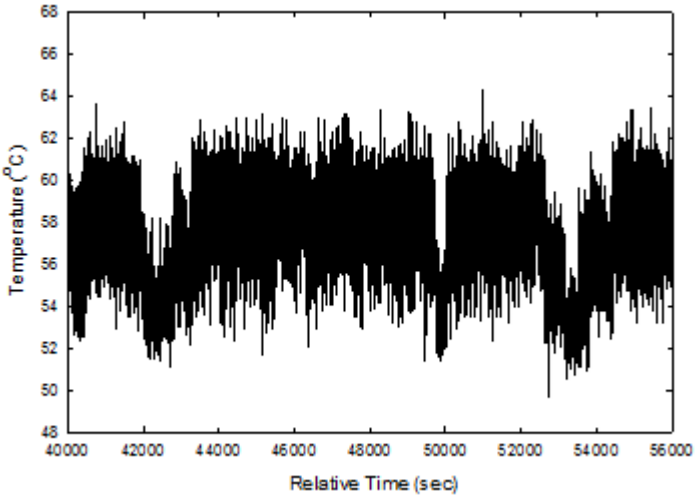

Figure 5.5 Experimental temperature record collected in a MTF (Reproduced from Sarchami's PhD thesis [12]).

Table 5.1 Key parameters used in the MTF experiments [12].

Nominal Conditions	Experimental (MTF) Conditions
Thermal power (kW)	1090
Average heat flux (kW/m2)	14.74
Total moderator mass flow rate (kg/s)	22.9
Number of nozzles	8
Number of outlets	2
Length of vessel [m]	5.9
Inlet flow temperature (°C)	40.1
Outlet flow temperature (°C)	51.5

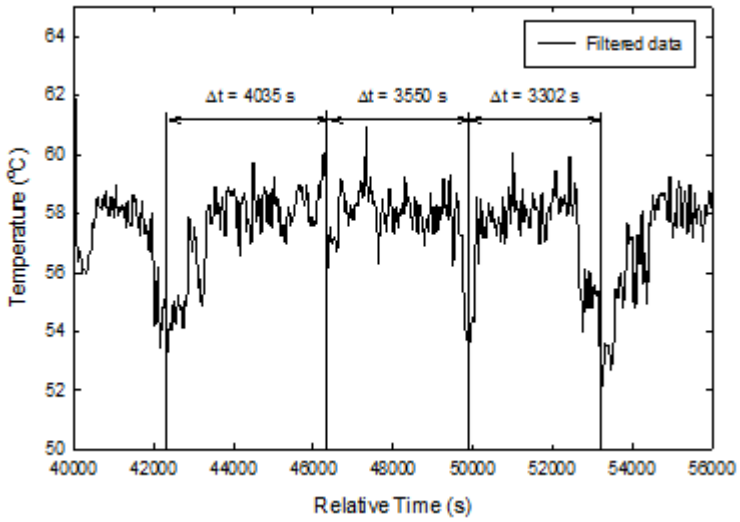

Figure 5.6 Filtered temperature data collected in the MTF [12].

is of main concern. Thus, such a prerequisite becomes more noteworthy when the flow adopts the mixed-type configuration schematically illustrated in Fig. 5.4b. In fact, under such flow conditions the presence of significant fluctuations for both flow velocity and temperature fields, having relatively low frequency components can be anticipated. To this aim, for a moderator flow characterized by a Richardson number of about 0.05, for which the flow is expected to assume a mixed-type configuration [76], several simulations covering physical-time intervals of 10 s were repeated using the following time steps ; 0.005 s, 0.01 s and 0.02 s. It must be pointed out that the use of time steps greater than 0.02 s produced severe numerical instabilities, consequently none of these simulations were able to converge. For time steps of $0.005\,s \leqslant \Delta t \leqslant 0.02\,s$ the values of simulated velocities were sampled along two diagonal planes inclined at 45° and 135°, respectively. In both cases, the averaged velocities were very close (0.2782 m/s for +45° and 0.2698 for 135°). The relative variations of the absolute flow velocities as a function of the time step are reproduced in Fig. 5.7. It is thus clear that the use of a time step of 0.01 s produces very good results ; in fact the relative velocity differences decrease by less than 0.1 % when they are compared with the results obtained for $\Delta t = 0.005$ s. Therefore, with the exception of one particular case that will be explained in the following section, most simulations presented in this paper were carried out using a time step of 0.01 s in conjunction with the spatial discretization presented in Section 5.3. For a mixed-type flow configuration, a particular attention was paid to cover at least 5000 s of physical-time.

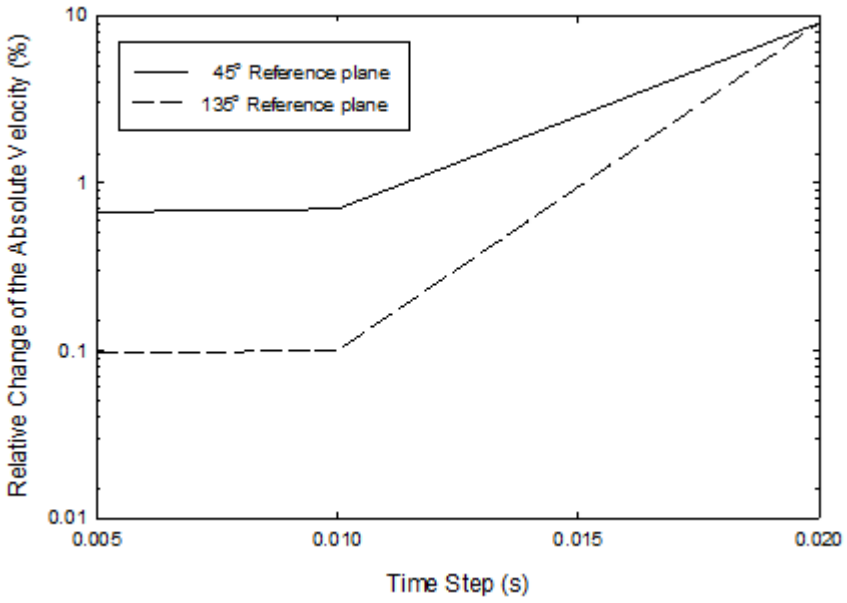

Figure 5.7 Convergence rate as a function of the time step.

5.6 Time-dependent CANDU-6 moderator flow simulations

The effect of five conditions were numerically studied for the flow of the moderator within the CANDU-6 calandria vessel. These conditions were selected to cover all the configurations shown in Fig. 5.4, as well as the transition between them. Based on our previous study [76], they are likely to correspond to the following values of the Richardson number : 0.002, 0.05, 0.07, 0.09 and 0.23. Nevertheless, the present work is mostly motivated to apply flow conditions which are able to bring about mixed-type configurations. In fact, for this type of flow distribution, the mutual competition between buoyancy and inertial forces triggers a time-dependent behavior. In turn, for inertia- and buoyancy-dominated cases (Fig. 5.4a and Fig. 5.4c) one of these forces becomes dominant and thus, overwhelms the effect of the other one ; consequently a more stable flow behavior is anticipated. It is important to mention that a single time step of 0.01 s was used to perform most simulations. However, for very high inlet flow velocity conditions (i.e. for Richardson's numbers lower than 0.05), to guarantee robustness and to avoid a possible numerical divergence due to the high Courant number in the domain ($\mathrm{CFL} > 20$), the time step was reduced from 0.01 s to 0.001 s.

5.6.1 Numerical results : analysis in the time-domain

As mentioned above, the time-dependent simulations were carried out for a wide range of the Richardson number. To this purpose, the same thermal power distribution shown in Fig.

5.2, as proposed by Rozon [69], was applied to the entire set of simulations; thus, the same average thermal power was assumed to be dissipated within the moderator for all the cases studied. Therefore, to achieve different values of Ri, in agreement with Eq. (5.1), the inlet moderator flow rate was changed by maintaining the geometry of the water injectors as given in the CANDU-6 reactor design manual [29]. Moreover, to accelerate the convergence, for each value of the aforementioned Richardson numbers, steady-state solutions were previously performed and their solutions were then subsequently applied as initial conditions. For the lowest value of Richardson number (i.e. Ri = 0.002), due to the small time step required, only 120 s of physical-time were simulated using $\Delta t = 0.001\,s$. Instead, for the rest of the cases a particular effort was deployed in order to cover a physical-time period as long as possible. In particular, for Ri = 0.05, where a previous work [76] shows a transition from inertia- to a mixed-type flow configuration (see Fig. 5.4b), more than 83 min of physical-time were covered. The time-dependent nature of the moderator flow was characterized by analyzing both the flow velocities and the temperatures sampled at the center of the calandria (i.e. x = 0, y = 0). Even though these variables were also sampled at other locations, due to the complexity of the flow behavior, the selection of the most appropriate sampling location was not necessarily straightforward. In particular, the treatment of a huge volume of numerical data collected at different locations can be redundant and cumbersome. Taking into account that most of the flow passes through the center of the vessel, for the present work we considered the aforementioned location as the most representative one. Furthermore, even though calculations were performed applying time steps of 0.001 and 0.01 s, to limit the amount of data, the numerical values were recorded only for every second.

Hence, for the entire set of simulations, Fig. 5.8 shows the time records of the variations of absolute flow velocities around their mean values (i.e. without bias). For a Ri number equal to 0.002, Fig. 5.8a shows a partial record of the flow velocity fluctuations versus time. It is observed that their amplitudes are extremely small, furthermore there is no indication of the existence of propagation of coherent flow structures. In fact, for this case, it is also observed that the flow is always in an inertia-dominated mode characterized by the impingement point between the two water-jets located at 90° with respect to the horizontal plane (Fig. 5.4a). It is important to mention that even though for this case the thermal power is different from zero, the effect of the flow density gradient is not strong enough to counterbalance inertia. Consequently, if the inlet flow velocities are high enough, the occurrence of an inertia-dominated flow configuration can occur even though the flow is not adiabatic, which seems to contradict previous studies [11, 15].

Based on predictions obtained from previous steady-state calculations for Richardson numbers higher than 0.04 [76], it is expected that a mixed-type of flow configuration should be

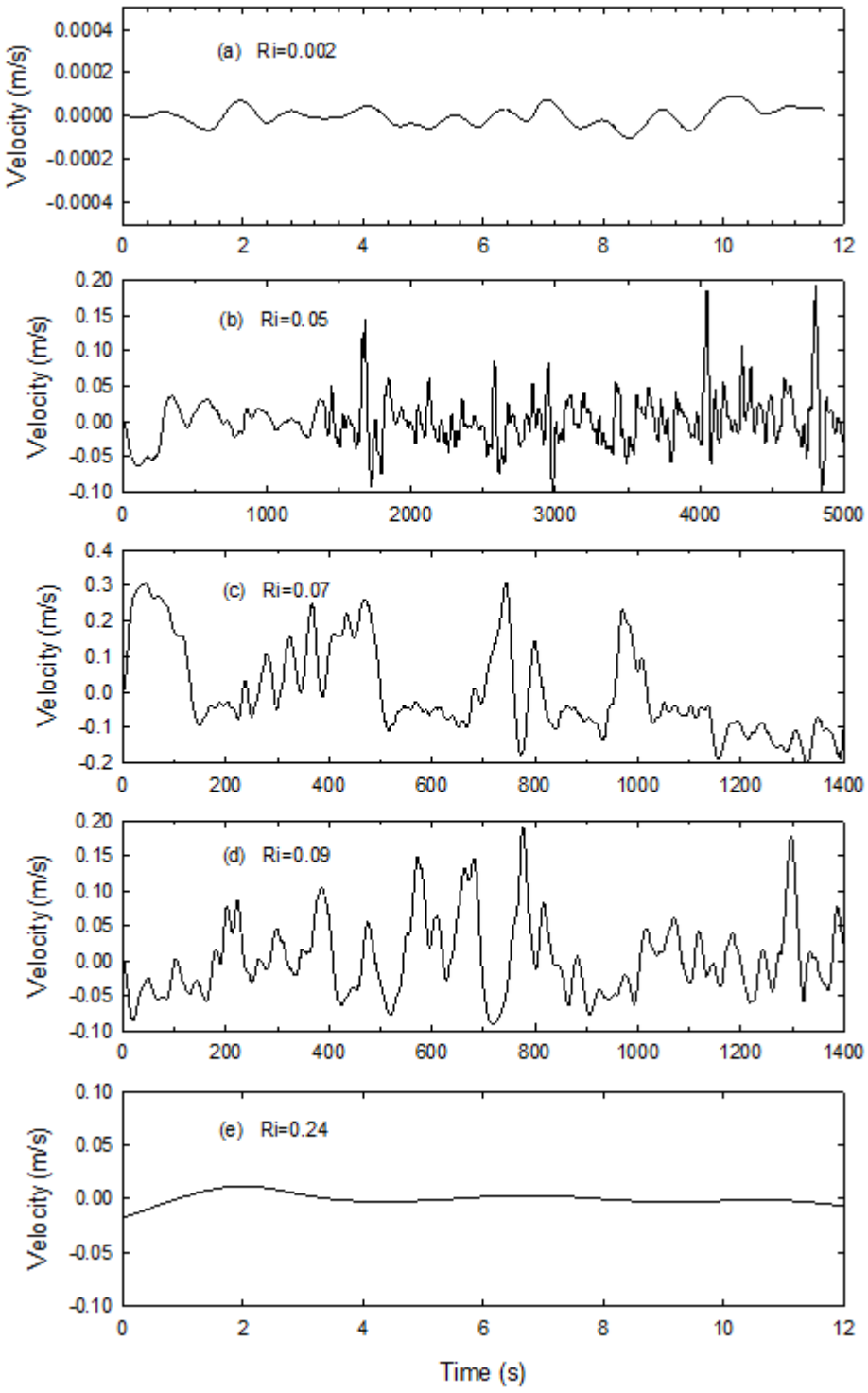

Figure 5.8 Time records of absolute flow velocity fluctuations (without bias) sampled at x = 0, y = 0. Simulations carried out with 17.17 MW/m of mean moderator thermal power. a) Ri=0.002 ; b) Ri=0.05 ; c) Ri=0.07 ; d) Ri=0.09 and e) Ri=0.23.

observed in the calandria vessel (see Fig. 5.4b). Furthermore, these steady state simulations have also indicated the existence of important flow asymmetries. It was also observed that the angle between the impingement point with respect to the horizontal plane increases with increasing the Richardson number. Therefore, time-dependent simulations were performed for Ri = 0.05. Similar to the former case (i.e. Ri = 0.002), previous steady state calculations performed using the same Richardson number were applied as initial conditions. Figure 5.8b shows a time record of the flow velocity collected at the center of the calandria. It can be observed that only after the first 1300 s of physical-time, the behavior of the flow is characterized by the presence of coherent fluctuating structures ; some of them seem to repeat with a strong periodicity. In fact, the snapshots extracted from a 5000 s video containing the entire set of simulated data, confirm that the impingement point moves angularly with an apparent periodicity. Some of these images are shown in Fig. 5.9, where the sign of the angle indicates the sense of rotation of the impingement point (i.e. (+) counterclockwise and (–) clockwise). It is obvious that for this flow condition, the moderator is characterized by a mixed-type flow configuration similar to that schematically representation in Fig. 5.4b. For a period of 630 s, Fig. 5.9 shows a clear oscillation of the impingement point occurring systematically on the right side of the calandria vessel. This behavior is quite possible due to the asymmetrical location of the flow discharge (see Fig. 5.1) and probably controlled by the lower resistance that the flow encounters within this region. From Fig. 5.9, it is also clear that for this type of configuration the flow oscillates forward and backward with a characteristic periodicity.
We have also observed that this particular angular movement continues to occur after the maximum lapse of time shown in the figure. In addition, it must be pointed out that this flow distribution has strong effects on both the flow velocity and the temperature determined at the center of the calandria vessel. To this purpose, Fig. 5.10 shows a 700 s time-window of the same record presented in Fig. 5.8b, where the sampling times corresponding to each snapshots are indicated as : (a)... (h) in Fig. 5.9.
The comparison of Fig. 5.9a to Fig. 5.9h with Fig. 5.10, proves the strong time-dependent correlation that exists between the presence of coherent flow structures within the calandria and the angular displacement of the impingement point. Hence, this observation confirms that the location of the impingement point can be used for characterizing (i.e. correlating) both steady and time-dependent moderator flows. As has been already discussed, amongst others in : Carlucci [15], Carlucci & Cheung [11] and Mehdi Zadeh et al. [76], the mixed-type configuration is characterized by important flow temperature excursions. For the same physical-time window of 700 s and for the same Richardson number (Ri = 0.05), Fig. 5.11 shows the simulated flow temperature collected at the center of the vessel.
This figure also contains the data numerically filtered using the algorithm given by Eq. (5.2).

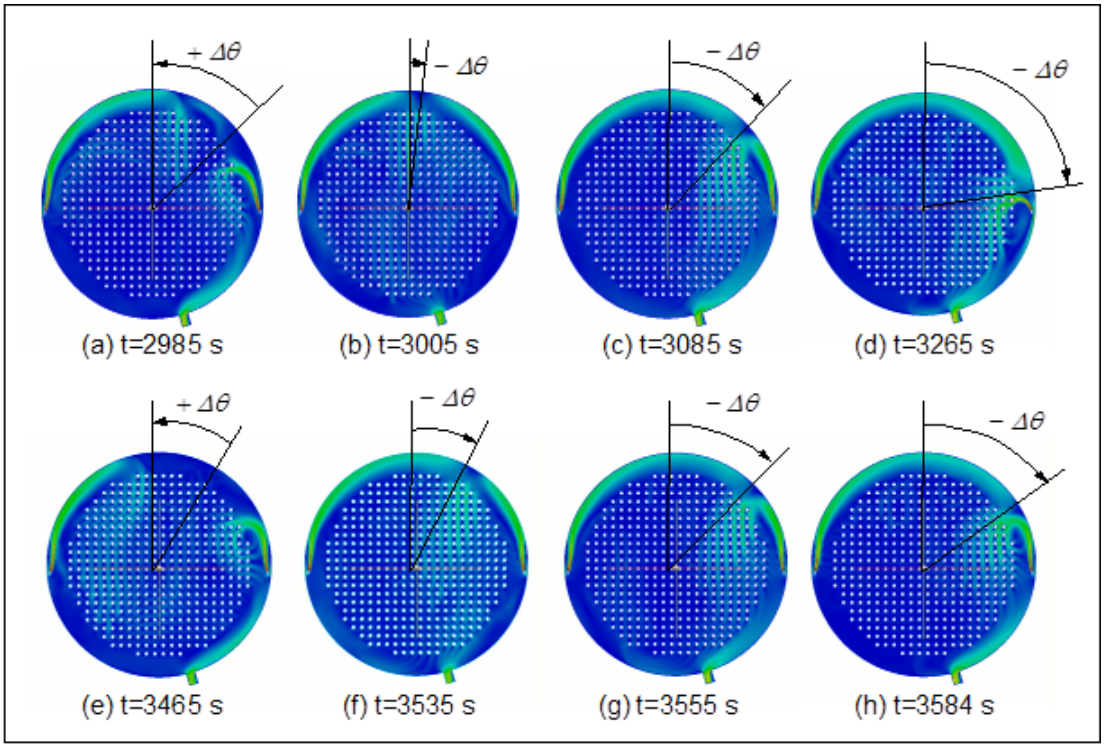

Figure 5.9 Snapshots taken from a 5000 s of physical-time video produced using the simulation data obtained with Ri = 0.05.

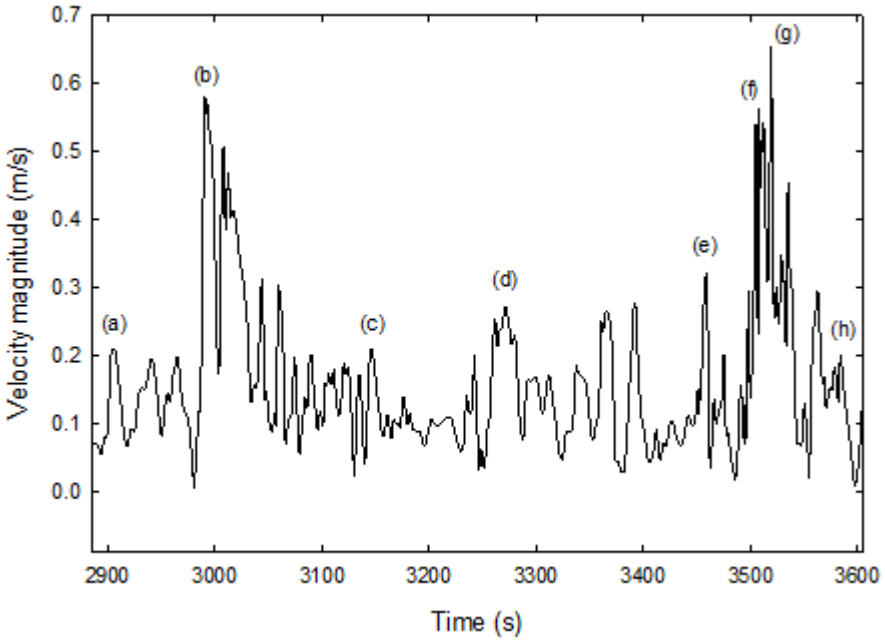

Figure 5.10 Absolute flow velocity collected at the center of the calandria for Ri = 0.05 and for the same time window of the snapshots given in Fig. 5.9.

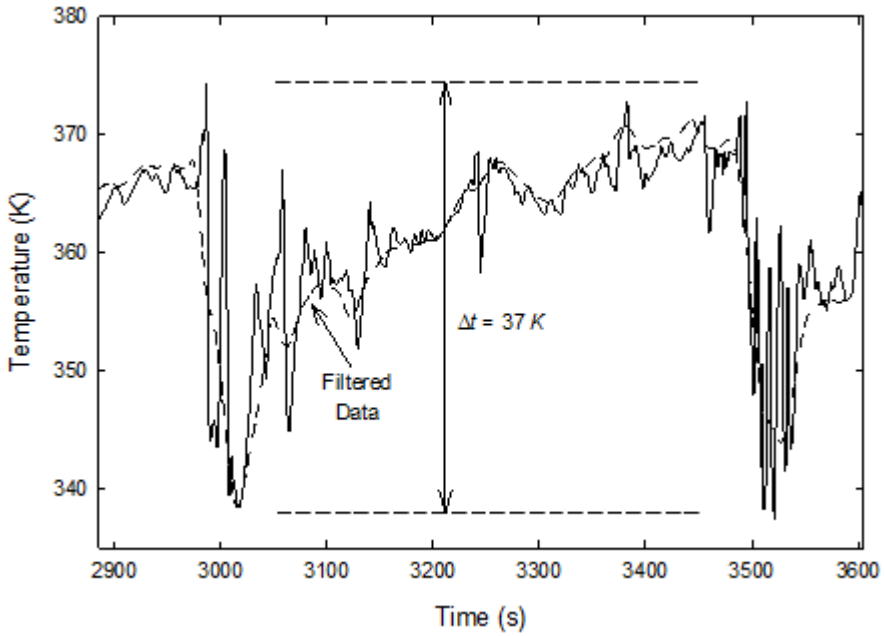

Figure 5.11 Flow temperature collected at the center of the calandria for Ri = 0.05 and for the same time window of the snapshots given in Fig. 5.9.

It is obvious that the temperature follows the flow velocity presented in Fig. 5.10, i.e. the temperature decreases with increasing velocity. Nevertheless, between the two major velocity peaks, the temperature shows a characteristic relaxation time along which it increases almost monotonically, as indicated by the dashed line. Note that this transition corresponds to the snapshots (b) and (g) in Fig. 5.9, which matches the reversal of the impingement point. This particular temperature behavior seems to indicate that the flow fluctuations are controlled by fluid density changes associated to non-negligible temperature variations. In fact, starting from its lowest value of the temperature, the fluid is heated up to the moment it becomes violently cooled down in a very short period of time. While the heating process requires more than 8 minutes (for this case), the cooling seems to occur in almost 50 s.

As illustrated by the filtered data (the dashed line curve in Fig. 5.11), the temperature behaves as the variation of the electrical potential across a capacitor ; it is initially charged with a characteristic response time and then it is discharged very rapidly. Following this analogy, it seems that after reaching the highest temperature, the hot fluid encounters a high velocity flow as shown in Fig. 5.10 which is extremely efficient in removing the accumulated thermal energy. Since both the flow velocity and the temperature shown in Figs 5.10 and 5.11, have been collected at the same location (i.e. x = 0, y = 0), the use of an electrical analogy is not necessarily correct ; nevertheless, it can be used to provide a plausible explanation

of the observed phenomena. For this particular case, the aforementioned heating-cooling process has been observed with impressive repeatability all along the entire simulation record. Furthermore, it is important to mention that both velocities and temperatures collected at x = 1.43 m, y = 0 m show similar trends to those presented in Fig. 5.9 and Fig. 5.10, respectively. Moreover, the peak-to-peak temperature difference at the center of the calandria can reach up to 37°C. For this particular case, nearby some calandria tubes, the flow approaches very closely saturation conditions. It is obvious that such a situation can affect both the neutron moderation and the absorption rates and consequently may bother the reactor's reactivity.
Time-dependent numerical simulations were also carried out by increasing Richardson number from 0.07 to 0.09. Similar to the former case, the moderator follows oscillatory motions characterized by coherent structures which propagate at a slower pace. In addition, it is also observed that the amplitudes of these fluctuations increase with increasing the Richardson number from 0.05 to 0.07 and then start decreasing with increasing this dimensional quantity (compare Fig. 5.8b, Fig. 5.8c and Fig. 5.8d). For higher values of this number, after 1300 s of physical-time, the amplitude of the oscillations are considerably attenuated and the flow becomes thermally stratified. In particular for the same location and for a relatively short period of time, Fig 5.8e shows the fluctuation of the flow velocity for Ri = 0.23. This results confirm that the increase of Richardson number brings about a noticeably change in the flow configuration. In fact, for this particular case the flow becomes thermally stratified without formation of an impingement point, as it is schematically shown in Fig. 5.4c. It must be pointed out that for similar Richardson numbers, a similar moderator flow configuration, without the presence of an impingement point was also observed in steady numerical simulations [76].

5.6.2 Analysis in the frequency-domain

In order to determine without ambiguity the existence of coherent flow structures that can be used to characterize the behavior of the moderator flow as a function of the Richardson number, a Fast Fourier Transform (FFT) was applied to the entire numerical data-set. However, before applying the FFT to the time dependent results, they were filtered by using the algorithm given by Eq. (5.2). Due to the relatively long response time of the flow, as indicated by Fig. 5.8, and the short time interval used for the simulations ($\Delta t = 0.01$ s and saving data every 1 s), a cut-off frequency of 0.5 Hz was applied to the entire data set. This value, which satisfies the Nyquist criterion, to some extent helps reducing the high frequency components that are not relevant for characterizing the overall moderator flow behavior. Furthermore, to avoid the overwhelming effect caused by zero frequency components, for each record the biases were calculated and subtracted from the data (see Fig. 5.8). For each velocity and temperature record, the dominant (fundamental) frequency components of their respective

power spectra were selected. Hence, instead of representing the power spectral density of the flow fields obtained for all Richardson numbers discussed in the former section, we plotted the locus of the dominant frequency vs. Ri, as shown in Fig. 5.12.

As illustrated in Fig. 5.12, the FFT results of the current temperature and velocity numerical simulations collected at (x = 0, y = 0) were also fitted by using a Pearson IV function [77] with a $r^2 = 0.98$. Note that this particular fitting does correspond to a double valued function ; for each value of Richardson number, it represents the locus formed by the dominant frequencies of both flow velocity and temperature records. As expected, it can be observed that for each Ri number, both flow fields are strongly correlated. It is obvious that this frequency locus identifies the range of flow conditions under which the moderator moves with a given periodicity. Thus, it delimits a region that seems to bring about mixed-type flow configurations similar to the schematically shown in Fig 5.4b. Even though for very low Ri numbers the data points are scarce, Fig. 5.12 shows that for Ri = 0.002 the moderator does not oscillate and consequently seems to be completely dominated by inertia, as schematically illustrated in Fig. 5.4a. The lack of information in this region does not permit us to rigorously identify the transition condition necessary to trigger a mixed-type configuration. Nevertheless, for very low values of Ri numbers, based on the trend of the Pearson's IV fitting function presented in Fig. 5.12, we can expect that this transition should take place for Ri > 0.01. In addition, these results confirm that inertia-dominated flows can be achieved, even though the thermal power is different from zero, which contradicts the arguments given amongst others by : Carlucci [15], Carlucci & Cheung [11]. Hence, depending on the magnitude of the inlet flow velocity, it seems that the flow is able to maintain an inertia-dominated configuration even though a considerable amount of thermal power is dissipated within the fluid.

By increasing the Ri number the fluid starts oscillatory motions with dominant frequencies that depends strongly on this number. However, due to the large dimensions of the CANDU-6, these frequencies are very low. This particular behavior confirms that in order to detect such a particular periodic fluid displacement across the calandria, very long physical-time periods are required for both experimental and numerical studies ; this is not necessary the case in most known research works performed up to now. Furthermore, Fig. 5.12 also shows that maximum frequencies ranging approximatively between 0.003 Hz to 0.004 Hz occur for Ri = 0.05 ; however, after this value the dominant frequencies decrease with increasing Ri. Since the current simulations were carried out by maintaining the thermal power constant, according to Eq. (5.1) the Richardson number increases very rapidly with decreasing the inlet flow velocity. Consequently, for a constant thermal power, the inertia of the flow decreases with increasing this number. Therefore, for Ri > 0.07, buoyancy tends to overwhelm inertia, which in turn forces the predominant frequencies to decrease. This particular behavior is clearly

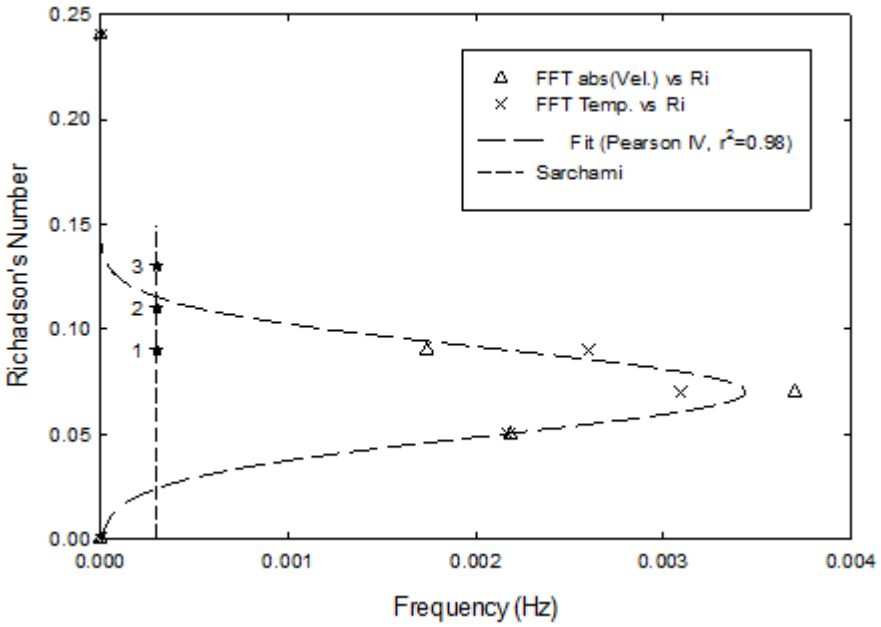

Figure 5.12 Locus of the dominant frequencies vs. Richardson number – current numerical data sampled at (x = 0, y = 0) and data given in : Sarchami [12].

indicated by the simulated data obtained for Ri = 0.23, where neither the flow velocities nor the temperatures present periodicities. As has been already mentioned, for high Ri values the moderator flow becomes controlled by buoyancy and consequently it turns into a completely thermally stratified distribution. Even though from the current available data the transition condition required to switch from one configuration to another (i.e. from mixed- to buoyancy-dominated) cannot be clearly determined, Fig. 5.12 seems to indicate that such a transition should occurs for Ri > 0.12.

For validation purposes, the same numerical treatment was also applied to the unique experimental data available in the open literature and reproduced in Fig. 5.5 [12], which satisfies the aforementioned requirements. Although, for this case, we do not have information about the exact location where the flow temperatures were measured, the Richardson number was estimated using the inlet and outlet flow conditions given in Table 5.1. In Fig. 5.12, these experimental points are identified by the numbers 1 and 2, respectively. Moreover, taking into account that within the range of inlet and outlet flow temperatures given in Table 5.1, the fluid expansion coefficient varies almost linearly, an interpolation was applied to determine the point 3 shown in the same figure. It is interesting to observe the excellent agreement between this “experimental” point and the proposed Pearson’s-IV fitting curve based on our simulations alone. Even though the amount of experimental information is extremely limited,

the behavior shown in Fig. 5.12 provides solid indications that the temperature fluctuations presented in [12] are not a product of experimental scattering or artifacts. In fact, they provide experimental evidences that for some values of Richardson numbers the moderator flow may follow a very complex behavior characterized by important oscillations.

5.7 Conclusion

The study of the time-dependent behavior of CANDU-6 moderator flow configurations constitutes a research field where the open literature material is very limited. This lack of information can possibly be explained by the resources, e.g. experimental and numerical, that such a type of work necessitates. In particular, due to the large dimension of the calandria vessel, the determination of flow conditions that can bring about transitions from a flow configuration to another requires the collection of extremely long flow physical-time records. To partially fulfils this gap, this paper presents 2-D time-dependent numerical simulations of full-size CANDU-6 moderator flows. To this purpose, the Code_Saturne developed by Électricité de France for simulating the thermal hydraulics of nuclear power reactors was used. The CANDU-6 flow domain was discretized using a grid containing 3.5×10^6 cells on a square topology. Furthermore, very short integration-time intervals necessary to guarantee a robust numerical convergence were implemented. Before simulating moderator flows, the performance of Code_Saturne was validated against available experimental data. Several time-dependent simulations were carried out for a wide range of the Richardson number (Eq. 5.1) by maintaining the moderator thermal power constant and by changing the inlet flow velocity. A particular effort was deployed to obtain up to 5000 s of physical-time records of flow velocities and temperatures for an integration time interval of 0.01 s. To determine moderator flow transition conditions, the numerical data collected at the center of the calandria (i.e. x = 0, y = 0) was analyzed both in the time and frequency domain. The foremost important results are summarized as :

– Due to the large dimensions of the calandria, the characterization CANDU-6 flow configurations necessitates considerable long physical-time records which are numerical intensive and very costly ;
– A comparison of time-dependent flow velocities for a wide range of Ri numbers collected at the center of the vessel, with snapshots reconstructed from films of the same simulations, confirms a strong correlation between the angular position of the impingement point and the configuration of the flow. As was initially proposed by Carlucci [15], this observation confirms the use of this angle as a function of Richardson number to represent both steady-state and time-dependent moderator flows ;
– The analysis in the frequency domain permitted us to construct a locus of dominant fre-

quencies as a function of the Ri number ;
– For Richardson numbers lower than 0.01 the moderator is able to maintain an inertia dominated configuration even though the thermal power is quite high ;
– The frequency locus representation indicates that for approximately $0.01 < \mathrm{Ri} < 0.12$ the moderator is characterized by the presence of coherent flow structures which oscillate with very low dominant frequencies (i.e. mixed-type configuration). Regardless, for Richardson numbers higher than 0.12 these fluctuations disappear and the moderator becomes thermally stratified ;
– Both flow temperatures and velocities show a very good correlation in the frequency domain ;
– The comparison of the proposed numerical frequency locus with the unique available experimental data shows an excellent agreement.

Based on numerical simulations, this paper provides a new way to determine the transition conditions between moderator flow configurations. Thus, we are able to confirm that they are controlled by quite complex time-dependent flow phenomena. Nevertheless, the limited number of data points for $\mathrm{Ri} < 0.01$ the flow is inertia-dominated, for $0.01 < \mathrm{Ri} < 0.12$ the flow shows a mixed-type behavior and becomes thermally stratified for $\mathrm{Ri} > 0.12$.

Acknowledgments

This work was partially funded by a discovery grant (RGPIN 41929) of the National Sciences and Engineering Research Council of Canada (NSERC). The authors are very grateful to the Fonds de Recherche du Québec-Nature et Technologies (FQRNT PhD excellence research fellowship), Compute Canada for the allocation of computational resources and the development group of Code_Saturne at EDF France for their technical assistances.

CHAPITRE 6 ARTICLE 3 : Effect of 3-D moderator flow configurations on the reactivity of CANDU-6 nuclear reactors

.

Authors : Foad Mehdi Zadeh, Stéphane Etienne, Guy Marleau, Richard Chambon, Alberto Teyssedou, submitted to Annals of Nuclear Energy.

6.1 abstract

The reactivity of nuclear reactors can be affected by thermal conditions prevailing within the moderator. In CANDU reactors, the moderator and the coolant are mechanically separated but not necessarily thermally isolated. Hence, in this type of reactors any variation of moderator flow properties may change the reactivity. Up to now, nuclear reactors calculations are performed by assuming uniform moderator flow temperature distribution. However, CFD simulations have predicted large time dependent flow fluctuations taking place inside the calandria, which can bring about local temperature variations that can exceed 323 K (*i.e.* 50°C). Within this framework, this paper presents robust CANDU-6 3-D CFD moderator simulations coupled to neutronic calculations. Thus, the proposed multiphysics numerical simulation strategy make it possible to study not only different moderator flow configurations but also their effects on the reactor reactivity coefficient.
Keywords : CANDU Reactor, Moderator Flow, 3-D CFD-Reactor Physics Coupled Simulations.

6.2 Introduction

About 5% of the total thermal power generated in a CANDU-6 nuclear reactor is transferred to the moderator. Around 70 to 80% of this heat is dissipated by the neutron slowing down process (*i.e.* by thermalization). Therefore, the spatial heat distribution is essentially controlled by the neutron distribution within the reactor core and thus, affects the thermal properties of the moderator. In particular its volumetric mass and macroscopic cross-section, and consequently the reactivity. Despite of the relatively low working temperature prevailing in the moderator of CANDU as compared to Pressurized Water Reactors (PWR), due to the relatively large dimension of the core (7.6 m $\times$ 6 m) the spatial neutron flux distribution locally determines the moderator flow temperatures affecting reactor's reactivity. In CANDU-6, the moderator (*i.e.* the heavy water) is confined in a big cylindrical vessel, *i.e.* the calandria, which contains 380 horizontal fuel channels. The moderator enters into this vessel via eight nozzles and two outlets permit the fluid to recirculate through an external heat re-

moval thermal-hydraulic circuit [29, 54]. The motion of the moderator is governed by inertial forces generated by the flow jets and gravitational forces (*i.e.* buoyancy) controlled by mass density differences. These forces coupled together with the complex geometry of the reactor, result in a quite intricate behavior of the flow within the calandria. Due to these reasons, performing moderator thermal-hydraulics simulations is not a straight forward task (*i.e.* very small nozzles as compared with the dimensions of the calandria, a multiple connected integration domain with several boundary conditions, inappropriateness of applying Boussineq's approximation, etc.) Therefore, prior to obtain information about the physics that controls the flow distribution, the use of any Computational Fluid Dynamic (CFD) model for such a purpose necessitates a rigorous assessment. It is obvious that the complexity of this problem increases very rapidly when reactor physics is coupled to hydrodynamic effects ; for instance the mutual interaction that exists between the neutron flux distribution and nuclear as well as thermophysical moderator properties. Consequently, the use of inappropriate physical and numerical simplifications to simulate such a system can dramatically mislead the predictions and subsequently results in incorrect analyses. From a thermal-hydraulic view point, due to the huge requirement of computational resources, the porous medium approach was extensively used by the nuclear industry to model the CANDU moderator flow around the calandria tubes [17, 18, 31, 49]. The use of this methodology is quite advantageous for obtaining fast results at relatively low costs. However, this technique cannot provide information about local flow effects close to calandria wall tubes. Therefore, the porous medium approach is limited to predict the overall behavior of the flow, such as the pressure drop and mean flow temperatures, but it is unable to generate local conditions which control heat transfer across the calandria tubes as well as the formation of wakes responsible of flow distributions. In particular, local effects such as the locations of stagnation points and the formation of wake zones, which may provoke partial wall dry out, cannot be estimated using this modeling approach. Moreover, it is obvious that local flow temperature distributions which control the mass density and the microscopic cross-sections, which can bring about spatial power changes cannot be correctly predicted as well. Therefore, the study of these local effects necessitates a more precise thermal-hydraulic model that should be coupled to reactor physics calculations. Performing this kind of thermal-hydraulic-neutronic coupled study by including all geometrical details as well as fluid thermo-physical properties, necessitates huge computational resources. Instead of using the porous medium approach, Kim et al. [24] performed 3-D CFD simulations by using the ANSYS Fluent-6.0 software. Even though in this work the authors demonstrated a good capability to predict the moderator flow, they did not analyze the discretization errors nor the numerical convergence of their calculations. Furthermore, the inlet velocity of the moderator used in this work (*i.e.* 5.3 m/s) was more than double

the inlet nominal velocity stipulated in the CANDU-6 design manual (approx. 2 m/s [29]). It is important to remark that the authors did not provide plausible explanation about this large value which can prevent getting realistic results. It must be pointed out that the lack of a rigorous estimation of numerical convergence is quite common, even for the more recent studies such as those given amongst others by : Farhadi et al. [31], Sarchami et al. [59] and Kim [9]. To this aim, Teyssedou et al. [65] concluded that a minimum of 3.6×10^6 cells are necessary for performing 2-D simulation of CANDU-6 moderator flows. It is obvious that this number must be much higher for 3-D calculations.

A modified version of a CANDU-6 design includes 480 horizontal fuel channels ; this type of reactor is currently in operation in Canada at Bruce and Darlington power plants. To characterize the moderator flow within this type of reactor, the Atomic Energy of Canada Limited (AECL) constructed a 1/4 Moderator Test Facility (MTF) [6,12]. This experimental setup contains 480 horizontal heated channels ; the data collected using this facility was used to validate moderator flow models. Within this framework, Sarchami et al. [10, 45] studied the effect of the surface heating method used during these experiments by comparing the results with the volumetric heating case encountered in real reactors. Based on numerical calculations, Sarchami [12] and Sarchami et al. [30, 46] concluded that the moderator is subjected to important hydrodynamic instabilities. In particular, they were able to show several scaling issues that were not necessarily satisfied during the design of the MTF ; for instance the Rayleigh (Ra) number which varies by two orders of magnitude between the experimental prototype and the CANDU-6, was considered critical [59]. This is a quite important remark because this number permits to determine the conditions that trigger buoyancy-driven flows (*i.e.* natural convection) which can occur within the large volume of the calandria. In fact, a competition between buoyancy and inertia forces may bring about important flow instabilities [78].

Based on a Canadian technology transfer agreement, India designed and manufactured a modified version of CANDU-6 reactors. Even though both technologies are very similar, the new design contains twelve moderator flow injectors and four outlets located at the bottom of the calandria vessel. Subsequent thermal-hydraulic studies of this flow circulation arrangement, indicated that the moderator flow distribution is more homogeneous as compared to CANDU-6 [47, 49, 79]. Nevertheless, for the next generation of the Indian Advanced Heavy Water Reactor (AHWR) that will use thorium as nuclear fuel, the calandria vessel is vertically oriented, which constitutes a major design change with respect to the former one. Recent CFD simulations [35] indicate that the maximum moderator temperature occurs at the outlet of the calandria located at the top of the reactor vessel, which is in agreement with the action of gravity (*i.e.* buoyancy effects). Mandal & Sonawane [55] carried out moderator

flow simulations by considering half of the reactor vessel and using an in house developed software. Similar to the previous work of Carlucci [15], they imposed symmetrical conditions along a vertical axially oriented midplane. Nevertheless, due to the time dependent behavior of almost natural convection, coupled to the geometrical asymmetric shape of the calandria (*e.g.* inclined outlets), symmetrical boundary conditions should affect the simulations. In fact, Carlucci & Cheung [11] observed a bifurcation of the flow configuration when such a boundary condition is applied ; thus, they concluded that to agree with real flows, the numerical simulations must take into account the entire calandria vessel. The available information in the open literature indicates that the works devoted to the simulation of moderator flows within the entire calandria vessel are very scarce. Most of existing works were performed in 2-D domains by introducing symmetrical boundary conditions (not recommended for treating this kind of problem) or by using simplified modelling approaches that do not satisfy real CANDU-6 operating conditions [76]. It must be pointed out that most of these works include neither a rigorous convergence analysis nor a coupling between thermal-hydraulics and reactor physics calculations. Within this framework and to partially fulfill this gap, this paper presents 3-D CANDU-6 full moderator CFD - reactor physics coupled simulations.

6.3 The CANDU-6 moderator hydrodynamic domain and flow equations

CANDU-6 nuclear power reactors use a large inventory of heavy water close to atmospheric conditions as moderator [29,54]. Under some postulated accidents, this large mass of low temperature water turn out to be a considerable energy sink for cooling down the reactor during the early moments of an accident. For this reason, the heat transfer from eventually damaged fuel channels to the moderator, constitutes an actual subject of study [80]. Notwithstanding this area of research which is of particular interest for performing nuclear safety analyses, under normal operation conditions, local moderator temperatures distributions may affect both the water density and the cross-sections bringing about substantial reactivity changes. In particular, the moderator temperature on the external wall of the calandria tubes should not reach saturation conditions. It is apparent that the study of these kinds of problems necessitates solving the distribution of moderator flow coupled to reactor physics using appropriate numerical tools. From the hydrodynamics standpoint, it is necessary to handle the entire reactor core which due to the presence of 380 horizontal channels constitutes a multiple connected domain having multiple boundary conditions. Figure 6.1 shows a schematic representation of the calandria vessel of a CANDU-6 nuclear reactor. The moderator flow is injected with a velocity of 2 m/s into the calandria through eight flow nozzles (*i.e.* four installed on each side of the vessel, as illustrated in figure 6.1).

The CFD portion of the simulations, which are coupled to neutronic ones, were performed

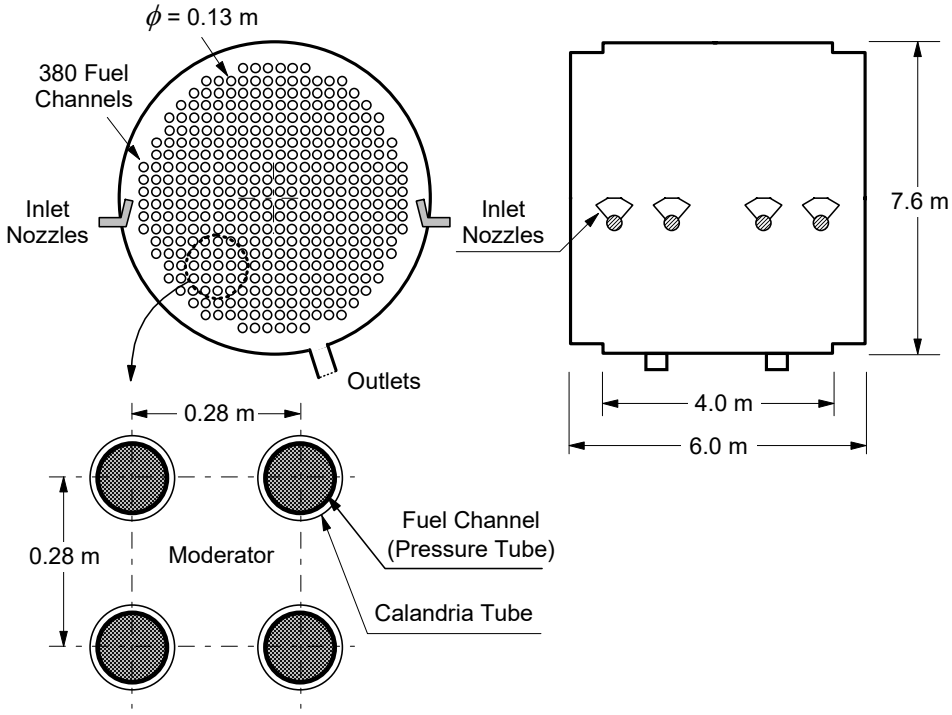

Figure 6.1 The calandria vessel of CANDU-6 reactors.

using the version 3 of Code_Saturne [1, 63] running on a high performance cluster of 7000 Intel Westmere EP X5650 (2.667 GHz). The Code_Saturne is a finite volume open-source software that has been developed by Électricité de France (EDF) for nuclear thermalhydraulic calculations. Since 2007, this software is distributed free of charge under the GNU general public license. It has the capability to solve the mass weighted time Reynolds-averaged Navier-Stokes set of equations [64] by using different solvers (*e.g.*, SIMPLE, SIMPLEC, etc.) and turbulence models (*e.g.* conventional turbulence models, LES, etc.). The governing equations can be written in a compact form as follows :

$$\begin{aligned}
\frac{\partial \rho}{\partial t} + \mathrm{div}\left(\rho \vec{u}\right) &= \Gamma \\
\frac{\partial \rho \vec{u}}{\partial t} + \mathrm{div}\left(\rho \vec{u} \otimes \vec{u}\right) &= -\mathrm{grad}\left(P\right) + \mathrm{div}\left(\underline{\underline{\tau}} - \rho \underline{\underline{R}}\right) + \vec{S}_u \\
\frac{\partial \rho a}{\partial t} + \mathrm{div}\left(\rho \vec{u} a\right) &= \mathrm{div}\left(\underline{J}_a - \overline{\rho a'' u''}\right) + S_a
\end{aligned} \tag{6.1}$$

where () indicates tensorial quantities. In this equation, Γ indicates the mass source term,

τ the viscous stress tensor, $\underline{\underline{R}}$ the Reynolds' stress tensor, S are the momentum and energy source terms, a is a scalar property, $\underline{J_a}$ is the vector flux of the scalar expressed by Fick-Fourier's law : $\underline{J_a} = \kappa_a \vec{\nabla} a$ and u'' and a'' are the fluctuating components of the Favre's decomposition method [64]. This set of equations is closed with an appropriate turbulence model. Based on our previous experience [65], we have selected the standard $\kappa - \epsilon$ model proposed by Launder and Spalding [66] in conjunction with the SIMPLEC algorithm [67]. In addition, to avoid using the Boussinesq's approximation, we have included into the thermal-hydraulic model the relationships required to evaluate the thermo-physical properties of the water as a function of its temperature. The calandria shell as well as the tubes are represented as wall boundary conditions.

The reactor physics calculations were carried out using the space-kinetic DONJON software developed at Polytechnique Montreal [81] ; more information about the reactor physics equations are given in Section 6.6. This numerical tool was used to generate the average power distribution within the reactor core required to start performing CFD moderator flow simulations. Thereafter, CFD simulated fluid temperature distributions were used by DONJON to recalculate new power distributions. This procedure was repeated until the changes were considered small enough ; more details about the methodology is presented in Section 6.6. The Figure 6.2 presents the power distribution of a CANDU-6 equilibrium core generated using the aforementioned method, which was then applied as initial conditions in Code_Saturne. It must be pointed out that these power distributions were obtained using a fuel burnup map of Gentilly-2 nuclear power station, before it was definitively shut down on December 28, 2012. The values of the power per bundle were implemented into the flow equations as space dependent volumetric thermal sources. In particular, it must be pointed out that the power distribution shown in Fig. 6.2 differs considerably to the power profile used amongst other by Sarchami [12]. In fact his power map does not represent real reactor values where, the neutron flux should be higher in the central zone of the reactor core and due to the presence of the reflector it cannot be equal to zero at the boundaries of the domain.

6.4 Study of boundary conditions used for the moderator injection system

From a CFD simulation viewpoint one of the major task that must be correctly handled along the calculations is the huge difference that exists between the dimensions of the injectors and the rest of the calandria vessel. Fig. 6.3 shows the principal geometrical characteristics of flow injectors used in CANDU-6 nuclear reactors [29]. They contain three baffles plates that distribute the total flow across four similar slightly divergent subchannels. It is obvious that a fine flow simulation inside the injectors necessitates a large number of discretization cells which in turn should not affect the refinement around the walls of calandria tubes. It is

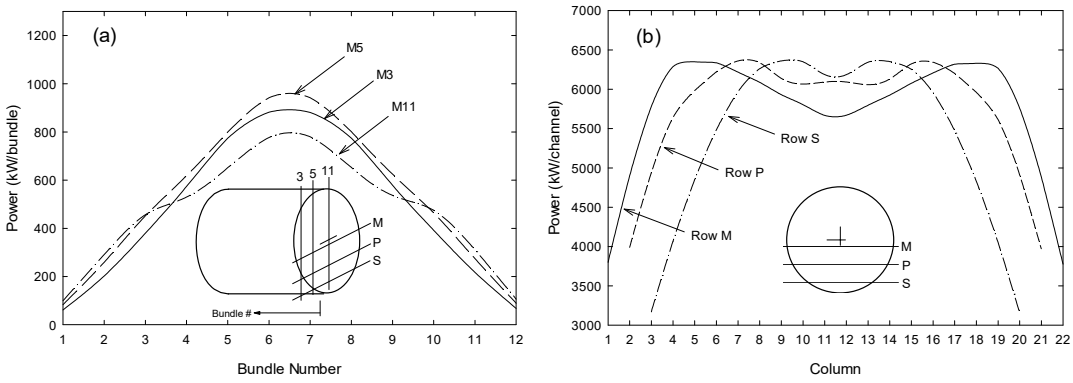

Figure 6.2 Representative time average power distribution of CANDU-6 reactors ; a) Axial distribution, b) Radial distribution.

apparent from Fig. 6.3, that the overall dimensions of the injectors are considerably smaller than the entire reactor vessel shown in Fig. 6.1. Furthermore, based on a hydraulic diameter of approximately 0.01 m, the Reynolds (Re) number inside each subchannel is quite high (Re = 379000) ; therefore, the flow is fully turbulent.

Implementing a turbulent jet model by increasing mesh refinement around them and adding them into the entire integration domain, increases considerably the required computational power. To limit this effect, some efforts were performed to implement analytical models of flow jets [68] and thus, retain the maximum computational resources for solving the rest of the flow within the calandria. Even though 2-D simulations performed using different flow injector models did not provide any apparent effect on moderator flows [39], some recent works demonstrate contradictory results which will be discussed in the following paragraphs.

The effect of outlet injector flow profiles in the configuration of the moderator has been the center of attention in several studies. In the development of MODTURC, Szymanski et al. [17] considered a uniform velocity profile with a constant value of about 2 m/s, *i.e.* close to the nominal design value given in [29]. Carlucci et al. [18] also implemented uniform velocity profiles in the MODTURC-CLAS flow solver to simulate the moderator flow in CANDU-9 reactors and validated the results against data collected in the MTF at AECL [6]. In general, the simulations were in very good agreement with the data. A similar approach was used amongst others by Kim et al. [24, 25] (*i.e.* uniform outlet jet velocity profile) ; nevertheless, they applied twice the nominal value of CANDU-6 without providing any explanation about this particular choice. Therefore, for a similar moderator power, this high inlet flow velocity predicted a moderator configuration which does not necessarily corresponds to actual reactor operation conditions. From these results it is difficult to infer how the outlet jet flow velo-

city distribution affect the configuration of the flow within the calandria vessel. In a more ambitious work, Sarchami [12] and Sarchami et al. [30] combined a complete discretization scheme of the injectors with the rest of the calandria vessel, *i.e.* they considered the injectors as parts of the hydrodynamic integration domain. Even though the authors deployed a substantial effort to simulate completely the moderator flow, the number of cells they used was not enough to assure converged solutions (They did not perform a grid sensitivity study.) Furthermore, they assumed a straight flow entrance pipe at the inlet of each diffuser. However, in the actual CANDU-6 design the flow enters into the injector system through a pipe elbow, as shown in Fig. 6.3. It is obvious that the presence of these curved structure affects the flow inside the diffuser and consequently the way the flow is distributed at the outlet.
Recently, Choi et al. [27] used the outlet flow injector velocity profile previously simulated by Yoon & Park [26], as inlet boundary conditions. In fact such a Dirichlet type boundary condition allowed them to reduce calculation costs (*i.e.* avoid full injector numerical modelling for a total of eight nozzles to be carried out). Nevertheless, the validity of the profile simulated by Yoon and Park as well as the method they implemented which was subsequently applied by Choi et al. are questionable. Furthermore, Choi et al. applied a linearly extruded 2-D profile arbitrarily selected from a 3-D one [26], to generate a pseudo 3-D distribution using coarse grids around the injectors. Transforming a 3-D vector profile using this methodology seems to be incorrect, in particular because the 3-D vectors of Yoon & Park show important re-circulation and reverse flows along the depth of the diffuser. However, one of the major weakness of this approach is due to wrong calculations performed by Yoon & Park, who simulated only the flow within the entire injector using a 3-D CFD model in Ansys-CFX software. They applied a very fine mesh grid and the $\kappa - \omega$ SST turbulence model ; the predicted velocity profile varied between negative (reverse flow) and very high positive values of up to 10 m/s. It must be pointed out that this velocity is about 5 times higher than the nominal CANDU inlet velocity [17, 29]. It is obvious that the 3-D extrusion of such a velocity profile, as was implemented by Choi et al. [27], largely overestimates the inlet flow velocity and thus, affects the moderator configuration. Moreover, in the simulations of Yoon & Park, a constant pressure of 1.5 bars at the diffuser outlet was imposed, therefore they did not take into account the fact the hydrostatic pressure affects the velocity distribution. Imposing such a boundary condition just at the outlet is not correct because such a constant pressure affects the distribution of the flow velocity. In order to analyze the effects of imposing hydrostatic boundary conditions to the velocity distributions at the outlet of the diffuser, we performed three 2-D simulations using the same CFD software (*i.e.* Ansys-CFX). For the first calculations, which are similar to those performed by Yoon & Park [26], we imposed a constant static pressure boundary condition just at the outlet of the diffuser ; this is represented by

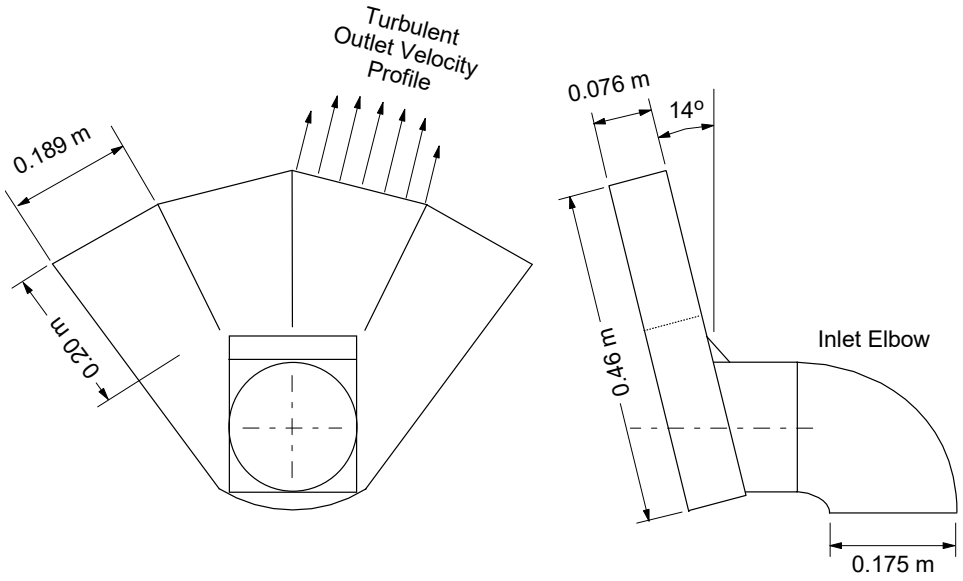

Figure 6.3 Inlet nozzle assembly of a CANDU-6.

the injector planes BC1 illustrated in Fig. 6.4. The two other numerical tests consist of the same injector geometry but implemented in a hydrodynamic domain with variable heights W and widths L. These values, which were changed from 10 to 20 times the diffuser hydraulic diameter, correspond to the boundary conditions BC2 and BC3 in Fig. 6.4, respectively.
The velocity profiles obtained by imposing the aforementioned boundary conditions, sampled at the outlet level are presented in Fig. 6.5. It must be pointed out that the use of boundary BC1 (*i.e.* similar condition applied by Yoon & Park [26]) produced unsatisfactory converged solutions. This is quite possibly due to the strong coupling between velocity and pressure imposed just at the outlet of the injector. Similar to Yoon & Park, the simulations present important flow recirculation with reversing flows occurring along the outlets (at about x/L=0.3 and x/L=0.7 in Fig. 6.5). Moving the pressure boundary conditions from BC2 to BC3 produced very similar results (they appear overlapped in Fig. 6.5) without flow recirculation zones. Therefore, based on these observations, the numerical convergence of the simulations presented by Yoon & Park is quite questionable, consequently their results should not be used as input boundary conditions for simulating CANDU-6 moderator flows.
According to the aforementioned discussion, the velocity profiles given in [26] represent a distorted flow distribution for CANDU-6 moderator flows, characterized by abnormal and extremely high narrow velocity peaks. Accordingly, only a small fraction of the outlet jet cross-sectional area contributes to the effective moderator flow rate, which should represent a major flaw of CANDU-6 design. However, previous works indicate that the moderator

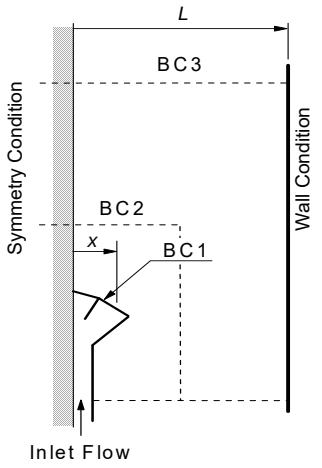

Figure 6.4 Studied cases for the flow diffuser.

flow distribution within the calandria is not sensitive to the water profile at the outlet of the injectors [39, 68]. The almost independent behavior of the moderator flow distribution with respect to inject flow profiles can be justified by the following facts. The injected water travels more than 12 m along the inner periphery of the reactor vessel (see Fig. 6.1) at a maximum velocity that is initially slightly higher than 2 m/s. Therefore, its interaction with the internal wall should modify the profile. In turn, towards the end of this almost circular trajectory the water jet interacts with a similar but opposite one coming from the symmetric injector counterpart. This interaction produces a very complex zero flow velocity region (*i.e.* a stagnation or flow impingement point), while the presence of horizontal channels tends to considerably scatter the flow.

Based on the above discussion, the simulations presented in this paper were carried out using a turbulent velocity profile. It was assumed that the flow becomes fully developed inside the subchannels formed by two consecutive injector baffle plates (see Fig. 6.3). Hence, Dirichlet boundary conditions were imposed at the outlet of each diffuser subchannel by implementing the following empirical power law [82] :

$$\frac{V(x)}{V_{\max}} = \left(1 - \frac{x}{L}\right)^{1/n} \tag{6.2}$$

where V(x) is the velocity profile, x is the relative coordinate of the injector with respect to its centerline and L is the half distance between two consecutive baffles. In this equation n is a constant that depends on the Reynolds number. For CANDU-6 diffusers (*i.e.* Re = 379000) we have estimated that this constant is equal to 8 [82].

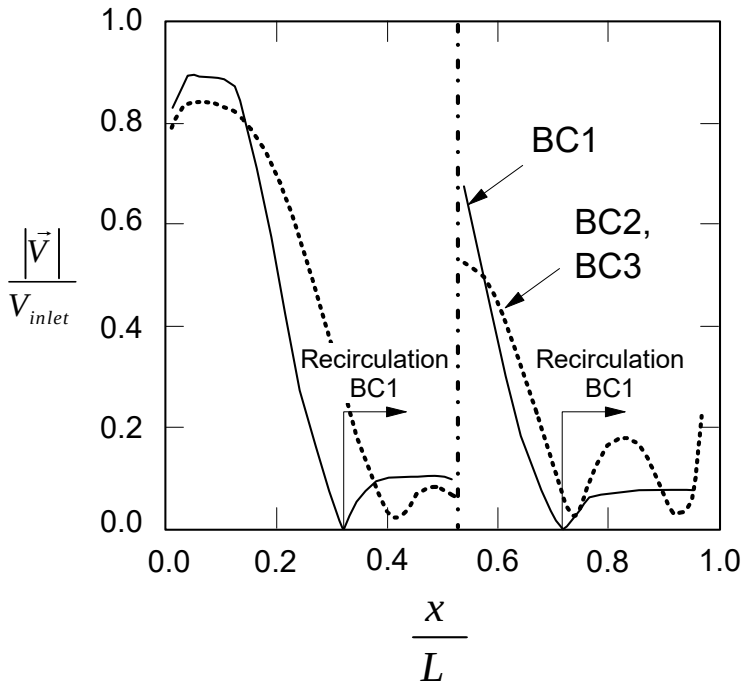

Figure 6.5 Velocity at the centerline of the flow diffuser using three different boundary conditions.

6.5 Numerical grid and sensitivity analysis

A 3-D grid was generated using the ICEM-CFD software [83] ; Fig. 6.6 shows the mesh topologies applied around the calandria tubes and the injectors, as well as in the outlet region. For the present work, the mesh is formed by 30×10^6 hexahedrons (dominantly) and tetrahedrons cells ; this value was selected after analysing the results vs. the number of cells. Before performing full 3-D moderator CFD simulations, the sensitivity of the calculations with respect to the number of cells was studied and analyzed. To this purpose, calculations were repeated by increasing the number of cells according to the following five steps : 2.5×10^6, 10×10^6, 20×10^6, 30×10^6 and 44×10^6 cells. The convergence threshold used for the current simulations was as recommenced in the user guide of Code_Saturne [1, 63]. Despite the complexity of the geometry, a particular care was taken to maintain the same cell stretching ratio along the three directions of the grids. The magnitude of the flow velocities, V_i, were sampled along the centerline of a plane tilted 60° with respect to a horizontal mid plane passing across the center of the calandria. To determine the convergence rate as a function of the number of cells, the results obtained using 44×10^6 cells were considered as reference to estimate the root mean square of the differences for flow velocities, according to :

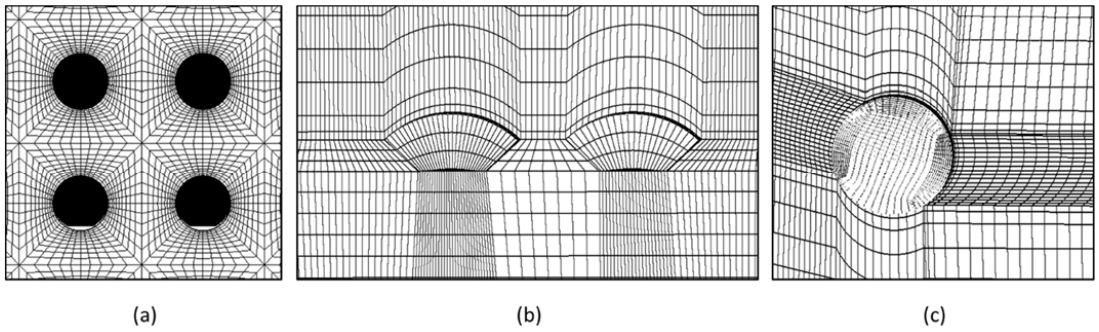

Figure 6.6 Mesh topology ; a) around the calandria tubes, b) around the injectors, c) moderator outlet.

$$\Delta V_{\mathrm{RMS}} = \sqrt{\frac{1}{N}\left[\sum_{i=1}^{N}\left(V_i - V_{\mathrm{ref},i}\right)^2\right]} \tag{6.3}$$

The results obtained from this equation for the entire set of numerical tests are presented in Fig. 6.7. At least two conclusions can be addressed from this figure. First, increasing the number of cells from 20×10^6 to 30×10^6 clearly indicates that the simulations become almost independent of the number of cells (*i.e.* the difference drops below +/- 0.004 m/s). Second, 3-D CFD simulations of CANDU-6 moderator flows necessitates at least 30×10^6 cells to converge. This is an important requirement that most numerical works performed in this field do not satisfy (see amongst others : [24, 27, 55, 59]). For this reason, most of these numerical simulations and in particular the conclusions given by their authors about the moderator flow behavior, should be considered with some care.

6.6 Validation of Code_Saturne flow simulations against experimental data

The objective of this section is to determine the capability of the Code_Saturne software for performing 3-D simulations of moderator flows. To this purpose, calculated velocities were compared to the recently published data collected at different locations in a Moderator Circulation Test (MCT) facility [9, 84–86]. This experimental set-up, which represents 1/4 scaled model of the calandria of a CANDU-6 reactor, was manufactured by the Korea Atomic Energy Research Institute to provide 3-D flow measured data. This model reproduces the most important features of the CANDU-6 by completely satisfying the geometrical similarity with respect to the real size nuclear reactor. Furthermore, the facility is instrumented with high precision PIV (Particle Image Velocimetry) measurement devices to determine local flow velocities in all directions.

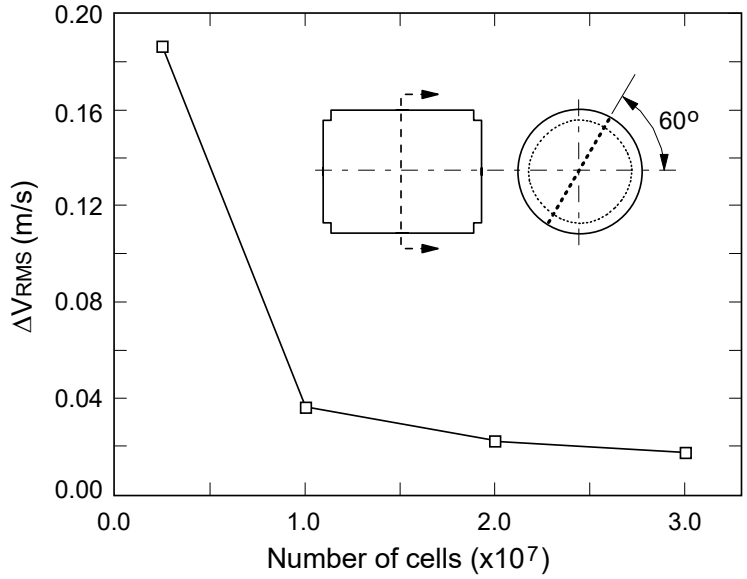

Figure 6.7 RMS of the difference between the magnitudes of 3-D flow velocities with respect to results obtained using 44×10^6 cells.

The topology of the discretization implemented to perform the CFD validation is similar to the one used for simulating the real CANDU-6 discussed in Section 6.3 (*i.e.* the same as Fig. 6.6). Furthermore, the velocity profile defined by Eq. 6.2 was also considered as inlet flow boundary conditions. The vertical velocity components predicted by Code_Saturne were then compared against experimental values collected along a radial direction on the following planes [9] : (x=0 m, z=-0.295 m), (x=0 m, z=-0.030 m), (x=0.216 m, z=-0.030 m) and (x=0.288 m, z=0.030 m) ; the results are shown in Fig. 6.8. Since Kim et al. [84] and Kim [9] have not provided information about the accuracy of their measurements, herewith we have assumed that they should be similar to those reported by Paul et al. [7] who used a similar PIV technique on a comparable configuration of horizontal tubes (*i.e.* +/- 5% of the readings). In general, as shown in Fig. 6.8, the simulations reproduce the experimental trends quite well. It is interesting to observe that close to the peripheral flow of the injector, they capture not only the high velocity region but also the low velocity imposed by the calandria wall condition which does not appear in the data. Moreover, the predicted fine flow fluctuations are due to the effect of the horizontal tubes on the flow which have not been captured by the experiments.

It must be pointed out that the results obtained by using the Code_Saturne software are substantially superior to those presented by Kim [9] who considerably underestimates the experimental trends. Hence, taking into account the complexity of this kind of flows and

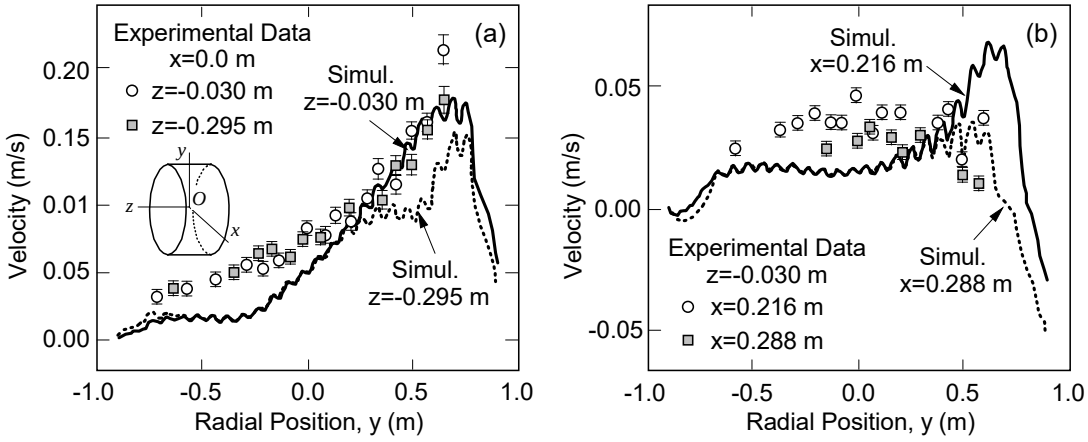

Figure 6.8 Comparison of the predictions of Code_Saturne against MCT experimental data [35] ;a) Lateral plane located at x = 0 m, b) Axial plane located at z = -0.03 m.

the uncertainty we have about the precision of the measurements, it is considered that Code_Saturne in conjunction with the proposed numerical scheme, is suitable for handling CANDU-6 moderator flows.

6.7 Moderator flow configurations in a 3-D domain

Khartabil et al. [6] carried out dimensional analyses to determine the most important flow parameters that can be used to characterize moderator flows. Consequently, they identified the Richardson number (Ri) as the key parameter for correlating moderator flow configurations ; this number is defined as :

$$Ri = \frac{g\alpha\dot{Q}D}{C_p\rho A_i V_i^3} \tag{6.4}$$

where g, α, $\dot{Q}$, D, C_p, A_i and V_i are the acceleration of gravity, the coefficient of thermal expansion, the heat generation rate, the vessel diameter, the specific heat at constant pressure, the cross sectional area of the nozzle and the inlet flow velocity, respectively. This number, which represents the ratio between gravitational and inertial forces, has been already used to correlate the moderator flows amongst others by : Carlucci [15] ; Carlucci & Cheung [11] ; Mehdi Zadeh et al., [76]. It is obvious from Eq. 6.4 that for adiabatic systems the Richardson number is equal to zero and it increases with increasing heat generation rate. According to previous works [76], depending on the value of Ri, three moderator flow configurations can be triggered within the CANDU-6 calandria vessel. These flow configurations are characterized

as : i) inertia-dominated, ii) mixed-type and iii) buoyancy-dominated. They are triggered by the competition between inertia and buoyancy forces acting on the fluid. Each of these flow configurations can bring about important moderator temperature distributions which in turn can affect the reactivity. As these configurations were characterised based on 2-D CFD simulations [11, 76], some authors [24, 59] argued that they are not representative of the 3-D flow distribution occurring in the reactor vessel. Within this context, the objectives of this section are twofold. First, to present the flow distributions obtained from 3-D steady state CFD simulations of a CANDU-6 carried out using the numerical scheme discussed in Section 6.3 and second, to generate the initial flow conditions required to couple CFD with reactor physics calculations. A first simulation for a nominal inlet flow velocity V_i =2 m/s was performed without heat addition, *i.e.* under almost isothermal flow conditions. The velocity contours as well as extracted velocity values sampled along an axial line with coordinates (-0.65 m, 1.75 m, 0 m) and (-0.65 m, 1.75 m, 6 m) are presented in Fig. 6.9.

Regardless of the asymmetric location of the outlets, it can be observed that with absence of thermal sources, the moderator adopts an almost symmetrical axial distribution. Nevertheless, it must be pointed out that the location of the injectors with respect to the vessel vertical mid-plane is not perfectly symmetric, which can explain the slight difference shown in Fig. 6.9b. Despite this fact, the values given in this figure illustrate an almost symmetric distribution with respect to the calandria mid plane, where peak velocities occur around the outlet regions, *i.e.* the maximum difference between outlet 1 and outlet 2 represents less than -4%. To further study the flow behavior as a function of inlet flow conditions, similar simulations were repeated for different values of Ri. To this purpose, the thermal power distributions given in Fig. 6.2 were applied to all the cases studied and the inlet flow velocity was consequently increased. To better determine whether or not the configurations depend on the axial location in the vessel, both flow velocities and temperatures were collected at two different planes. One of these planes corresponds to the calandria mid-plane (*i.e.* at z=0) and the second one passes across one of the outlets (*i.e.* where the axial velocity distributions present the peaks shown in Fig. 6.9b). For $Ri < 0.04$ the flow distribution is mainly governed by inertia (*i.e.* buoyancy forces are very small [76]). Consequently, two opposite flow jets are able to meet at the top of the calandria vessel forming a stagnation region (impingement point) which triggers a strong downward flow across the tubes. The comparison of the velocity maps collected over two planes at different axial locations, as shown in Figs. 6.10a and 6.10b, indicates that in both cases the impingement point occurs at the upmost region of the vessel forming an angle of 90° with respect to the horizontal plane.

It must be pointed out that any dissimilarity between these two figures are mainly due to the apparent difference in the color scales. In fact, the presence of a high velocity outlet flow

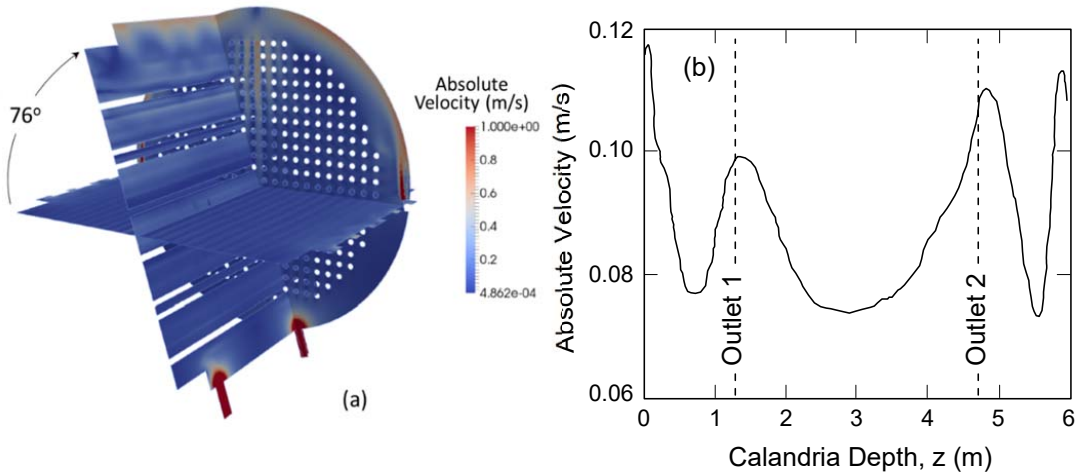

Figure 6.9 Simulation at adiabatic flow conditions; a) Velocity map, b) Absolute velocity along an axial axis.

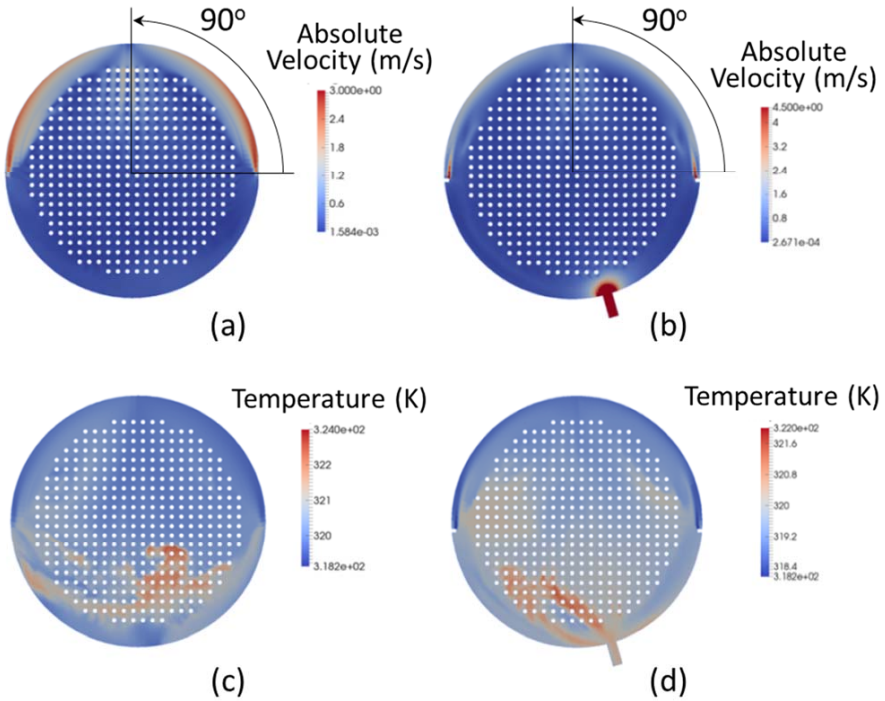

Figure 6.10 Velocity and temperature maps of the inertia-dominated flow configuration for Ri = 0.01; a) and c) center plane at z = 0 m,b) and d) plane crossing one of flow outlets.

region in Fig. 6.10b, tends to overwhelm the colors within the uppermost circumferential zone. Figures 6.10b and 6.10d show the flow temperature distributions predicted at the aforementioned calandria planes. At both locations, the temperatures increase toward the center and bottom of the vessel. Consequently, for this type of configuration the upper half of the moderator has an average temperature much lower than the central one. Furthermore, it is clear that the differences observed between Figs. 6.10c and 6.10d are caused by the presence of the outlet. Despite this fact, the inertia-dominated moderator configuration seems to occur simultaneously everywhere within the calandria vessel, independent of the axial location.

From full size 2-D numerical simulations and for $\mathrm{Ri} > 0.04$, it has been observed that adding heat into the moderator provokes a transition from inertia-dominated to a mixed-type configuration [76]. This behaviour is mainly due to the competition between inertia and buoyancy forces. In fact, the addition of heat increases the mass density gradients and thus, brings about an upward flow that counterbalances the downward one. Under these conditions, the flow undergoes significant hydrodynamic instabilities [78]. Both the amplitude and the dominant frequency of these fluctuations increase with increasing Ri number, that is when the magnitudes of inertial and buoyancy forces become comparable. Nevertheless, increasing further the Richardson number provokes a remarkable reduction in frequency and amplitude. Consequently, there is a limited range of Ri numbers ($0.04 < \mathrm{Ri} < 0.12$) for which the moderator shows almost periodic angular oscillations. Within this range, the impingement point moves more or less periodically along almost a quarter of the calandria outermost circumferential length and the flow distribution becomes completely asymmetric. Mehdi Zadeh et al. [78] observed that this angular displacement occurs preferentially toward the right hand side of the vessel (see Fig. 6.1). They argued that this behavior is controlled by the uneven location of the outlets. Fig. 6.11 shows velocity and temperature maps obtained from 3-D simulations carried out in a similar manner to the former case, but for $\mathrm{Ri} = 0.05$ (*i.e.* for a mixed-type moderator flow).

For both sampling planes, Figs. 6.11a and 6.11b show quite similar angular clockwise displacements of the impingement point (*i.e.* $\theta < 90\ ^\circ$). 2-D time dependent simulations indicate that this point moves clockwise and counter clockwise with a predominant frequency that depends on the value of Richardson's number [78]. As discussed above, this flow behaviour characterizes a mixed-type moderator configuration. In addition, the flow temperature maps obtained from the same 3-D simulations, shown in Figs. 6.11c and 6.11d, indicate a higher flow dispersion, as compared with the inertia-dominated flow given in the Figs. 6.10c and 6.10d. In particular, it can be also observed that the mean flow temperature increases toward moderator regions located above the horizontal mid plane (Compare Figs. 6.11c and 6.11d with Figs. 6.10c and 6.10d.) Furthermore, the moderator temperature distribution is affected

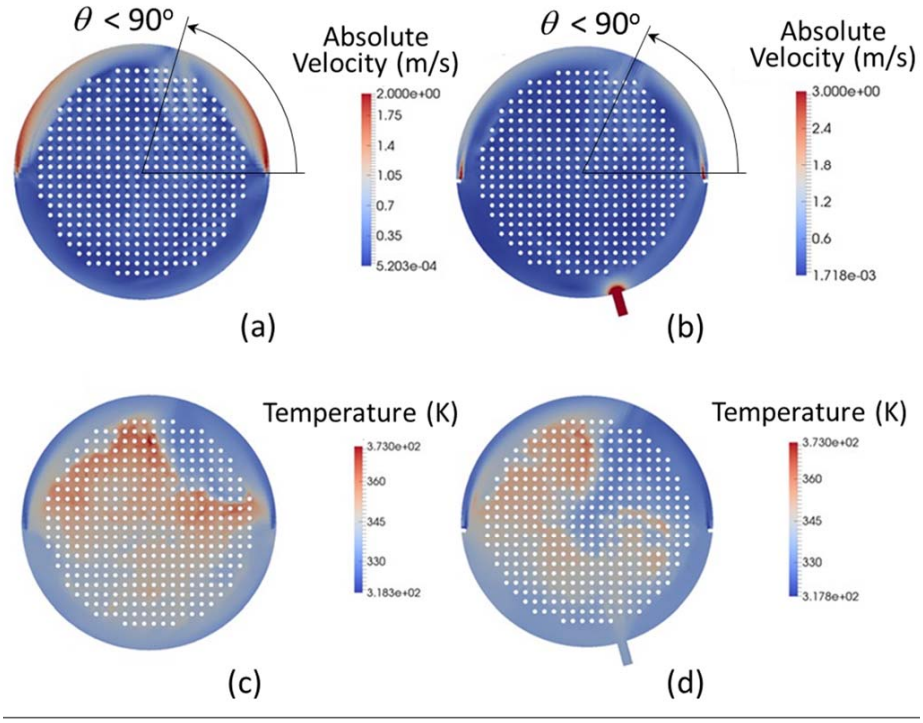

Figure 6.11 Velocity and temperature maps for a mixed-type configuration, for Ri = 0.05 ; a-c) center plane at z = 0 m, b-d) plane crossing one of the outlets.

by the highest thermal load taking place at the center of the reactor (see the Fig. 6.2), as can be observed by the difference between Figs. 6.11c and 6.11d.

For relatively high Richardson numbers, above Ri =0.12 (increasing the thermal power or decreasing the inlet flow velocity (Eq. 6.4), the moderator flow adopts a buoyancy-dominated configuration [76, 78].

Under these conditions, buoyancy counterbalances completely flow inertia, therefore the water jets are unable to penetrate into the high temperature region that develops at the top of the calandria. Consequently, the moderator becomes thermally stratified. Velocity and temperature maps collected from 3-D CFD simulations are presented in Fig. 6.12. For the two sampling planes, Figs. 6.12a and 6.12b unambiguously show that for Ri = 0.12 there is no evidence about the formation of a jet impingement point. In fact, the temperature maps presented in Figs. 6.12c and 6.12d, confirm that for this Ri number the moderator is thermally stratified, characterized by temperature distributions that are very similar and independent of the calandria axial location. It is obvious from Eq. 6.4 that this kind of flow distribution must spread out by increasing Richardson's number.

The numerical results presented in this section provide solid indications that the moderator flow configurations, as described in the open literature for 2-D simulations [11, 15, 76], also

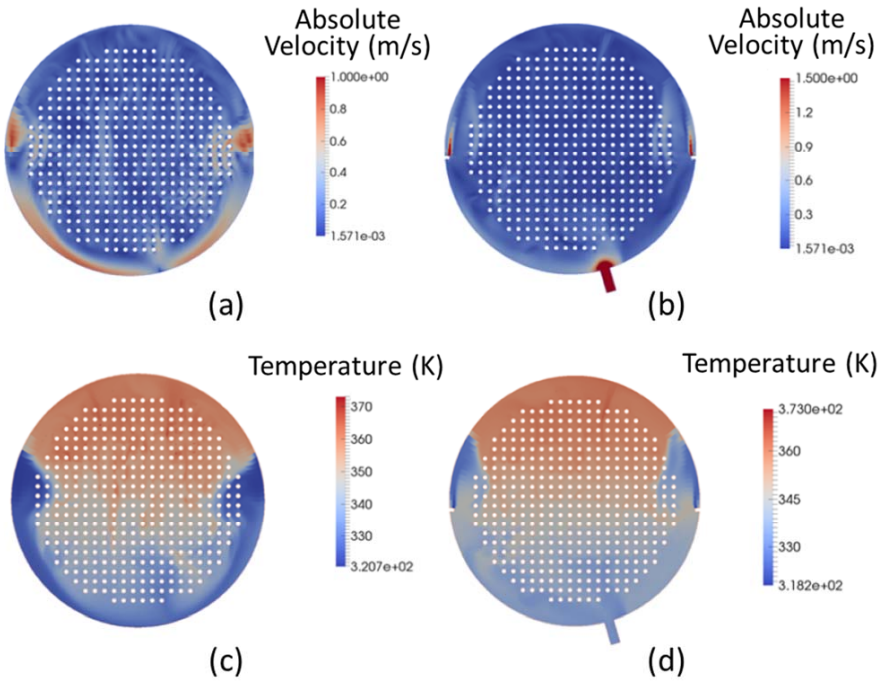

Figure 6.12 Velocity and temperature maps for a buoyancy-dominated configuration, for Ri = 0.12 ; a-c) center plane at z = 0 m, b-d) plane crossing one of the outlets.

occurs within the entire reactor core. Furthermore, asymmetric locations of the outlets and the injectors (Fig. 6.1) introduce slight distortions in the axial flow distributions which do not noticeably affect the moderator configurations as a function of Richardson number. The transitions from one configuration to another vs. this number determined at different axial planes, correspond to similar values determined from 2-D studies. It is obvious that this argument contradicts those given by other authors [12, 24, 59] who claimed the existence of strong axial flow asymmetries which in turn affect the radial and angular flow distributions. The major differences perceived amongst the simulations given in these works with respect to the present one, are very possibly due to inconsistent convergent calculations caused by the limited number of discretization meshes they used. From this discussion, we conclude that both the CFD modelling approach and the numerical scheme implemented for simulating the thermal-hydraulics behavior of the moderator are accurate enough to couple them with reactor physics calculations. In particular, we are interested to determine how different moderator flow configurations (*i.e.* the heavy water temperature distribution) may affect reactor's reactivity.

6.8 Coupling 3-D CFD moderator flow simulations with reactor physics calculations

. As discussed above, the temperature of the moderator can vary substantially in the calandria vessel, locally affecting the heavy water mass density. It is then possible that these variations have a nonnegligible impact on macroscopic cross-sections. Thus, the aforementioned moderator configurations influence both neutron moderation and absorption rates and consequently reactivity. Within this framework, this section presents thermal-hydraulics reactor physics coupled calculations. The latter ones were carried out using Version 3.02 of the DONJON numerical code. This is an open source reactor physics software, developed at Polytechnique Montréal [2, 81], that solve space – kinetic diffusion equations in the entire core ; the equations can be written in a compact form as :

$$\begin{aligned} &\Sigma\left(\vec{r},E\right)\phi\left(\vec{r},E\right)-\operatorname{div}\left(D\operatorname{grad}\left(\phi\left(\vec{r},E\right)\right)\right)= \\ &\int_0^\infty dE'\Sigma_{a0}\left(\vec{r},E'\rightarrow E\right)\phi\left(\vec{r},E'\right)+\frac{\chi\left(E\right)}{k_{\text{eff}}}\int_0^\infty dE'\nu\left(E'\right)\Sigma_f\left(\vec{r},E'\right)\phi\left(\vec{r},E'\right) \end{aligned} \tag{6.5}$$

where, Σ is the total macroscopic cross section, $\vec{r}$ the spatial coordinates, E the neutron energy, ϕ the neutron flux, D the diffusion coefficient, Σ_s the isotropic scattering cross-section, χ the fission spectrum that takes into account delayed neutrons, ν the average number of neutrons generated per fission and Σ_f the fission macroscopic cross-section. DONJON code has the capability of handling all CANDU-6 neutron flux control devices (*i.e.* control rods, zonal neutron absorbers, etc.) ; nevertheless, for the purpose of the present work these features were not included during the calculations and the simulations were performed at steady state conditions. It must be pointed out that the performance of DONJON to simulate CANDU reactors has been largely validated by comparing its predictions with reactor physics benchmarks [87]. This is one of the reasons that this code is largely used not only by the Canadian nuclear industry but also internationally. The strategy implemented to couple fluid to neutronic calculations was established as follows :

a) Perform an initial estimation of the neutron flux distribution for a constant reactor thermal power of 2060 MW (*i.e.* 103 MW dissipated within the moderator), using an iso-thermal moderator at 346.15 K (73°C). This value was selected because it corresponds to typical operating conditions of CANDU-6. In addition, this calculation was performed for a core at equilibrium and a real burnup of Gentilly-2 nuclear power plant.

b) For a given value of Richardson's number, apply the neutron flux calculated at a) to perform a first CFD calculation. The thermal power dissipated within the moderator is

assumed proportional to the power produced in the fuel ; thus, the inlet moderator flow velocity is adjusted to obtain the required value of Ri (see Eq. 6.4).

c) Use the actual moderator temperature distribution obtained in b) to calculate the volumetric mass of the moderator flow everywhere.

d) Calculate the average mass density of the heavy water (moderator) around each of the 4560 fuel bundle and use these values as new inputs in the DONJON code.

e) Recalculate the moderator temperature distributions for the actual moderator thermal power obtained from step c).

f) Repeat steps c) to e) until both CFD and neutron flux simulations converge simultaneously. The convergence criterion applied in Code_Saturne was the same presented in Section 6.3, in DONJON it was $\left|k_{\text{eff}}^{i-1} - k_{\text{eff}}^{i}\right| / k_{\text{eff}}^{i-1} \leq 10^{-6}$.

Figure 6.13 shows the initial thermal power distribution predicted by DONJON in step a). The values shown in Fig. 6.13 were then considered as a reference to determine the effect of the moderator temperature distribution on the k_{eff} . Furthermore, due to the unsteady nature that characterizes the mixed-type moderator configuration [78], only the following two cases were treated : i) inertia dominated and ii) buoyancy-dominated.

The effect of the moderator temperature distribution was initially studied for an inertia-dominated configuration ; thus, the Richardson number was kept constant (*i.e.* Ri = 0.01) for the entire simulation set. In order to determine possible moderator temperature effects on the neutron flux distribution (*i.e.* the thermal power), after achieving convergence, the reference power distribution calculated in the step a) and shown in Fig. 6.13 (*i.e.* reference values) were subtracted from the last ones. Therefore, we consider that any difference observed between them must be related to the effect of the moderator flow configuration ; the results are presented in Fig. 6.14. It must be pointed out that for the same simulation (with heat addition) it was also observed that along the axial position at the calandria centre, the maximum averaged flow temperature distribution changed very slightly (about +/- 1 K). This result confirms that the axial flow distribution does not affect the moderator flow configuration in a normal plane, which seems to develop similarly to the adiabatic case presented in Fig. 6.9. As shown in Figs. 6.10c and 6.10d, for the same Ri number the moderator temperature is lower in the upper region as well as in the periphery of the calandria and it is higher toward the center, increasing slightly close to the outlets. In view of this, the distribution shown in Fig. 6.14a seems to be mainly controlled by the moderator density ; the change in density affects the moderator macroscopic cross-sections. A comparison of Fig. 6.14a with Fig. 6.14b indicates that higher the moderator temperature is, the lower is the averaged power distribution. Thus, the local moderator temperature seems to have a negative

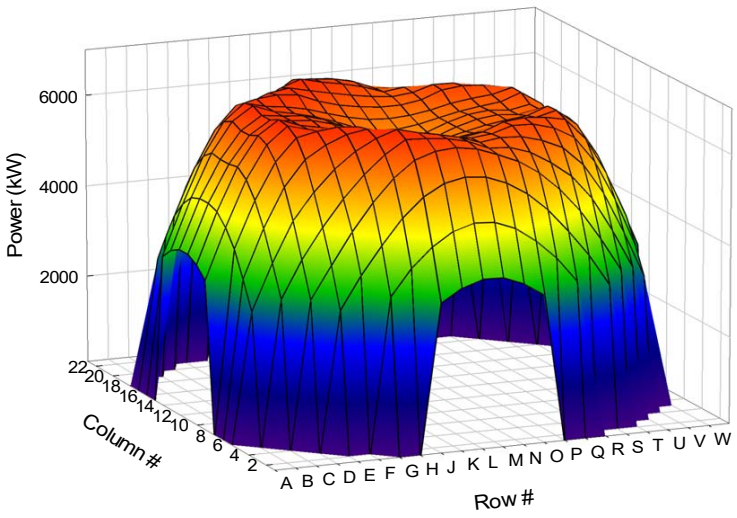

Figure 6.13 Reference time averaged bundle thermal power predicted by DONJON for an isothermal moderator at 346.15 K (73°C).

effect on the reactor thermal power distribution.

Similarly to the former case, the effect of moderator temperatures on the reactor power distribution were simulated for a buoyancy-dominated configuration. The Richardson number and the overall reactor power were maintained constant at Ri = 0.21 and 103 MW, respectively. After satisfying the convergence criteria for both CFD and reactor physics calculations, the reference values of the power distribution (Fig. 6.13) calculated in step a) were subtracted from the last ones. The results of this difference as well as the flow temperature collected at different positions over the calandria mid-plane, are shown in Fig. 6.15. It is obvious that for a buoyancy-dominated flow the variations in the power distribution are much apparent than for the previous case. In fact a maximum change between the bottom and the top of the reactor of about 100 kW for the central channels (*i.e.* column 11) is observed. A comparison of this quite net tendency with the temperature distribution given in Fig. 6.15b, clearly indicates the local effect that the moderator temperature has on the reactor power distribution. Once again, the higher the local temperature is, the lower is the local thermal power.

In order to further investigate such a notable coupling that seems to exist between local moderator temperatures and power, a typical CANDU-6 nuclear reactor lattice was simulated using version 3.6 of the neutron transport software DRAGON developed at Polytechnique Montréal [88, 89]. These simulations were performed applying the same channel geometry as well as the same cross-section library used before in DRAGON software to generate the DONJON cross-section data base. To determine the effect of local moderator temperature

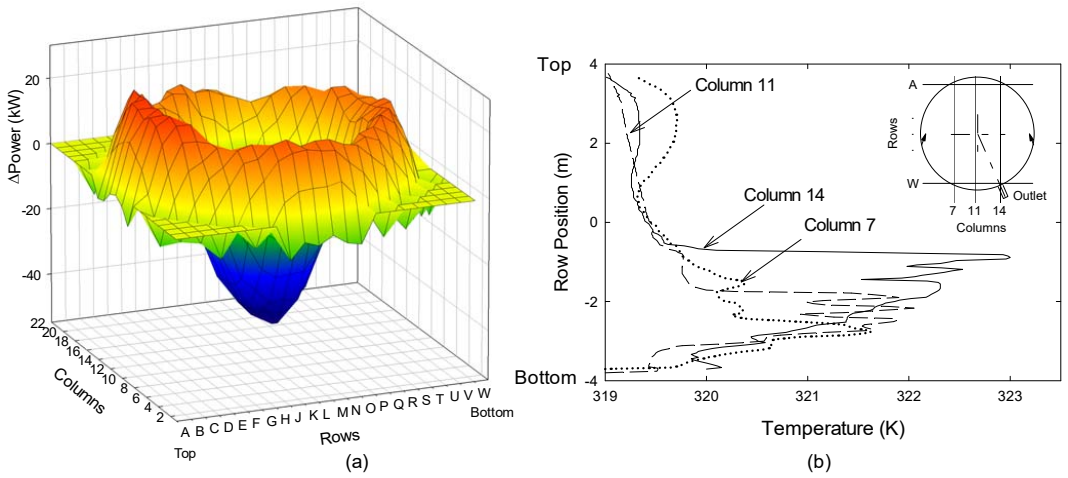

Figure 6.14 Predicted time averaged bundle power taking into account the moderator temperature distribution for an inertia-dominated flow configuration (Ri = 0.01) ; a) Difference between the actual averaged power and reference averaged power, b) Moderator temperature distribution at the mid-calandria plane.

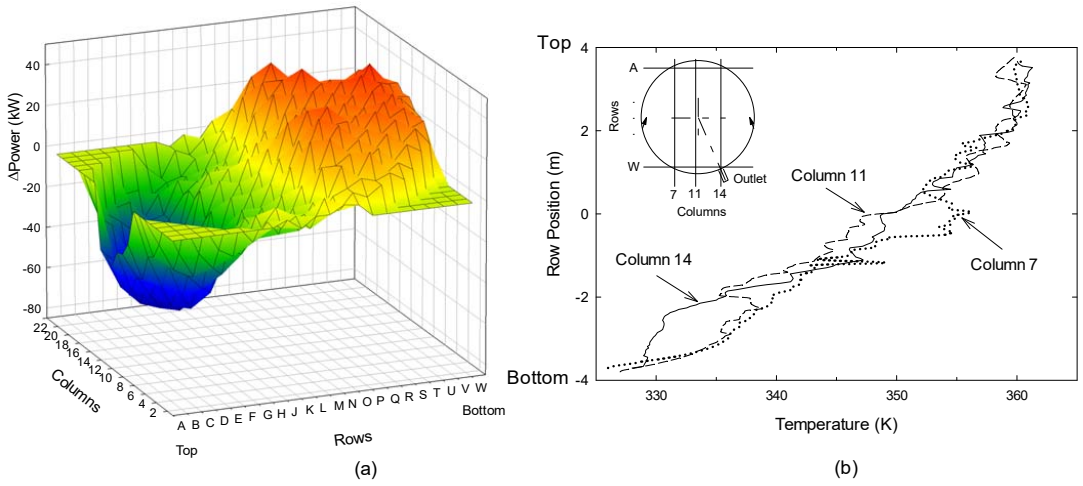

Figure 6.15 Predicted time averaged channel power taking into account the moderator temperature distribution for a buoyancy-dominated flow configuration (Ri = 0.21) ; a) Difference between the actual averaged channel power and reference averaged channel power, b) Moderator temperature distribution at the mid-calandria plane.

changes, for three different fuel burnups (*i.e.* fresh fuel at 0 days, as well as 150 and 300 days) the moderator mass density was modified only around 5 mm of water thickness layers surrounding the calandria tubes. The results, shown in Fig. 6.16a, indicate that the effective multiplication factor k_{eff} is affected negatively by a local decrease in the moderator density taking place very close to the walls of calandria tubes. Furthermore, it is also observed that the negative effect of the moderator temperature on k_{eff} increases with increasing burnup. This particular behavior is obviously reflected in the reactor multiplication factor calculated with DONJON, as shown in Table 6.1 for the three cases discussed above : isothermal moderator (reference case), Ri=0.01 and Ri=0.21. With respect to the reference case, k_{eff} slightly increases for the inertia-dominated configuration and decreases for the buoyancy-dominated case. This somewhat strange behaviour seems to indicate that the value of the multiplication factor is sensitive to local macroscopic cross-sections which are affected by moderator temperature distributions, which depend strongly on the moderator flow configuration. To this aim, Fig. 6.16b shows the results obtained from similar neutron transport calculations performed for the cell, but when the temperature is uniformly changed everywhere in the moderator. In this case, the effect of the temperature on the reactivity is completely different ; a negative effect occurs only for a fresh fuel, *i.e.* before Pu^{239} starts appearing. This is clearly shown by the positive slop that increases with increasing burnup.

Nevertheless, a comparison of Fig. 6.16a and 6.16b seems to indicate that the negative reactivity temperature effect observed when reactor physics calculations are coupled with the CFD of the moderator, are triggered only when local mass density changes occur. It is apparent that these results contradict those given in the open literature [5], where reactivity increases with increasing moderator temperature. Once again, it must be pointed out that these estimations were carried out by assuming that the temperature in the entire moderator changes uniformly, similar to the case shown in Fig. 6.16b. For this reason, this conclusion should be taken with some care because most reactivity vs. temperature studies do not consider local effects as given in the present work.

Even though the results presented in this paper were collected under steady state conditions, they provide some indications about a possible dynamics of moderator flows. Within this view-point, it is important to remark that the observed temperature-reactivity coupling behavior, should force the moderator flow distribution to oscillate ; the thermal power decreases in those regions where the temperature increases and vice versa. Hence, even under buoyancy-dominated flow conditions, the local reduction in thermal power should reverse the flow distribution bringing about a better moderator mixing, *i.e.* a safer mode of operation. Eventually, this kind of thermal oscillation can be attenuated by the action of dissipative mechanisms such as friction, formation and destruction of wakes, etc. with a relaxation time

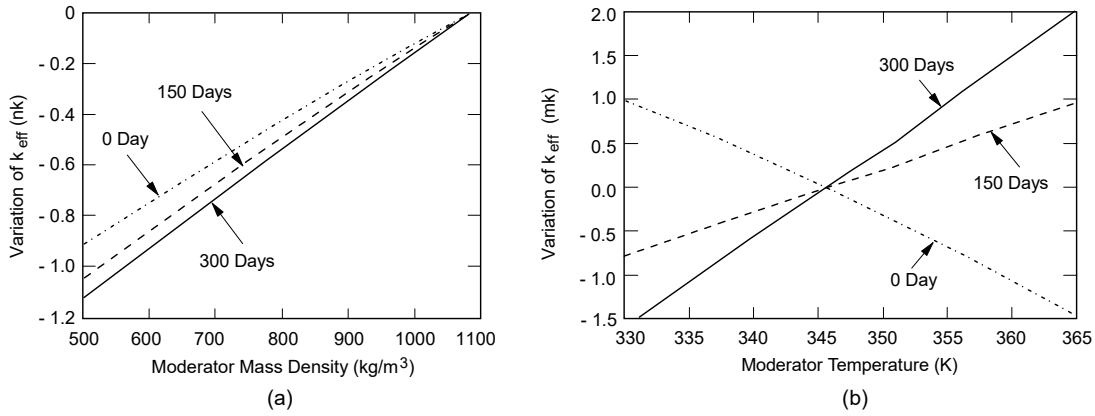

Figure 6.16 Variations of the effective multiplication factor vs. the moderator temperature calculated using DRAGON 3.06 neutron transport software ; a) Effect of local heavy water density changes around 5 mm thickness layers close to calandria tubes ; b) Effect of uniform temperature variations applied to the entire moderator.

Table 6.1 Effect of the moderator flow configuration on the neutron multiplication factor.

Moderator Flow Conditions	k_{eff}
Uniform temperature (346.15 K)	1.065545
Inertia-dominated (Ri = 0.01)	1.067747
Buoyancy-dominated (Ri = 0.21)	1.065371

controlled by the geometry, the fluid velocity and the thermal power (*i.e.* the Richardson number). According to our knowledge, up to now, thermal moderator flow oscillations have been observed only in scaled experimental facilities [6, 78]. Due to the large dimensions of CANDU-6 reactors, their numerical predictions, however, necessitate huge computational resources to perform extremely long periods of time-dependent CFD-nuclear physics coupled simulations.

6.8.1 Variation of reactivity vs. local moderator temperatures : a plausible explanation

For the first case, the trend observed in Fig. 6.16b for the change in reactivity as a function of temperature for different fuel burnup is similar to that presented in Reference [5]. An increase in fuel temperature leads to a global reduction in the moderator density. As a result the average energy of the neutron slowed down by the moderator is increased. This leads to a reduction in k_{eff} for fresh fuel (*i.e.* fewer neutron absorbed in the fuel lead to fission in U^{235}). Nevertheless, the presence of Pu^{239} for burned fuel reverses this trend because the absorption cross-section of this isotope increases with the neutron energy. This leads to a reduction in the unproductive neutron absorption in the fuel (*i.e.* higher chance that a neutron captured in the fuel produces fission).

For inertia-dominated moderator configurations, the change in the fluid density occurs locally. Thus, for the case where the reduction in moderator density is mainly concentrated around the fuel bundle, one observes in Fig. 6.16a that instead of becoming positive the slope of k_{eff} versus moderator density becomes more negative with increasing fuel burnup. This reduction in density does not change dramatically the averaged energy of the neutrons that have been slowed down in the moderator after crossing a cell. However, it decreases substantially the number of fast neutron reflected back directly in the cell after exiting the calandria tube (in such a case we can consider that the moderator acts as a reflector) thereby decreasing the probability of fast fission in Pu^{239}. The global interaction of these two competing effects for the problem studied here is a further reduction in k_{eff} with burnup. It must be pointed out that we were able to obtain the same trends shown in Fig. 6.16 by using stochastic calculations performed with SERPENT code [90].

For the thermally stratified moderator shown in Fig. 6.15a (a buoyancy-dominated configuration), the lowest half of fuel channels are surrounded by high-density heavy water. The upper portion of the core, including the reflector in this region is characterized by a much lower moderator density as indicated by the temperature distribution illustrated in Fig. 6.15b. The difference in the density between the upper and lower regions of the core unbalances the neutron leakages, *i.e.* the leakage increases with increasing moderator temperature. Hence,

the high moderator density zone will have a higher population of thermal neutrons. If it is assumed that the content in Pu^{239} is almost uniformly distributed in the core the fission rate should be higher in the lower half portion of the core and consequently the power must be higher in this region. This spatial power unbalance corresponds to the results shown in Fig. 6.15a. In turn, if the extent of the low-density moderator region becomes slightly larger than the high-density one then, k_{eff} must decrease, which corresponds to the trends given in Table 6.1.

Even though these explanations support the results observed from the CFD reactor physics coupled simulations, they do not necessarily satisfy those presented in Fig. 6.16b. In this particular case, for each moderator temperature, the density is evenly distributed within the core ; therefore there is no competition between different core regions and thus, the neutron flux follows a pattern similar to Fig. 6.13. Consequently, any modification in the moderator temperature affects simultaneously the entire reactor core. For a core at equilibrium a slight increase in neutron energy will increase the fission of Pu^{239} everywhere and accordingly will increase the reactivity.

6.9 Conclusions

Three dimensional CFD simulations of CANDU-6 moderator flows, coupled to reactor physics calculations constitutes a research area where the scientific material in the open literature is very scarce. This limited information can be partially explained by the huge computational resources that such a work necessitates. In particular, due to the large dimensions of the calandria vessel, the determination of flow conditions that can bring about different moderator flow distributions requires an intensive computational work, by using a minimum of 30 million of discretization cells. Nevertheless, most numerical works performed in this field do not satisfy this critical requirement. To solve this problem, we present in this paper 3-D CANDU-6 full moderator CFD simulations that guarantee a rigorous numerical convergence constrain. These calculations, are carried out using a thermal-hydraulic software (*i.e.* Code_Saturne) developed by the French nuclear industry, coupled to reactor-physics calculations obtained using the DONJON code, which is used for reactor core simulations.

One of the principal problem encountered in 3-D moderator flow simulations is due to the extremely large difference that exists between the dimensions of the moderator flow injectors (*i.e.* few centimeters) and the large size of the calandria vessel (*i.e.* several meters). To overcome this difficulty, some authors extrapolated flow jet profiles obtained from separate numerical simulations. In this work, however, we demonstrate that this approach is not necessarily correct due to the wrong boundary conditions they implemented. Therefore, some results given in the open literature are inappropriate and they produce misleading interpre-

tations, which contradict the CANDU-6 moderator design criterion.

After validating, against experimental data, the capability of Code_Saturne to handle CANDU-6 moderator flows, it is used to simulate 3-D moderator configurations under isothermal conditions. It was thus observed that the flow distribution takes place almost angularly, *i.e.* very small differences are observed in the axial direction. Furthermore, it is quite possible that these differences are mainly produced by the asymmetric position of the outlets with respect to a calandria vertical mid plane. Consequently, at isothermal conditions, the moderator follows very closely the behavior already observed in 2-D simulations.

A methodology was implemented to couple CFD simulations with reactor physics calculations. In all the cases studied, an initial neutron flux distribution, calculated by using a Gentilly-2 nuclear power plant burnup map and assuming an isothermal moderator at 346.15 K (73°C) was used to determine reference thermal power values. Similar CFD-nuclear physics coupled calculations were repeated, but permitting the moderator temperatures to satisfy local flow variations as dictated by CFD. Hence, it was observed that local moderator temperatures have a non-negligible effect on k_{eff}. In particular, the higher is the local temperature the lower is the local thermal power. This is an unexpected result that seems to contradict similar studies performed by keeping the moderator temperature constant everywhere within the reactor core. To validate such an observation, a neutron transport calculation using the DRAGON code, in a typical lattice and including local mass density changes around calandria tubes were carried out. The results indicate that local moderator temperature variations bring about a negative reactivity behavior that increases with burnup. Similar neutron transport calculations performed for the entire reactor core by applying the same moderator temperature everywhere, produce opposite results, *i.e.* reactivity increases with increasing both the moderator temperature and burnup. In view of these results, a plausible mechanism which can explain our observations is thus proposed.

Acknowledgments

The authors would like to thank the Fonds de recherche du Québec-Nature et technologies (FRQNT B-2 PhD excellence research fellowship) for their financial support, Compute Canada for the allocation of computational resources and the development group of Code_Saturne at Électricité de France for their technical assistances. This work was funded by a discovery grant (RGPIN 41929) of the National Sciences and Engineering Research Council of Canada (NSERC).

CHAPITRE 7 DISCUSSION GÉNÉRALE

Dans cette section, les discussions globales et les principales conclusions de la recherche ainsi qu'un point sur le profil de l'injection de l'écoulement sont présentés. Toutefois, les problématiques de la recherche ainsi que les résultats et les analyses détaillées ont été présentés aux chapitres 4, 5, 6 et en annexe A.

7.1 Synthèse des résultats

La première partie des résultats obtenus dans le cadre de cette thèse (présentés en annexe A) consiste à compléter les travaux de recherche réalisés dans la cadre du projet de maîtrise de Romain Necciari [39]. Une série de simulations numériques a été effectuée sur des configurations de tubes afin d'évaluer les plateformes numériques ainsi que les algorithmes de calcul dans le but de simuler l'écoulement du modérateur. Il a été conclu qu'en utilisant le modèle de turbulence κ - ϵ classique en conjonction avec une topologie de maillage structuré de type carré qui englobe les tubes de calandre, on peut améliorer les prédictions numériques de ce type d'écoulement. Ce travail nous a permis de trouver un nombre minimal de cellules requis afin de réaliser des simulations de l'écoulement du modérateur au sein du réacteur CANDU-6.
La deuxième partie du travail est présentée au chapitre 4 de la thèse. En premier lieu, celui-ci a pour but d'évaluer la validité des modèles physiques, les méthodes ainsi que les conditions utilisées pour la simulation de l'écoulement du modérateur dans les réacteurs nucléaires de type CANDU-6. Dans ce contexte, avant d'effectuer les simulations, les approximations couramment utilisées pour une étude thermohydraulique du modérateur ont été analysées. En particulier, il en est ressorti que l'utilisation de l'hypothèse de Boussinesq induira des erreurs numériques qui ne peuvent pas être négligées.
Les simulations présentées dans ce travail prédisent l'existence de trois configurations d'écoulement de modérateur respectivement contrôlées par l'inertie, mixte et contrôlée par la flottabilité. Les transitions entre ces configurations se font en fonction du rapport entre la puissance thermique générée par le réacteur dissipé dans le modérateur et la vitesse d'injection du modérateur. Ce rapport correspond à la définition du nombre de Richardson (Ri). Il a été observé que :

- Pour $\mathrm{Ri} < 0.04$ l'écoulement semble adopter une configuration contrôlée par l'inertie.
- Pour $0.04 < \mathrm{Ri} < 0.09$ l'écoulement est soumis à une concurrence entre les forces d'inertie et de flottabilité. Cette configuration mixte résulte en des asymétries de l'écoulement. Dans

ces conditions, la répartition de l'écoulement commence à passer vers un côté de la calandre, en provoquant d'importantes différences de température à travers le modérateur.

– Pour $0.09 < \mathrm{Ri} < 0.12$ une zone de transition entre les configurations mixte et contrôlée par la flottabilité est obsérvée.

– Pour $\mathrm{Ri} > 0.12$ les forces de flottabilité deviennent dominantes dans la calandre. Ceci crée une zone chaude dans la partie supérieure du modérateur où les jets ne peuvent pas pénétrer. On observe que le modérateur devient thermiquement stratifié.

La détermination du positionnement du point de rencontre des jets est très importante, car, dans une configuration avec des asymétries (c.-à-d. une configuration mixte), la différence de température est directement reliée à la rencontre entre les jets. En conséquence, cette position doit être considérée lors des analyses de sûreté nucléaire.

Le développement d'un modèle CFD dépendant du temps constitue la troisième partie de cette étude. Il a été observé que les simulations stationnaires ne peuvent pas prédire de manière appropriée la structure de l'écoulement du modérateur quand l'ordre de grandeur des forces agissant sur le système est proche. Plusieurs simulations instationnaires ont été réalisées pour une large gamme du nombre de Richardson. Les données numériques extraites au centre de la calandre ont été analysées à la fois dans le domaine temporel et fréquentiel. L'analyse dans le domaine fréquentiel nous a permis de construire une trajectoire fréquentielle dominante, en fonction du nombre de Richardson. Il a été observé que pour les valeurs Richardson inférieures à 0.01, le modérateur est capable de maintenir une configuration d'inertie dominante. Pour des valeurs du nombre de Richardson comprises ente 0.01 et 0.12, l'écoulement de modérateur est caractérisé par la présence de structures cohérentes qui oscillent avec de très faibles fréquences. Dans de telles conditions, il a été observé que le point de rencontre des jets était complètement dépendant du temps, oscillant d'un côté à l'autre avec de grandes amplitudes. Néanmoins, pour des valeurs du nombre de Richardson supérieures à 0.12, ces fluctuations disparaissent et le modérateur devient thermiquement stratifié. En conséquence, les prédictions des modèles CFD en régime stationnaire ne sont pas loin des distributions de l'écoulement en fonction du temps. La comparaison de la trajectoire fréquentielle proposée avec les données expérimentales montre un excellent accord.

La quatrième partie de cette thèse porte sur des simulations 3-D CFD du modérateur couplées à des calculs de physique du réacteur (neutronique). Suite à une étude de convergence numérique, le nombre nécessaire de mailles dans le cadre d'une étude 3-D a été déterminé. Les simulations thermohydrauliques de cette étude ont été réalisées à l'aide du Code_Saturne [1] alors que la partie neutronique a été faite par le code DONJON [2] appliqué à des simulations du cœur du réacteur. Une méthodologie a été mise en place pour coupler les simulations

CFD avec les calculs de physique des réacteurs. Il a été observé que les variations locales de distribution de température du modérateur ont un effet non négligeable sur le k_{eff} du réacteur. En se basant sur des calculs en transport neutronique et aussi des calculs de diffusion de neutrons, il a été observé qu'une température locale plus élevée du modérateur réduit la puissance thermique locale dans le coeur du réacteur. Cette prédiction contredit des études similaires effectuées en gardant uniforme la température du modérateur partout dans le coeur du réacteur. À cet égard, une explication physique a été proposée dans ce dernier article soumis au journal "Annals of Nuclear Energy".

7.2 Discussion sur le profil de vitesse lors de l'injection du modérateur

Étant donné que l'objectif de la recherche réalisée dans le cadre de cette thèse était d'analyser l'écoulement du modérateur pour différentes conditions de fonctionnement caractérisées par des paramètres clés, l'utilisation d'un profil global de l'écoulement turbulent (ayant une distribution semi-constante) comme entrée du jet dans la calandre était indispensable. D'ailleurs, implémenter un profil de vitesse dans un domaine bidimensionnel utilisé dans certaines parties de ce travail était impossible. Toutefois, il est évident que l'écoulement du modérateur après son passage dans les sections de l'injecteur ayant chacune une géométrie complexe n'aura pas un profil uniforme au moment de quitter l'injecteur pour entrer dans la calandre. Il a été mentionné à la section 2.1.2 que Sarchami [12] a combiné les huit injecteurs du CANDU-6 dans le domaine hydraulique de la calandre. Bien que cette combinaison semble donner des prédictions précises sur l'écoulement du modérateur dans les injecteurs, Sarchami n'a pas correctement fait la modélisation géométrique des injecteurs. En effet la géométrie qu'il a employée est présentée à la figure 7.1. Selon le manuel du CANDU-6 [29], un raccordement courbé à 90° conduit l'écoulement vers l'entrée du diffuseur. Cependant, cette conduite n'a pas été prise en compte dans la modélisation de Sarchami. Nos simulations (qui seront présentées plus tard dans cette section) ont prédit d'importantes distributions de l'écoulement proprement générées par la présence de cette conduite courbée (ce point est aussi discuté dans le troisième article, voir la figure 6.3 dans la section 6.4).

Une deuxième approche utilisée pour déterminer le profil de l'écoulement consiste à simuler l'écoulement au sein d'un injecteur complètement isolé c.-à-d. à l'intérieur d'un volume sans la présence des canaux de combustible. Comme mentionné à la section 2.1.2, l'imposition des conditions aux frontières posées pour effectuer cette modélisation est très délicate. À titre d'exemple, les vecteurs de vitesse du modérateur ainsi que le profil de vitesse tel que prédit par Yoon et al. [26] sont présentés à la figure 7.3. On peut observer que les comportements de l'écoulement dans les deux segments intérieurs et extérieurs de l'injecteur sont complètement différents. Ceci semble être une erreur numérique générée par l'imposition d'une mauvaise

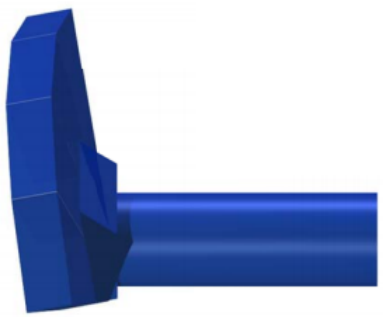

Figure 7.1 Modélisation géométrique de l'injecteur utilisée par Sarchami et al. [10].

condition aux frontières placée directement à la sortie de l'injecteur.

Afin de pouvoir corroborer la validité du profil proposé par Yoon et al. [26], nous avons modélisé l'écoulement du modérateur dans les injecteurs tout en imposant des conditions aux frontières prenant en compte l'écoulement extérieur à l'injecteur. Le domaine hydrodynamique utilisé pour cette étude est présenté à la figure 7.3. Il s'agit d'un seul injecteur placé dans un domaine hydraulique représentant 1/8 du volume de la cuve du CANDU-6. Les frontières du domaine de la cuve ont été définies comme suit : des conditions aux frontières symétriques pour toutes les surfaces qui se trouvent à l'intérieur de la calandre réelle ; des parois sans glissement pour les parois extérieures de la calandre, pour la canatisation de sortie ainsi que les parois de l'injecteur. L'écoulement entre dans ce domaine avec un débit volumique correspondant à 1/16 de la valeur nominale utilisée dans les réacteurs CANDU-6. Quant à la sortie, une condition aux frontières de type pression a été imposée. Pour ces simulations, le modèle de turbulence κ - ϵ avec une loi de paroi évolutive (c.-à-d. "scalable" en anglais) pour un maillage non structuré suffisamment fin, composé de 1.5×10^6 cellules ont été utilisées. Le critère de convergence sélectionné pour ces simulations a été que les valeurs des résidus normalisés soient inférieures à 10^{-5}.

Les vecteurs ainsi que les contours de vitesse à la sortie des segments de l'injecteur sont présentés aux figures 7.4 et 7.5 respectivement.

Le décollement de l'écoulement dû à la pression négative générée dans l'injecteur crée une zone de recirculation assez importante comme on l'observe dans la figure 7.4 a. De plus, la distribution de la vitesse est beaucoup plus importante près de la paroi se trouvant en face de la conduite d'entrée de l'injecteur (voir la figure 7.4 b). Il faut noter qu'un comportement similaire est observé pour les deux segments de l'injecteur, c'est-à-dire que l'écoulement a tendance à rester collé aux parois qui se trouvent en face de la conduite d'entrée (voir figure 7.4 b et d). D'ailleurs, les effets de la conduite courbée à l'entrée de l'injecteur (c.-à-d.

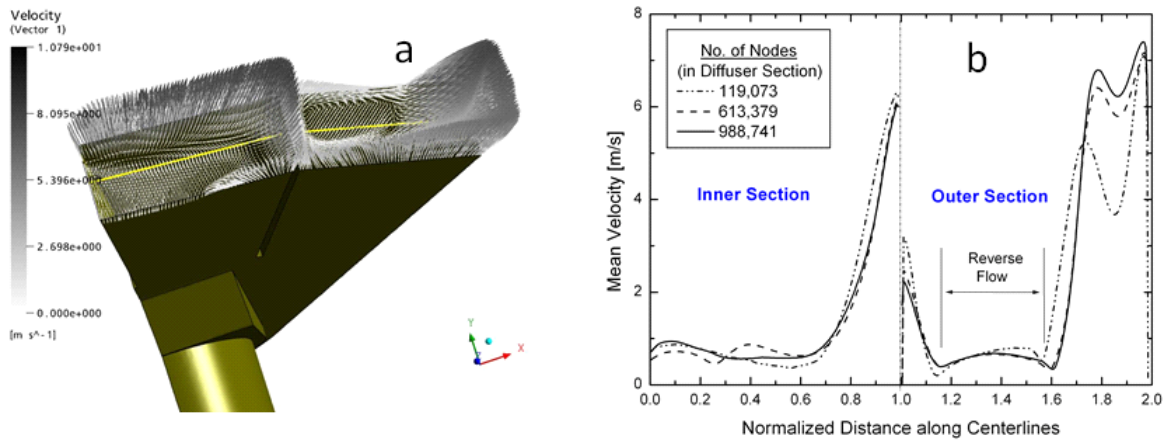

Figure 7.2 Simulation du jet du modérateur présenté par Yoon et Park [26] (Copyright June 22 2016 by the American Nuclear Society, La Grange Park, Illinois). a) Vecteurs de vitesse ; b) Profil de vitesse sur la ligne du centre.

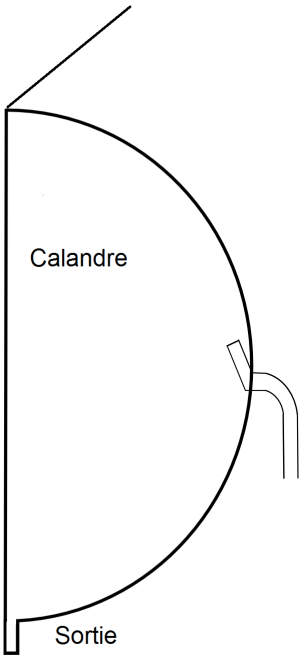

Figure 7.3 Position de l'injecteur du modérateur employé lors des validations des simulations présentées par Yoon et Park [26].

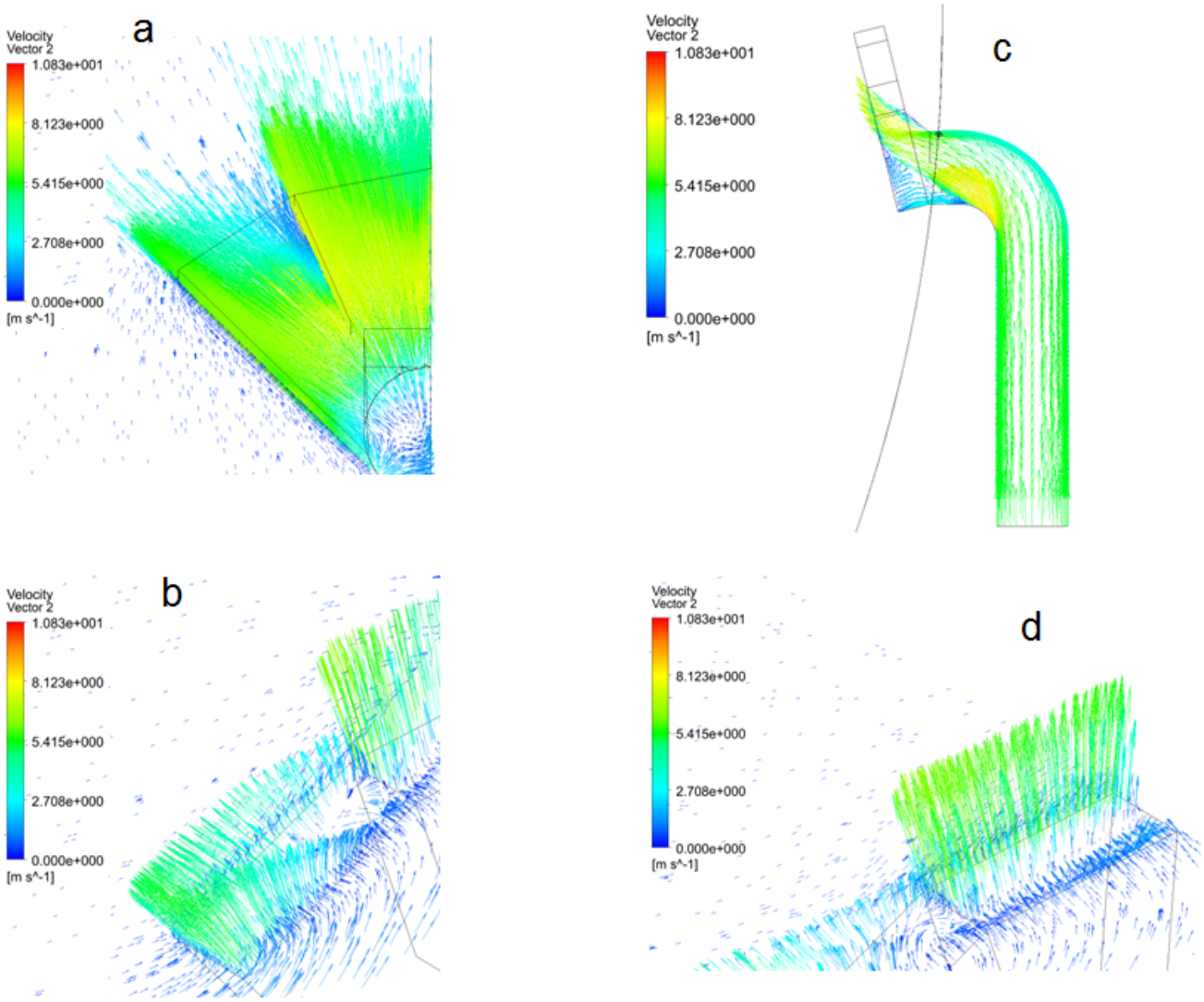

Figure 7.4 Vecteurs de la vitesse causée par l'injection de l'eau du modérateur. a) Selon le plan traversant les conduites ; b) À la sortie du segment extérieur ; c) Dans le plan médian ; d) À la sortie du segment intérieur.

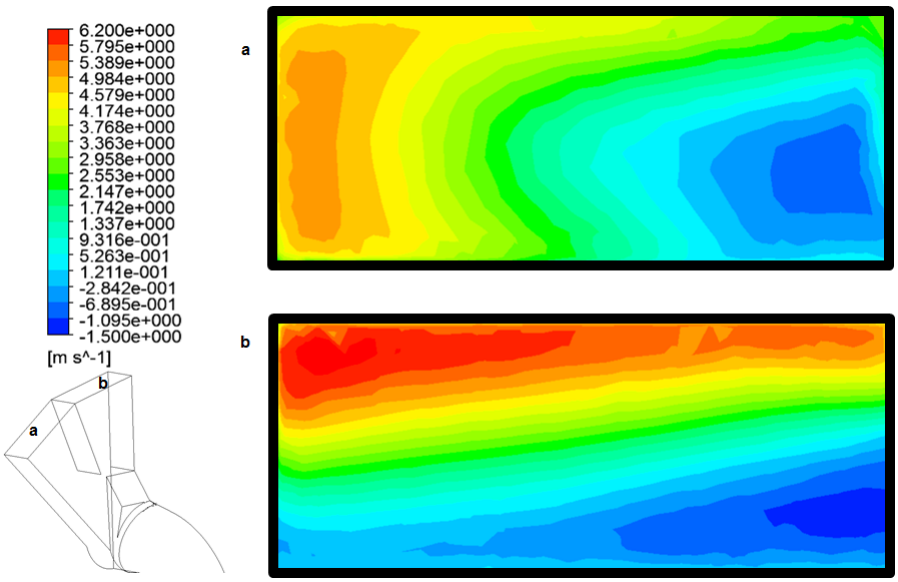

Figure 7.5 Contours de vitesse à la sortie du diffuseur. a) Segment extérieur ; b) Segment intérieur.

décollements) qui ont été discutés plus haut sont remarquables dans la figure 7.4 c où une zone de recirculation se forme en amont du diffuseur.

Afin d'illustrer les distributions de l'écoulement au moment de quitter l'injecteur, les sorties des deux segments, extérieur et intérieur sont présentés respectivement aux figures 7.5 a et 7.5 b. Ces figures présentent les contours de la composante de vitesse dans la direction normale au plan à la sortie de l'injecteur. On peut remarquer sur ces contours que les zones de recirculation ainsi que les valeurs maximales à la vitesse de sortie de l'écoulement sont beaucoup plus petites que celles prédites dans les simulations de Yoon et al. [26].

Une analyse détaillée de ces simulations en utilisant d'autres modèles de turbulence ainsi que des validations avec des données expérimentales seront l'objet d'un article de recherche qui est en ce moment dans la phase de rédaction.

CHAPITRE 8 CONCLUSION ET RECOMMANDATIONS FUTURES

Cette recherche visait l'étude thermohydraulique de l'écoulement du modérateur au sein de la cuve du réacteur CANDU-6. En premier lieu, cette recherche a conduit au développement d'une carte des configurations du modérateur couvrant une large gamme des conditions. Une analyse détaillée des asymétries et des oscillations a été réalisée à l'aide de simulations transitoires du modérateur pour de nombreuses conditions d'écoulement. Les prédictions thermohydrauliques du modérateur ont été ensuite couplées avec les équations de la physique des réacteurs afin d'étudier l'impact des fluctuations du modérateur sur la réactivité du réacteur CANDU-6.

8.1 Revue des objectifs

Afin d'évaluer les contributions de cette thèse, il faut mettre en valeur les réalisations des objectifs présentés à la section 1.4.

L'un des objectifs de cette thèse a été d'établir une stratégie numérique pertinente pour simuler l'écoulement de modérateur. Les études de convergence et les développements analytiques (dans le cadre de la vérification de la validité de l'hypothèse de Boussinesq) nous ont permis de choisir une plateforme numérique (c.-à-d. nombre de cellules, le modèle de turbulence, l'algorithme de calcul ainsi que le pas de temps) suffisamment précise pour réaliser cette étude. Le code de calcul utilisé pour cette étude (c.-à-d. le Code_Saturne développé chez Électricité de France [1]) a été validé avec des données expérimentales disponibles dans la littérature. Plus précisément, les prédictions du Code_Saturne ont été en très bon accord avec les données de la MCT [9], qui est un modèle expérimental du CANDU-6 parfaitement mise à l'échelle.

Quant à un autre objectif de cette recherche, les valeurs de puissance thermique pour chaque grappe de combustible de CANDU-6 ont été importées dans le domaine thermohydraulique de l'écoulement du modérateur. Ces valeurs de puissance ont été calculées à l'aide du logiciel DONJON [2], développé à Polytechnique Montréal.

Dans le cadre de cette recherche, une carte des configurations de l'écoulement du modérateur a été développée. Cette carte prédit la configuration de l'écoulement du modérateur en fonction du nombre de Richardson.

Afin de pouvoir déterminer tous les mouvements périodiques ayant lieu dans l'écoulement du modérateur, des simulations allant jusqu'à 5000 secondes réelles ont été effectuées. Les analyses de données ont prédit des fréquences d'oscillation très faibles dans le modérateur. Les mouvements observés dans ces simulations n'ont jamais été prédits dans les simulations

précédentes puisque cette grandeur (de l'ordre de 10^{-3} Hz) nécessite une longue durée (plus que 1000 s) de simulation.
Comme dernier objectif de cette recherche, l'effet des distributions de l'écoulement de modérateur sur la réactivité des réacteurs CANDU-6 a été simulé. D'importantes variations de la réactivité proprement due à la distribution de la température du modérateur ont été observées (de l'ordre du mK). Une explication physique de ce phénomène a été proposée (voir le troisième article présenté au chapitre 6).

8.2 Recommandations

Les recommandations suivantes sont proposées pour les travaux de recherches futurs.

- *Utilisation des modèles plus précis que RANS (Reynolds Averaged Navier-Stokes).* Afin de minimiser le temps de calcul pour les simulations de cette recherche, nous avons utilisé le modèle de turbulence à deux équations $\kappa - \epsilon$ (standard). Ce choix a été basé sur des études comparatives avec des données expérimentales disponibles. Toutefois, nos choix étaient limités aux modèles de turbulence à deux équations dans le but de réduire les coûts de calcul. Il est évident que les modèles LES (Large Eddy Simulation) ou DES (Dettached Eddy Simulation) donnent des prédictions plus précises que les modèles RANS tout en nécessitant des ressources de calcul considérables. On suggère une investigation sur la précision apportée par ces méthodes aux prédictions de l'écoulement du modérateur. Les données expérimentales de Paul et al. [74] et/ou celles du laboratoire STERN [8] sont des cas simples 2-D et pourront être considérées comme cas tests pour une telle étude.
- *Modélisation géométrique de la calandre en utilisant la géométrie exacte des 8 injecteurs afin d'éviter l'utilisation d'un profil développé comme condition aux frontières.* On a utilisé un profil global dans nos études afin d'éliminer les huit injecteurs du domaine hydraulique de la calandre et par conséquent alléger les calculs numériques. Ce choix est justifiable, car l'objectif de cette étude était de caractériser l'écoulement pour différentes conditions de fonctionnement. Toutefois, une analyse précise du comportement de l'écoulement pour chacune des configurations prédites par cette étude nécessitera la prise en compte des injecteurs dans le domaine. Les simulations présentées à la section 7.2 ont illustré que les distributions de l'écoulement à la sortie des injecteurs ne peuvent pas être précisément représentées par un profil 1-D. Par conséquent, la géométrie des injecteurs doit être considérée dans les simulations. Cependant, selon notre étude de maillage, la modélisation des injecteurs ajoutera 12×10^6 cellules de plus au domaine (1.5×10^6 pour chacun des injecteurs). Il faut noter que ceci va encore augmenter les coûts de simulations surtout si les simulations sont faites en régime transitoire.

– *Étude 3D dépendant du temps pour prédire les fluctuations dans le temps dans la direction axiale de la calandre*. Il a été observé que pour certaines conditions, les simulations en régime stationnaire ne sont pas capables de correctement prédire des phénomènes pouvant être importants au point de vue de la sûreté nucléaire comme celui des oscillations observées. Alors qu'une simulation 3-D transitoire semble être très coûteuse compte tenu des temps caractéristiques de l'écoulement, certaines simplifications peuvent être apportées au domaine afin d'alléger les calculs et rendre le temps des simulations acceptable. Dans ce contexte, on propose d'effectuer les simulations uniquement sur une moitié axiale de la calandre. Malgré certaines asymétries dans la géométrie (c.-à-d. les positions des injecteurs dans la direction axiale), cette simplification ne va pas grandement influencer les distributions de l'écoulement. Cependant, il n'est pas recommandé de couper la calandre de plus de la moitié. On recommande que le domaine réduit contienne au moins 4 injecteurs, car l'interaction des jets voisins a un effet majeur sur la distribution de l'écoulement du modérateur.
– *Développement d'un modèle simplifié de mouvements oscillatoires de l'écoulement pour la configuration mixte*. Les oscillations observées pour la configuration mixte de l'écoulement sont des phénomènes pouvant être cruciaux pour la sûreté nucléaire. Le développement d'un modèle analytique de l'oscillateur capable de prédire les mouvements périodiques de l'écoulement du modérateur permettra de réduire les coûts de simulations.

8.3 Publications

Cette thèse a conduit à quatre articles de revues et un article de conférence. La liste de ces publications est la suivante.

1. Moderator flow simulation around calandria tubes of CANDU-6 nuclear reactors, Teyssedou, A., Necciari, R., Reggio, M., Mehdi Zadeh, F. and Etienne, S., Taylor & Francis Engineering Applications of Computational Fluid Mechanics, v. 8, 1, pp 178–192, 2014.
2. A cartographical study of the moderator flow in CANDU-6 nuclear reactors, Mehdi Zadeh, F. and Teyssedou, A., Étienne, S., CFD-SC, Toronto, CANADA, June 2014.
3. CFD simulation of the moderator flow in candu-6 nuclear reactors. Mehdi Zadeh, F., Etienne, S. and Teyssedou, A. Accepted in Fabruary 2016. ASME Journal of Nuclear Engineering and Radiation Science. doi :10.1115/1.4032874.
4. 2-D CFD Time-dependent thermal-hydraulic simulations of CANDU-6 moderator flows. Mehdi Zadeh, F., Etienne, S. and Teyssedou, A. Submitted to Elsevier Nuclear Engineering and Design in January 2016.
5. Effect of 3-D moderator flow configurations on the reactivity of CANDU-6 nuclear

reactors. Mehdi Zadeh, F., Etienne, S., Marleau, G., Chambon, R. and Teyssedou, A. Submitted to Elsevier Annals of Nuclear Energy in April 2016.

RÉFÉRENCES

[1] EDF - Électricité de France, "Code_Saturne 3.0.0 theory guide," http ://code-saturne.org/cms/sites/default/files/theory-3.0.pdf, 2014, accessed : 2014-02-10.

[2] A. Hébert, D. Sekki et R. Chambon, "A user guide for donjon version5," *Report IGE–344, École Polytechnique de Montréal*, 2014.

[3] A. V. Nero, *A guidebook to nuclear reactors*. University of California Press, 1979.

[4] S. Glasstone et A. Sesonske, *Nuclear reactor engineering : reactor systems engineering*. Springer Science & Business Media, 2012.

[5] Canteach lecture, *Reactivity Effects Due to Temperature Changes and Coolant Voiding, Module 12, URL : https ://canteach.candu.org/Content%20Library/20041112.pdf*. Notes du cours 22106, 1997.

[6] H. Khartabil, W. Inch, J. Szymanski, D. Novog, V. Tavasoli et J. Mackinnon, "Three-dimensional moderator circulation experimental program for validation of CFD code MODTURC-CLAS," 2000.

[7] S. Paul, M. Tachie et S. Ormiston, "Experimental study of turbulent cross-flow in a staggered tube bundle using particle image velocimetry," *International Journal of Heat and Fluid Flow*, vol. 28, no. 3, pp. 441–453, 2007.

[8] R. Huget, J. Szymanski et W. Midvidy, "Status of physical and numerical modelling of candu moderator circulation," dans *Proceedings of 10th Annual Conference of the Canadian Nuclear Society, Ottawa*, 1989.

[9] H. T. Kim, "Preliminary test results and CFD analysis for moderator circulation test (MCT)," *Annals of Nuclear Energy*, 2015.

[10] A. Sarchami, N. Ashgriz et M. Kwee, "Comparison between surface heating and volumetric heating methods inside candu reactor moderator test facility (MTF) using 3d numerical simulation," *Int. J. Nucl. Energy Sci. Eng.*, vol. 3, pp. 15–21, 2013.

[11] L. Carlucci et I. Cheung, "The effects of symmetric/asymmetric boundary conditions on the flow of an internally heated fluid," *Numerical Methods for Partial Differential Equations*, vol. 2, no. 1, pp. 47–61, 1986.

[12] A. Sarchami, *Investigation of Thermal Hydraulics of a Nuclear Reactor Moderator*. Ph.D. Thesis, University of Toronto, 2011.

[13] S. K. Park, J. J. Jeong, J. R. Lee, H. Y. Yoon et H. T. Kim, "Assessment of the CUPID code applicability to the thermal-hydraulic analysis of a candu moderator system," *Progress in Nuclear Energy*, vol. 75, pp. 72–79, 2014.

[14] G. I. Hadaller, R. A. Fortman et al., "Frictional pressure drop in aligned and staggered tube banks with large pitch diameter ratio," 1996.

[15] L. Carlucci, "Numerical simulation of moderator flow and temperature distributions in a CANDU reactor vessel," dans *Proceedings of La Modélisation fine des Écoulements, ISBN : 2829780467, Paris*, 1982, pp. 533 – 543.

[16] A. Gosman et W. Pun, *Calculation of Recirculating Flows, Report no. HTS/74/12*. Imperial College, London, 1974.

[17] J. Szymanski, M. Garceau, K. Ng et W. Midvidy, "Numerical modelling of three-dimensional turbulent moderator flow in calandria," dans *Proceedings of the international conference on numerical methods in nuclear engineering. Volume 1*, 1983.

[18] L. Carlucci, V. agranat, G. Waddington, H. Khartabil et J. Zhang, "Predicted and measured flow and temprature distribution in a facility for simulating in-reactor moderator circulation," dans *Proceedings of 8th International Conference of CFD Canada, Montreal*, 2000.

[19] C. Yoon, B. W. Rhee et B.-J. Min, "3-D CFD analysis of the CANDU-6 moderator circulation under normal operating conditions," *J. Korean Nucl. Soc*, vol. 36, no. 6, p. 559, 2004.

[20] ——, "Development and validation of the 3-D computational fluid dynamics model for CANDU-6 moderator temperature predictions," *Nuclear technology*, vol. 148, no. 3, pp. 259–267, 2004.

[21] C. Yoon et J. H. Park, "Development of a CFD model for the candu-6 moderator analysis using a coupled solver," *Annals of Nuclear Energy*, vol. 35, no. 6, pp. 1041–1049, 2008.

[22] J. R. Lee, S. G. Park, H. Y. Yoon, H. T. Kim et J. J. Jeong, "Numerical study for candu moderator temperature prediction by using the two-phase flow analysis code, CUPID," *Annals of Nuclear Energy*, vol. 59, pp. 139–148, 2013.

[23] L. Carlucci, V. Agranat, G. Waddington, H. Khartabil et J. Zhang, "Predicted and measured flow and temperature distributions in a facility for simulating in-reactor moderator circulation," Atomic Energy of Canada Limited, Chalk River, Ontario (Canada), Rapp. tech., 2000.

[24] M. Kim, S.-O. Yu et H.-J. Kim, "Analyses on fluid flow and heat transfer inside calandria vessel of CANDU-6 using CFD," *Nuclear Engineering and Design*, vol. 236, no. 11, pp. 1155–1164, 2006.

[25] H. T. Kim et B. W. Rhee, "Scaled-down moderator circulation test facility at Korea atomic energy research institute," *Science and Technology of Nuclear Installations*, 2015.

[26] C. Yoon et J. H. Park, "Simulation of the internal flows of an inlet diffuser assembly for the CANDU-6 moderator analysis," *Nuclear Technology*, vol. 160, no. 3, pp. 314–324, 2007.

[27] S. R. Choi, J. J. Jeong, J. R. Lee, H. Y. Yoon et H. T. Kim, "Numerical investigation of the CANDU moderator thermal-hydraulics using the cupid code," *Progress in Nuclear Energy*, vol. 85, pp. 541–547, 2015.

[28] B. W. Rhee et H. T. Kim, "A review of the scaling study of the CANDU-6 moderator circulation test facility," *Journal of Power and Energy Engineering*, vol. 2, no. 09, p. 64, 2014.

[29] A. Manzer, *Design Manual Gentilly-2 Nuclear Generating Station.* Report #DN-66-37000. Atomic Energy of Canada Limited., 1979.

[30] A. Sarchami, N. Ashgriz et M. Kwee, "Three dimensional numerical simulation of a full scale candu reactor moderator to study temperature fluctuations," *Nuclear Engineering and Design*, vol. 266, pp. 148–154, 2014.

[31] F. Farhadi, N. Ashgriz, M. Kwee, R. Girard, Y. Parlatan et M. Ali, "Temperature fluctuations in a CANDU moderator test facility," dans *Proceeding of International Conference on Nuclear Engineering.* ASME, Brussels, 2009, pp. 569–577.

[32] D. Koroyannakis, R. Hepworth et G. Hendrie, "An experimental study of combined natural and forced convection flow in a cylindrical tank," *AECL Report. TDVI-382*, 1983.

[33] M. Quraishi, D. Koroyannakis et W. Waters, "Study of combined forced and natural convection flow using an analytical indicator flow visualization technique." Ann Arbor, MI, USA, 1985, pp. 743 – 747.

[34] C. Yoon, B. W. Rhee et B.-J. Min, "Validation of a CFD analysis model for predicting CANDU-6 moderator temperature against SPEL experiments," dans *10th International Conference on Nuclear Engineering.* American Society of Mechanical Engineers, 2002, pp. 131–138.

[35] A. K. Kansal, J. B. Joshi, N. K. Maheshwari et P. K. Vijayan, "CFD analysis of moderator flow and temperature fields inside a vertical calandria vessel of nuclear reactor," *Nuclear Engineering and Design*, vol. 287, pp. 95–107, 2015.

[36] R. Huget, J. Szymanski et W. Midvidy, "Experimental and numerical modelling of combined forced and free convection in a complex geometry with internal heat generation," dans *Proceedings of 9th International Heat Transfer Conference*, vol. 3, 1990, p. 327.

[37] R. Huget, J. Szymanski, P. Galpin et W. Midvidy, "MOUDTURC-CLASS :an effcient code for analysis of moderator circulation in CANDU reactors," dans *Third International Conference on Simulation Methods in Nuclear Engineering*, 1990.

[38] H. T. Kim et S.-M. Chang, "Computational fluid dynamics analysis of the Canadian deuterium uranium moderator tests at the Stern laboratories inc." *Nuclear Engineering and Technology*, vol. 47, no. 3, pp. 284–292, 2015.

[39] R. Necciari, *Simulations de l'écoulement et du transfert de chaleur du modérateur du réacteur CANDU*. M.Sc. thesis, École Polytechnique de Montréal, 2011.

[40] H. T. Kim, J. E. Cha, H. Seo et I. C. Bang, "Measurement of velocity and temperature profiles in the 1/40 scaled-down CANDU-6 moderator tank," *Science and Technology of Nuclear Installations*, vol. 501, p. 439863, 2015.

[41] B. W. Rhee, H. Kim et Y. Song, "Reconsideration of a scaling study of candu-6 moderator tank scaled-down test facility," dans *22nd International Conference on Nuclear Engineering*. American Society of Mechanical Engineers, 2014, pp. V02AT09A042–V02AT09A042.

[42] H. Seo, H. T. Kim, J. E. Cha et I. C. Bang, "Measurements and visualization of velocity profiles in a scaled CANDU6 moderator tank using particle image velocimetry," *Annals of Nuclear Energy*, vol. 73, pp. 361–372, 2014.

[43] C. Yoon, B. W. Rhee et B.-J. Min, "A review on 3-D CFD model development for the CANDU-6 moderator analysis in KAERI," 2003.

[44] H. F. Khartabil et R. B. Duffey, "Velocity and temperature distribution measurements inside a scaled calandria in support of CANDU X passive moderator cooling system design," *GENES4/ANP2003, Kyoto, Japan*, 2003.

[45] A. Sarchami, N. Ashgriz et M. Kwee, "Effect of scaling of the thermalhydraulics of the moderator of candu reactor," dans *International Conference on Mathematics and Computational Methods Applied to Nuclear Science and Engineering Rio de Janeiro, RJ, Brazil, May 8-12, 2011*, 2011.

[46] ——, "Temperature fluctuations inside the CANDU reactor moderator test facility (MTF)," *Annals of Nuclear Energy*, vol. 60, pp. 157–162, 2013.

[47] S. Ravi, N. Rajan et P. Kulkarni, "Computational and experimental studies of fluid flow and heat transfer in a calandria based reactor," dans *Computational Fluid Dynamics 2008*. Springer, 2009, pp. 233–238.

[48] K. Prabhakaran, P. Goyal, A. Dutta, V. Bhasin, K. Vaze, A. Ghosh, A. V. Pillai, et J. Mathew, "Studies on flow induced vibration of reactivity devices of 700MWe Indian PHWR," *Nuclear Engineering and Design*, vol. 244, pp. 1–16, 2012.

[49] A. M. Vaidya, N. K. Maheshwari, P. K. Vijayan et D. Saha, "Computational study of moderator flow and temperature fields in the calandria vessel of a heavy water reactor using the PHOENICS code," *Kerntechnik*, vol. 73, no. 1-2, pp. 33–40, 2008.

[50] R. Sinha et A. Kakodkar, "Design and development of the AHWR—the Indian thorium fuelled innovative nuclear reactor," *Nuclear Engineering and Design*, vol. 236, no. 7, pp. 683–700, 2006.

[51] G. Austman, J. Szymanski, M. Garceau et W. Midvidy, "Measuring moderator temperature in a CANDU reactor," dans *6^{th} Annual Conference of CNS, Ottawa, Canada*, 1985.

[52] World Nuclear Association, "Nuclear power in Canada," http://www.world-nuclear.org/info/Country-Profiles/Countries-A-F/Canada--Nuclear-Power/, Mise à jour : Novembre 2015 (Repéré le 1 décembre 2015).

[53] IAEA, "Power reactor information system," http ://www.iaea.org/PRIS/WorldStatistics/OperationalReactorsByCountry.aspx, accessed : 2014-04-01.

[54] D. G. Cacuci, *Handbook of Nuclear Engineering*. Springer, 2010.

[55] J. C. Mandal et C. R. Sonawane, "Simulation of moderator flow and temperature inside calandria of CANDU reactor using artificial compressibility method," *Heat Transfer Engineering*, vol. 35, no. 14-15, pp. 1254–1266, 2014.

[56] J. Szymanski, M. Garceau, K. Ng et W. Midvidy, "Numerical modelling of three-dimensional turbulent moderator flow in calandria," dans *Proceedings of the international conference on numerical methods in nuclear engineering. Volume 1*, 1983.

[57] R. Huget, J. Szymanski, P. Galpin et W. Midvidy, "Modturc_clas : An efficient code for analyses of moderator circulation in candu reactors," dans *Proceedings 3rd International Conference on Simulation Methods in Nuclear Engineering, Montreal*, 1990.

[58] R. Arsene, I. Prisecaru et Ş. NICOLICI, "Improvement of the thermalhydraulic characteristics in the calandria vessel of a CANDU 6 nuclear reactor," *UPB Scientific bulletin*, 2013.

[59] A. Sarchami, N. Ashgriz et M. Kwee, "Three dimensional numerical simulation of a full scale candu reactor moderator to study temperature fluctuations," dans *Proceedings of World Academy of Science, Engineering and Technology*, no. 63. World Academy of Science, Engineering and Technology, 2012.

[60] A. J. Chorin, "A numerical method for solving incompressible viscous flow problems," *Journal of Computational Physics*, vol. 2, no. 1, pp. 12–26, 1967.

[61] J. Boussinesq, *Théorie analytique de la chaleur : mise en harmonie avec la thermodynamique et avec la théorie mécanique de la lumière*. Gauthier-Villars, 1901, vol. 1.

[62] D. D. Gray et A. Giorgini, "The validity of the Boussinesq approximation for liquids and gases," *International Journal of Heat and Mass Transfer*, vol. 19, no. 5, pp. 545–551, 1976.

[63] F. Archambeau, N. Méchitoua et M. Sakiz, "Code_Saturne : A finite volume code for the computation of turbulent incompressible flows-industrial applications," *International Journal on Finite Volumes*, vol. 1, no. 1, 2004.

[64] A. Favre, *La turbulence en mécanique des fluides.* Gauthier-Villars, 1976.

[65] A. Teyssedou, R. Necciari, M. Reggio, F. Mehdi Zadeh et S. Étienne, "Moderator flow simulation around calandria tubes of CANDU-6 nuclear reactors," *Engineering Applications of Computational Fluid Mechanics*, vol. 8, no. 1, pp. 178–192, 2014.

[66] B. E. Launder et D. Spalding, "The numerical computation of turbulent flows," *Computer Methods in Applied Mechanics and Engineering*, vol. 3, no. 2, pp. 269–289, 1974.

[67] J. Van Doormaal et G. Raithby, "Enhancements of the simple method for predicting incompressible fluid flows," *Numerical Heat Transfer*, vol. 7, no. 2, pp. 147–163, 1984.

[68] M. Bouquillon, *Modélisation numérique de jets et leurs applications dans la simulation des écoulements dans la cuve du modérateur du réacteur CANDU.* M.Sc. Thesis, Polytechnique Montréal, 2008.

[69] D. Rozon, *Gestion du combustible nucléaire.* Notes du cours ENE6109, Polytechnique Montréal, 2007.

[70] L. F. Richardson, "The approximate arithmetical solution by finite differences of physical problems involving differential equations, with an application to the stresses in a masonry dam," *Philosophical Transactions of the Royal Society of London. Series A, Containing Papers of a Mathematical or Physical Character*, pp. 307–357, 1911.

[71] I. Celik, "Procedure for estimation and reporting of discretization error in CFD aplications," *ASME Journal of Fluids Engineering*, vol. 1, no. 06, p. 2008, 2004.

[72] S. S. Paul, *Experimental and numerical studies of turbulent cross-flow in a staggered tube bundle.* M.Sc. Thesis, University Of Manitoba, 2007.

[73] Ansys Inc., "Ansys fluent 12.0 users guide," *275 Technology Drive, Cansburg, PA 15317, USA*, 2009.

[74] S. Paul, S. Ormiston et M. Tachie, "Experimental and numerical investigation of turbulent cross-flow in a staggered tube bundle," *International Journal of Heat and Fluid Flow*, vol. 29, no. 2, pp. 387–414, 2008.

[75] A. Sarchami, N. Ashgriz et M. Kwee, "Effect of scaling on the thermalhydraulics of the moderator of a candu reactor," dans *Proceedings oInternational Conference on Ma-*

thematics and Computational Methods Applied to Nuclear Science and Engineering, no. May 8-12. American Nuclear Society (ANS), 2011.

[76] F. Mehdi Zadeh, S. Étienne et A. Teyssedou, "CFD simulation of the moderator flow in CANDU-6 nuclear reactors," *In press : Journal of Nuclear Engineering And Radiation Sciences*, vol. doi :10.1115/1.4032874, 2016.

[77] M. Abramowitz et I. A. Stegun, *Handbook of mathematical functions : with formulas, graphs, and mathematical tables*. Courier Corporation, 1964, no. 55.

[78] F. Mehdi Zadeh, S. Étienne et A. Teyssedou, "2-D CFD time-dependent thermal-hydraulic simulations of candu-6 moderator flows," *Submitted to : NED*, vol. paper # NED-D-16-00090, no. under revision, 2016.

[79] K. Prabhakaran, P. Goyal, A. Dutta, V. Bhasin, K. Vaze, A. Ghosh, A. V. Pillai, et J. Mathew, "Studies on flow induced vibration of reactivity devices of 700MWe Indian PHWR," *Nuclear Engineering and Design*, vol. 244, pp. 1–16, 2012.

[80] A. Behdadi et J. Luxat, "Comparison of turbulent models for candu moderator following a pressure tube to calandria tube contact," dans *31th Annual Conference of the Canadian Nuclear Society and 34th Annual Conference of the Canadian Nuclear Association*, may 2010.

[81] É. Varin, *Intégration des algorithmes du systeme de régulation du réacteur dans un code de cinétique espace temps*. M.Sc. thesis, École Polytechnique de Montréal, 1995.

[82] H. Schlichting et K. Gersten, *Boundary-layer theory*. Springer Science & Business Media, 2000.

[83] ANSYS Inc., "Ver. 13 ICEM-CFD," 2011.

[84] H. T. Kim, B. W. Rhee, J. E. Cha et H.-L. Choi, "Status of moderator circulation test at Korea atomic energy research institute," dans *Proceedings of Korea Nuclear Society Spring Meeting, Gwangju, Korea*, 2013.

[85] H. T. Kim, H. Seo, S. Im, B. W. Rhee et J. E. Cha, "Experimental study of moderator circulation in CANDU6 calandria tank," dans *22nd International Conference on Nuclear Engineering*. American Society of Mechanical Engineers, 2014, pp. V02BT09A052–V02BT09A052.

[86] H. T. Kim, B. W. Rhee et H.-L. Choi, "PIV measurement of velocity distribution in the moderator circulation test (MCT)," *Journal of Power and Energy Engineering*, vol. 2, no. 09, p. 74, 2014.

[87] E. Varin, R. Roy, R. Baril et G. Hotte, "CANDU-6 operation post-simulations using the reactor physics codes DRAGON/DONJON," *Annals of Nuclear Energy*, vol. 31, no. 18, pp. 2139–2155, 2004.

[88] N. Martin, *Développement de la méthode Sn à schémas diamants d'ordres élevés en géométrie 3D cartésienne.* M.Sc. thesis, École Polytechnique de Montréal, 2008.

[89] G. Marleau, A. Hébert et R. Roy, "A user guide for DRAGON release 3.06 l. tech. rep. IGE-174 rev. 12," 2013.

[90] J. Leppänen *et al.*, *Development of a new Monte Carlo reactor physics code.* VTT Technical Research Centre of Finland, 2007.

ANNEXE A Cadre Numérique de l'étude

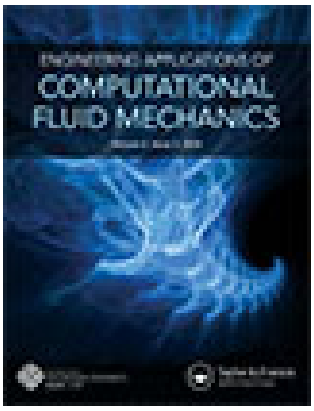

Engineering Applications of Computational Fluid Mechanics
Publication details, including instructions for authors and subscription information:
http://www.tandfonline.com/loi/tcfm20

Moderator Flow Simulation Around Calandria Tubes of Candu-6 Nuclear Reactors

A. Teyssedou[a], R. Necciari[a], M. Reggio[b], F. Mehdi Zadeh[a] & S. Étienne[b]
[a] Nuclear Engineering Institute, Engineering Physics Department École Polytechnique de Montréal, Québec, Canada,
[b] Mechanical Engineering Department, École Polytechnique de Montréal, Québec, Canada

Published online: 19 Nov 2014.

To cite this article: A. Teyssedou, R. Necciari, M. Reggio, F. Mehdi Zadeh & S. Étienne (2014) Moderator Flow Simulation Around Calandria Tubes of Candu-6 Nuclear Reactors, Engineering Applications of Computational Fluid Mechanics, 8:1, 178-192, DOI: 10.1080/19942060.2014.11015506

To link to this article: http://dx.doi.org/10.1080/19942060.2014.11015506

MODERATOR FLOW SIMULATION AROUND CALANDRIA TUBES OF CANDU-6 NUCLEAR REACTORS

A. Teyssedou[#]*, R. Necciari [#], M. Reggio[+], F. Mehdi Zadeh[#] and S. Étienne [+]

[#]*Nuclear Engineering Institute, Engineering Physics Department*
École Polytechnique de Montréal, Québec, Canada,
[+]*Mechanical Engineering Department, École Polytechnique de Montréal, Québec, Canada*
**E-Mail: alberto.teyssedou@polymtl.ca (Corresponding Author)*

ABSTRACT: CFD simulations of cross-flows along in-line and staggered tube bundles which emulate those encountered in the calandria of CANDU-6 reactors are presented. The knowledge of external wall temperature distributions around calandria tubes is a major concern during normal and off-normal operating conditions of CANDU reactors. Calculations are performed using the FLUENT software with several turbulence models using segregated and Coupled algorithms. It is observed that κ-based models are able to reproduce mean velocities in staggered bundles. In most cases, the Coupled algorithm yields convergence even if it requires a longer computational time. Based on this work, the standard κ-ε model is recommended to perform this kind of simulations. Improved κ-ε models do not lead to better results while the κ-ω model predicts very well the physics only around the first row but it is unable to predict the flow around tubes located far downstream in the bundle.

Keywords: computational fluid dynamics, CANDU reactors, moderator flow, calandria tubes, tube bundles

1. INTRODUCTION

The knowledge of flow velocity and temperature distributions of the moderator in the vessel of CANDU-6 nuclear reactors is a major concern in safety analysis. In particular, numerical simulations of local fluid velocities around calandria tubes may help in providing fundamental heat transfer predictions. We have observed that in most cases CFD codes are not rightfully used, i.e., the number of nodes is insufficient to satisfy numerical convergence and turbulence models are not appropriate to treat particular problems. From this viewpoint, we try to clarify some of these flaws by validating numerical results against experimental data obtained from the open literature.

Fig.1 shows a cross-sectional view of a CANDU-6 reactor calandria vessel; its total depth is 6 m. Its design is such that the moderator (i.e., heavy water) circulates around a bank of 380 tubes, in general at a very low flow velocity. For an isothermal flow of the moderator in the calandria (without heat transfer neither from the tubes, nor from neutron slow-down processes), the two water jets and a symmetrical flow discharge will create two quasi-symmetrical vortices, i.e., one on the left side of a vertical mid plane and another on the right side. Under normal operation conditions and due to the real geometrical arrangement of the tubes, inlet nozzles and water outlet, mostly cross-flow distributions will develop around the tubes. In addition, the multi-connected region of the calandria vessel imposes a serious challenge to realize numerical simulations of the phenomenon.

In order to deal with this problem, a porous medium approach, where the tubes are replaced by appropriate distributed hydraulic resistances was introduced in the 1980's. Based on this idea, the Canadian nuclear industry developed the MODTURC (MODerator TURbulent Circulation; Huget et al., 1990) and MODTURC-CLAS (MODerator TURbulent Circulation Co-Located Advanced Solution; Huget et al., 1989) software. These models are nowadays largely used to perform nuclear safety analysis calculations.

It is clear that porous medium modeling does not allow fine flow information to be predicted. In fact, these types of calculations provide only average values of flow velocities and temperatures and do not give any information about local flow variables near tube solid walls, which are necessary to implement accurate heat transfer calculations. Along this line of thinking, the CFX commercial CFD code was applied with the porous media approach using segregated (Yoon et al., 2004 and 2006) and coupled solvers (Yoon and Park, 2008) to simulate Calandria type experiments.

Simulations were enhanced by Kim et al. (2006) who used FLUENT to calculate moderator's flow across all calandria tubes. Yoon et al. (2004 and 2006) and Yoon and Park (2008) employed

Received: 8 Aug. 2013; Revised: 20 Oct. 2013; Accepted: 22 Nov. 2013

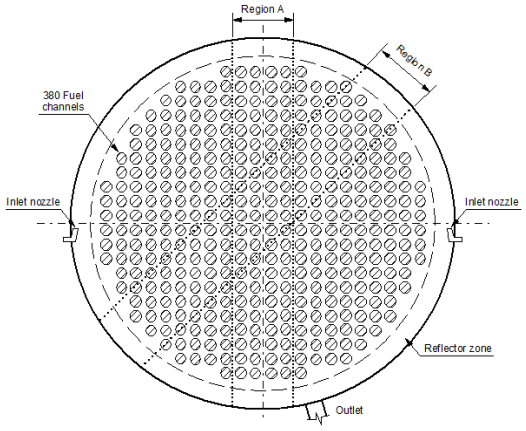

Fig. 1 Cross-sectional view of calandria vessel of CANDU- 6 nuclear power reactor.

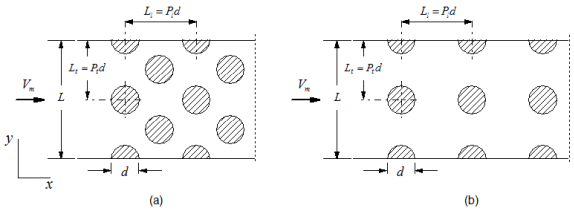

Fig. 2 Schematics of: (a) staggered and (b) in-line tube-bundles.

frictional pressure loss data collected for incompressible flows along in-line and staggered tube bundles to validate distributed hydraulic resistances. The experiments, performed at the Stern laboratories (Hadaller et al., 1996) used a quarter scale test section to simulate an axial slice of a CANDU-6 calandria vessel. As shown by "region A" in Fig.1, an in-line tube distribution can be considered. In turn, "region B" (in the same figure) corresponds to a staggered type of tube distribution. Therefore Hadaller et al. (1996) collected frictional pressure drop data from measurements taken in test sections having in-line and staggered tube bundles to represent only a partial section of a calandria vessel. These pressure drop data are in general quite small (a few Pa), which make them quite difficult to measure or simulate with acceptable accuracy.

Cross-flow in tube bundles has been largely studied because they are encountered in numerous heat exchangers or cooling systems used by the power industry. Investigations and visualizations have been carried out among others by Zukauskas (1989), who has also proposed pressure drop and heat transfer correlations. He has performed experiments under four different flow conditions: (*i*) predominant laminar flow ($Re < 10^3$), (*ii*) mixed or subcritical flow ($Re < 2 \times 10^5$), (*iii*) predominant turbulent or critical flow ($2 \times 10^5 < Re < 4 \times 10^5$) and (*iv*) supercritical flow ($4 \times 10^5 < Re$). A detailed review of this kind of flows can be found among others in: Beale and Spalding (1999), Paul (2006), Paul et al. (2007 and 2008) and Liang and Papadakis (2007). However, most of the flow visualizations have been performed in tube bundles having a few number of rows as compared to Stern Laboratories experiments (Hadaller et al., 1996). Moreover, when results for large tube bundles are presented, most of the works do not provide complete data sets. For instance Iwaki et al. (2004) performed cross-flow visualizations for 20 rows but the measurements were carried out only along the first row of tubes.

From a numerical simulation point of view, several studies were carried out, among others by Balabani and Yianneskis (1996) and Simonin and Barcouda (1988). A detailed review is given in Paul (2006) and Liang and Papadakis (2007). The latter reproduces experiments performed by Simonin and Barcouda (1988) using a 3D Large Eddy Simulation of an entire tube-bundle. Within this context, the goal of the present work is twofold: first to validate 2D cross-flow simulations with data collected in both in-line and staggered tube-bundles, and second to test the ability of various numerical schemes to handle Hadaller et al. (1996) experiments. To fulfill these objectives, a preliminary validation is performed by using flow velocity data given in Paul (2006) and Paul et al. (2007 and 2008). The simulations are carried out using FLUENT with the following turbulence models: (i) κ-ε, (ii) κ-ε realizable, (iii) κ-ε RNG and (iv) κ-ω.

2. SELECTED EXPERIMENTAL DATA

In this section, the experimental data given in Paul (2006) and Paul et al. (2007 and 2008) and Hadaller et al. (1996) are described. The experimental set-ups used by these authors are schematically shown in Fig. 2; key geometrical parameters and experimental conditions are summarized in Table 1. In all cases, the test sections have rectangular or square geometry. The selected experiments are performed using water under constant temperature conditions and uniform velocity distributions at the inlets of the channels. Furthermore, the Reynolds number is based on the tube diameter and inlet uniform flow velocity. Paul (2006) and Paul et al. (2007 and 2008) used a PIV (Particle Image Velocimetry) technique to collect local velocity data whereas Hadaller et al. (1996) used differential pressure

Table 1 Summary of key parameters.

	Paul et al. (2006-2008)	Hadaller et al. (1996) Config. 1		Hadaller et al. (1996) Config. 2
Type*	S	S		I
Number of rows	6	33		24
Number of arrays	3 ; 2	4 ; 3		4
L (mm)	193.04	346		286
Depth (mm)	200	200		200
d (mm)	25.4	33.02		33.02
L_l (mm)	53.34	50.49		71.4
L_t (mm)	96.52	100.98		71.4
P_l	2.1	≈1.53		≈2.16
P_t	3.8	≈3.06		≈2.16
Vm (m/s)	0.340	0.054	0.07	0.103
T (°C)	23.0	39.5	63.6	79.8
Re	9300	2746	5237	9392

* I = in-line, S = staggered

transducers to collect static flow pressure drop. According to Paul (2006) and Paul et al. (2007 and 2008), the uncertainties of mean velocity at 95% confidence level are ±3% in the central portion of the channel and ±5% close to tube walls. It must be pointed out that the current numerical study was performed in 2D while the above experiments are 3D in nature. It is therefore anticipated that numerical predictions may show some discrepancies with respect to the experimental data.

3. MODELING EQUATIONS

The governing equations used in FLUENT are based on the Reynolds Averaged Navier-Stokes equations (RANS). For 2D steady state incompressible flows, the RANS conservation equations for mass and momentum are written as:

$$\frac{\partial U_i}{\partial x_i} = 0 \tag{1}$$

$$\rho \frac{\partial \left(U_i U_j \right)}{\partial x_i} = -\frac{\partial P}{\partial x_j} + \frac{\partial}{\partial x_i}\left(\mu \frac{\partial U_j}{\partial x_i} - \rho \overline{u_i' u_j'} \right) + \rho \, \overline{f}_j \tag{2}$$

where $\overline{f}_j$ represents average values of body forces (in the present study they are considered equal to zero), U_i is the average i velocity component, P is the mean pressure and $\overline{u_i' u_j'}$ is the ij component of the Reynolds stress tensor. In addition, turbulence models are based on Boussinesq's hypothesis that links the Reynolds stress tensor to a turbulent viscosity (or eddy-viscosity), hence:

$$\overline{u_i' u_j'} = \nu_t \left(\frac{\partial U_j}{\partial x_i} + \frac{\partial U_i}{\partial x_j} \right) - \frac{2}{3} \delta_{ij} \kappa \tag{3}$$

where ν_t is the turbulent viscosity which is not constant, κ is the turbulent kinetic energy and δ_{ij} is the Kronecker delta function. In the present work the following four two-equation turbulence models were used: (*i*) the standard κ-ε model proposed by Launder and Spalding (1972), (*ii*) the κ-ε realizable introduced by Shih et al. (1995), (*iii*) the κ-ε RNG introduced by Yakhot and Orszag (1986), and (*iv*) the standard κ-ω based on the work of Wilcox (1998). It must be pointed out that the Shear-Stress Transport κ-ω model proposed by Menter (1994) was also tried; however, contrary to what seems to be observed in aerodynamic applications, convergence was difficult to achieve. Therefore, these results are not discussed here; however, additional information about the above turbulence models is given in Necciari et al. (2010).

FLUENT uses a finite volume approach to solve the conservation equations and it offers to the user several discretization schemes. Because of the nature of the actual problem, the pressure based solver is chosen over the density based one. To this purpose, SIMPLE (Semi-Implicit Pressure Link Equations) and Coupled algorithms have been used. The PRESTO! (PREssure STaggering Option) was applied for the pressure interpolation, whereas the second-order upwind scheme was selected to discretize the convective terms for the simulations.

For all cases, the residuals were used as a convenient convergence metric. In this study, calculations were considered to converge when they showed a neat decreasing trend or they stayed around 10^{-5}. In addition, before stopping the calculations, relative variations of key physical variables, such as flow velocities and pressures were imposed to be lower than 10^{-3} *m/s* and 1 *Pa*, respectively.

4. COMPUTATIONAL MESH AND BOUNDARY CONDITIONS

To conduct a flow simulation, the computational domain must be appropriately discretized. In this work, this task is performed using GAMBIT, former companion software for FLUENT. In this paper, discussions about the different mesh types and alternatives are not presented. This can be found in a previous work given in Necciari et al. (2010). However, multiple meshes based on different geometrical decomposition and/or mesh type (i.e. quadrilateral and triangular) and mesh refinement were tested. In particular, a square based mesh type with multi-block quadrilateral structured meshes was used in this study (Fig. 3). Various reasons support using this type of mesh: it is simple to implement and it allows an easy control of the mesh density (structured mesh) to be achieved, it requires relatively fewer cells than the triangular one, it is well suited to solve the boundary layer and provides similar results to those obtained with more complex meshes.

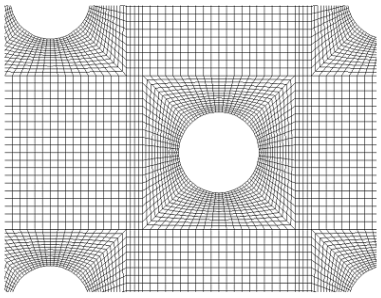

(a) Mesh structure

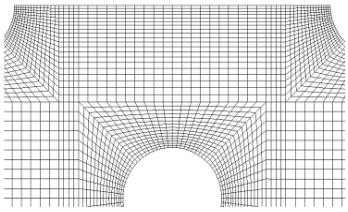

(b) Mesh geometry around cylinders

Fig. 3 Square-based mesh.

As boundary conditions, a uniform velocity was used at the inlet boundary, a no-slip condition was used over solid walls and outflow condition in FLUENT was applied at the outlet of the channel. A turbulent intensity of 4% was imposed at the inlet and an enhanced wall treatment was used to model the boundary layer (y+≈1).

5. COMPARISONS OF SIMULATIONS WITH DATA

Paul (2006) and Paul et al. (2007 and 2008) presented flow data collected in a staggered tube bundle having the geometry given in Table 1. Fig. 4 shows the experimental set-up and the locations where the numerical results were sampled and compared with experimental values.

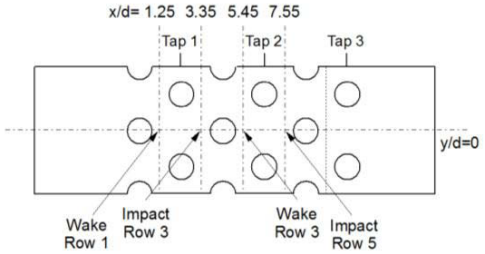

Fig. 4 Paul (2006) and Paul et al. (2007 and 2008) flow channel and locations where results of simulations are sampled.

Before studying the numerical performance of different algorithms and turbulent models, and to select the appropriate grid size that produces a suitable error level, a grid convergence study was performed. To this aim, the same experiments were simulated by using the κ–ε Standard turbulence model and the SIMPLE algorithm. Simulations were repeated for grid sizes of 1 772, 8 200, 32 800, 132 000 and 528 000 using the grid topology shown in Fig. 3. The value of the selected working parameter was the normalizedstreamwise velocity, i.e., U_x/V_m. For different locations, Fig. 5 illustrates computed RMS differences of U_x/V_m as a function of the

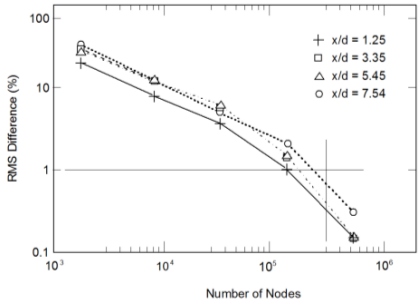

Fig. 5 Grid convergence for RMS difference at different locations.

mesh size. The solution obtained using a very fine grid with 1 209 600 nodes was used as a reference case. These results show that decreasing the mesh size with increasing number of elements up to 200 000, the expected RMS difference is less than 1%. Therefore, it was determined that the use of a mesh having 528 000 elements constitutes a good compromise between computational performance and error level. It is important to mention that this convergence study provides an approximate estimation of the minimum number of nodes required to perform 2D simulations of the calandria vessel of CANDU reactors. In fact, the results indicate that to guarantee a satisfactory convergence for 2D calculations, each tube should be meshed with a minimum of 9 500 elements which necessitates at least 3.6 millions of elements. Nevertheless, we have observed that in recent CFD simulations, numerical codes are not rightfully used, i.e., the number of nodes is insufficient to satisfy convergence and turbulent models are not appropriate to treat cross-flows. In fact, some of these observations contradict works where 2D and even 3D CANDU simulations were carried out using a limited number of nodes (Mangoong et al., 2006; Sarchami et al., 2013). Thus, it is quite possible that in these studies convergence was not completely achieved. Therefore, herewith, we find it useful to validate and clarify some of these key aspects.

5.1 Performance of SIMPLE and Coupled algorithms

The experimental conditions given in Paul (2006) and Paul et al. (2007 and 2008) were also used to evaluate the performance of particular algorithms implemented in the FLUENT code. To this aim, both SIMPLE and Coupled schemes were applied. Only two turbulence models were used for this study: the standard κ-ε and the κ-ω models. The others κ-ε alternatives are not presented here; the κ-ε RNG behaves like the standard κ-ε while it was observed that the κ-ε Realizable does not converge well when the SIMPLE algorithm is invoked.

Figs. 6, 7 and 8 show comparisons of velocity profiles along several surfaces obtained with the aforementioned algorithms with both the κ-ε and the κ-ω models. Experimental data are also shown in the figures. The velocity profiles are given in terms of non-dimensional quantities; the velocity is scaled by the uniform inlet velocity while distances are referred to the diameter of the cylinder. Simulations are compared using a variance, defined as:

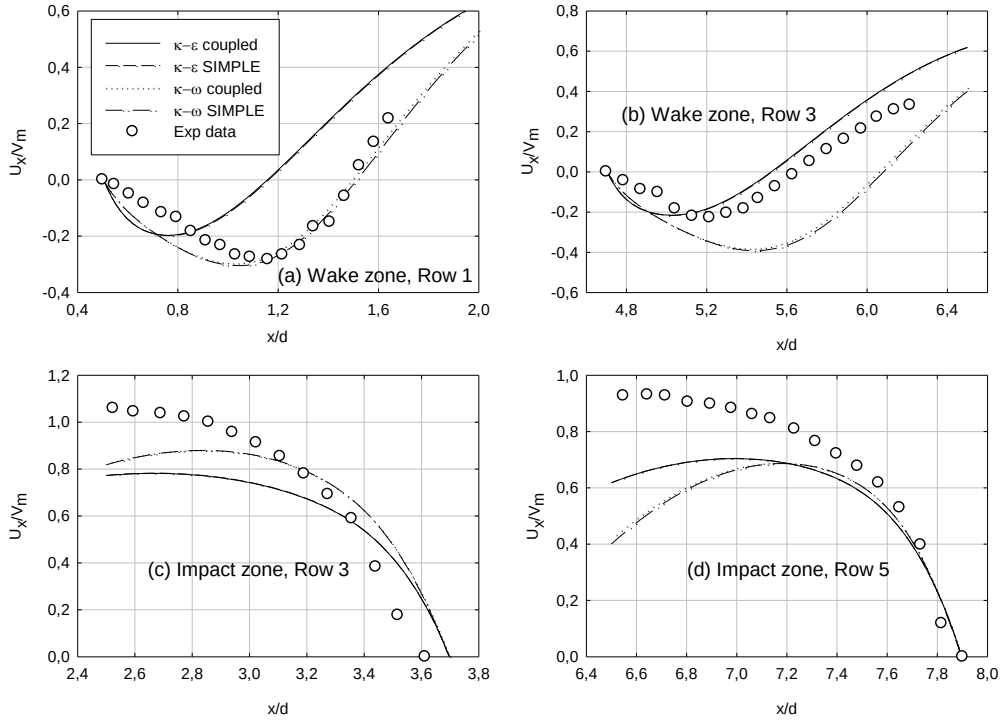

Fig.6 Comparison of streamwise velocity profiles obtained with SIMPLE and Coupled algorithms using κ-ε and κ-ω turbulence models (y/d=0).

$$\sigma^2 = \frac{1}{n}\sum_{i=1}^{n}\left(x_{\exp} - x_{num}\right)^2 \qquad (4)$$

Fig. 6 shows streamwise velocities on surfaces at *y/d=0* (Fig. 4); it is observed that in all cases the turbulence models underestimate the velocity upstream of impact zones. In the wake zones behind the tubes, all models predict the correct trends with a recirculation zone in which the streamwise velocity is negative. In the wake zone at row 1, the κ-ω model produces the best prediction. For the wake zone downstream of row 3, the standard κ-ε behaves better which is contrary to the results of Paul et al. (2008); probably due to the grid structure used to perform the present calculations. The values of the variances given in Table 2 confirm these observations. For the four surfaces shown in Fig. 4, the results obtained with SIMPLE and Coupled algorithms by using the κ-ε models are extremely close, the differences are not noticeable on the velocity profiles. Instead, when the κ-ω model is used, the differences are larger, even if the two algorithms produce similar results. However, the principal differences are observed to occur in the wake zones. For the κ-ω model it is also observed that the Coupled algorithm seems to produce results closer to the experimental data than the SIMPLE one.

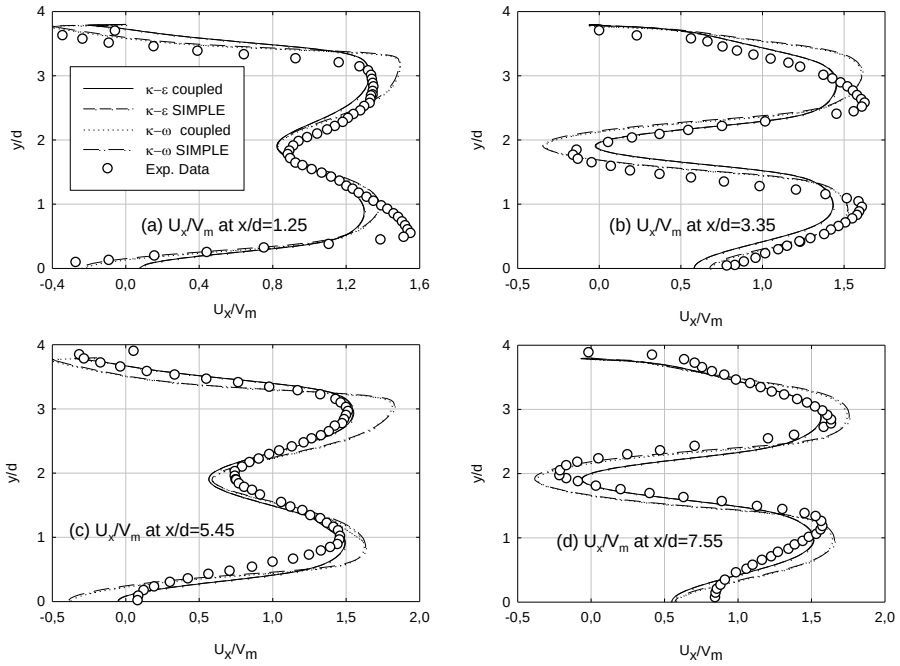

Fig. 7 Streamwise velocity profiles obtained with SIMPLE and Coupled algorithms using κ-ε and the κ-ω turbulence models (*x*/*d*=1.25, 3.35, 5.45 and 7.55).

Table 2 Variance of simulation as function of experimental data.

Surface	Velocity	Variance			
		Standard κ-ε		κ-ω	
		SIMPLE	Coupled	SIMPLE	Coupled
Impact Row 3	S	38.2	39	24	24.1
Impact Row 5	S	26.5	26.2	52.6	48.6
Wake Row 1	S	44.9	46.4	3.1	2.7
Wake Row 3	S	8.6	9.2	58.6	50.4
x/d = 1.25	S	75.7	79.5	53.6	57.1
	T	3.2	3.3	2.8	2.7
x/d = 3.35	S	95.7	98.8	105.8	107
	T	7	7.3	7.1	7
x/d = 5.45	S	25.9	27.1	64.9	57.9
	T	2.8	2.9	4.8	4.5
x/d = 7.55	S	48.1	47	63.8	56.7
	T	5.4	5.5	12.1	11.3

*S = streamwise and T = transverse

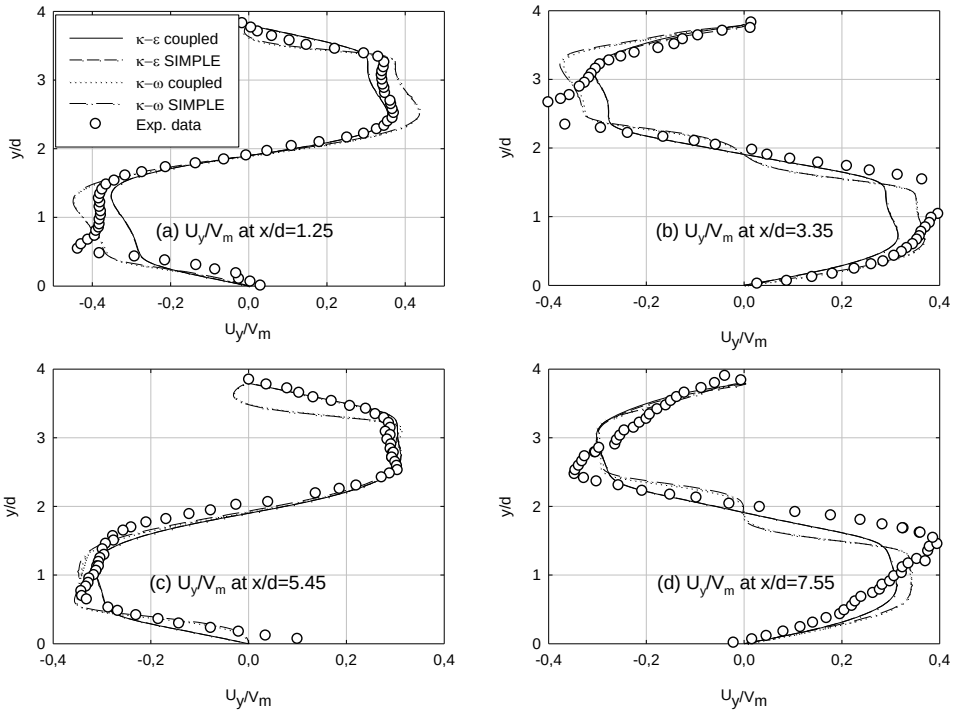

Fig. 8 Transverse velocity profiles obtained with SIMPLE and Coupled algorithms using κ-ε and the κ-ω turbulence models (*x*/*d*=1.25, 3.35, 5.45 and 7.55).

Figs. 7 and 8 present the streamwise and transverse velocity profiles determined along lateral surfaces (see Fig.4), respectively. The differences when the κ-ε model is used are larger on lateral surfaces than on the y/d=0 surface, but they are not very noticeable on the profiles. Once again, the differences are more pronounced when the κ-ω model is used. Nevertheless, these differences are much smaller for these velocity profiles than for the one at *y/d=0* (see Fig. 6). Despite these observations, it is almost impossible to determine which algorithm is better for simulating all cases (i.e., for all velocity profiles). However, for the κ-ε model, the SIMPLE algorithm seems to provide globally better results than the Coupled one. In turn, when the κ-ω model is used, the Coupled algorithm seems to behave better than the SIMPLE one.

In view of the previous results, we can therefore infer that both algorithms are able to predict similar velocity profiles, especially when the κ-ε turbulence model is used. The observed differences do not allow us to clearly determine which of the two algorithms performs better for treating this kind of complex flows. Nevertheless, we recommend choosing the Coupled algorithm jointly with the κ-ω model or the SIMPLE with the κ-ε model.

It is noted, however, that the κ–ω model yields slower convergence rate when SIMPLE is used, while the κ-ε Realizable model is not able to converge when the same algorithm is invoked. Moreover, the Coupled algorithm always converges unconditionally; instead SIMPLE seems to be more cumbersome even if quite low under-relaxation coefficients are used. For instance, for in-line tube bundles, the SIMPLE algorithm does not converge at all. Further, the Coupled algorithm produces smaller residuals enabling a better accuracy to be achieved. In general, a single iteration is more expensive when the Coupled algorithm is used. In practice this means that for a domain requiring a large number of cells, the Coupled algorithm necessitates more computational time per iteration than SIMPLE; nevertheless, it requires a lower number of calculation cycles. It is clear that a trade-off between these conditions must be established.

In practice, after several tests conducted with different turbulence models and for both algorithms, we recommend using SIMPLE with low under-relaxation factors (if needed) in conjunction with κ-ε or κ-ε RNG turbulence models for staggered tubes-bundles, in particular fine meshes. When convergence is difficult to achieve, or when very low residuals are expected,

the Coupled algorithm is better suited. It is important to note that depending on the initial guess, the Coupled algorithm may also diverge. In such a case it is suggested to start the calculation using the SIMPLE algorithm and then switch to the Coupled one to reach a stricter convergence. This progression also permits faster calculations to be achieved.

5.2 Comparison between simulations performed using different turbulence models with data

Simulations were performed by using four turbulence models. The results were compared with experimental data. Fig. 9 shows average streamwise velocity profiles over the surfaces located at *y/d=0*, where the data are presented in dimensionless form. Figs. 10 and 11 show streamwise and transverse velocity profiles along lateral surfaces, respectively. The variances of the simulations with respect to the experimental data are given in Table 3.

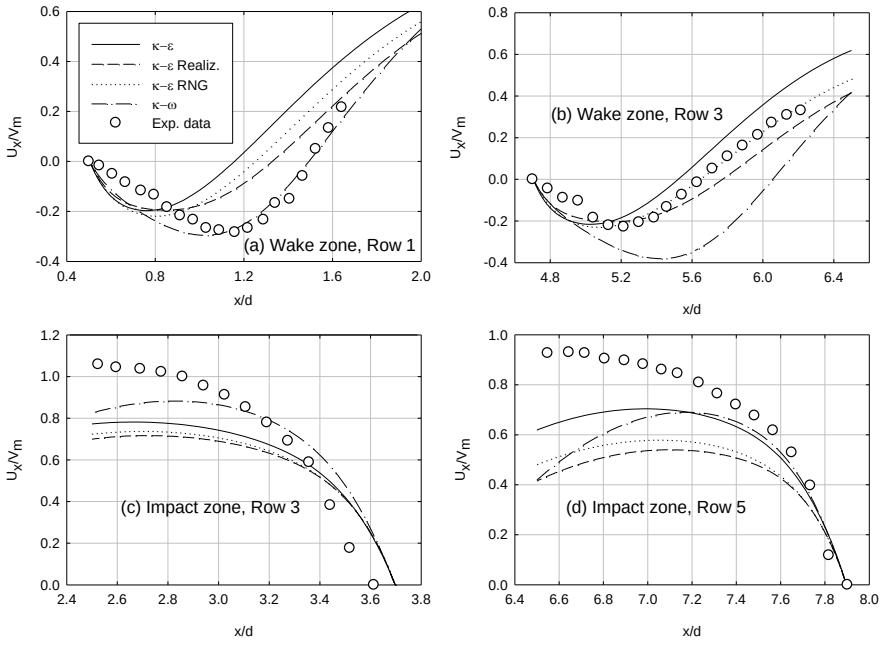

Fig. 9 Comparison of simulated streamwise velocity profiles with data of Paul (2006) and Paul et al. (2007 and 2008) (axial location *y/d*=0).

Table 3 Variance of simulations as function of experimental data (four turbulence models).

Surface	Velocity	Variance			
		κ-ε Standard	κ-ε Realizable	κ-ε RNG	κ-ω
Impact Row 3	S	39.9	58	50.9	24.1
Impact Row 5	S	26.2	90.4	69.4	48.6
Wake Row 1	S	46.4	14.1	26.1	2.7
Wake Row 3	S	9.2	4	1.7	50.4
x/d = 1.25	S	79.5	60	64.8	57.1
	T	3.3	3.1	3.4	2.7
x/d = 3.35	S	98.8	102.1	101.6	107
	T	7.3	7.6	7	7
x/d = 5.45	S	27.1	32.9	27.4	57.9
	T	2.9	3.6	3.2	4.5
x/d = 7.55	S	47	58	53.1	56.7
	T	5.5	0	7.1	11.3

*S = streamwise and T = transverse

Fig. 9 and Table 3 confirm that for both the impact and the wake zones, all turbulence models correctly predict the experimental trends. Nevertheless, for the impact zones, they underestimate the velocity upstream the cylinders. It is also observed that with the exception of the standard κ-ε model, the other models predict the first impact zone better than the second one. In addition, it is also observed, that the κ-ω model predicts quite well the first wake region, in particular it provides a correct recirculation length, while κ-ε models underestimate this length by up to 35%. For the second wake zone, the κ-ε RNG seems to produce better results, while the κ-ε Realizable and the κ-ω model overestimate the recirculation length by up to 30% and the standard κ-ε underestimates this length by 10%. Concerning the predictions of the wake zone, it seems that they are better for the third cylinder than for the first one when κ-ε models are used; instead they get worst when the κ-ω model is implemented in the calculations. In general, an improvement is observed by using the standard κ-ε model along the entire flow, whereas the κ-ω model seems to better predict the flow only in a region close to the first row of tubes.

It must be pointed out that we are concerned about possible involuntary systematic errors that could be introduced during the experiments. In fact, the comparison of Figs. 9a with 9c and Figs. 9b with 9d, indicates that there is almost a perfect continuity along the present simulated values. For instance, comparing the values of $U_x/V_m \approx 0.6$ at $x/d=2$ in Fig. 9a with $U_x/V_m \approx 0.7$ at $x/d=2.4$ in Fig. 9c shows that they are not only close but they also have the right extrapolation slope. The same observation can be drawn from Figs. 9b and 9d. In turn, at the same location, experimental data are not only quite different but their extrapolation trends diverge. This argument seems to be supported by simulations of the lateral velocity profiles (Figs. 10 and 11), which are in very good agreement with the data.

For the velocity profiles along lateral surfaces, shown in Figs. 9 and 10, it is observed that in general all turbulence models predict the correct trends. The κ-ε models produce quite similar predictions, while there are significant differences between these results and those obtained when the κ-ω model is used. With the exception of the streamwise velocity along the surface x/d=5.45 predicted by the κ-ω model, it is also observed

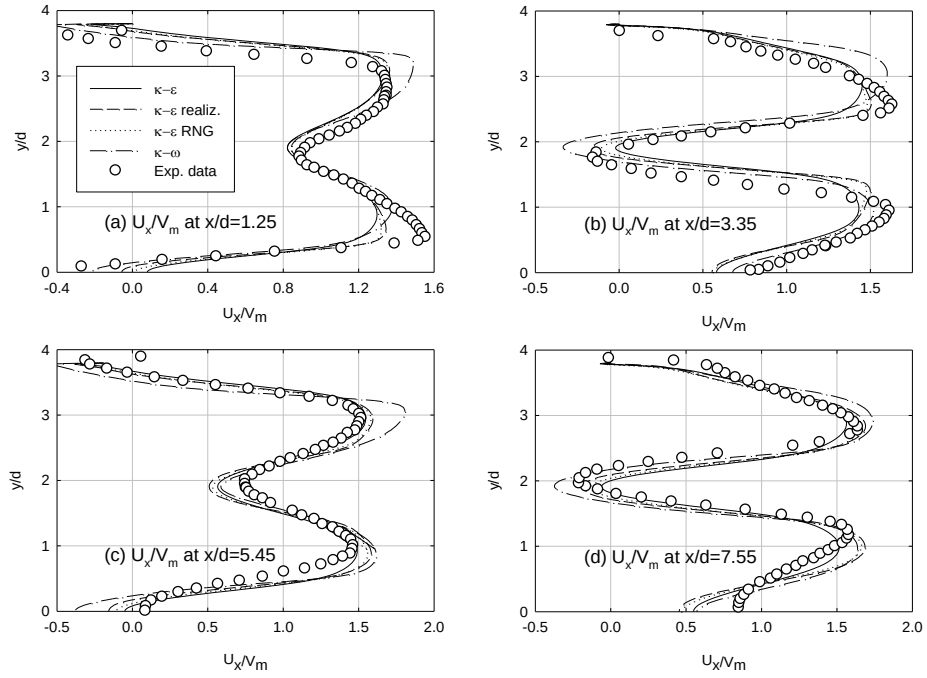

Fig. 10 Comparison of simulated lateral velocity profiles with data of Paul (2006) and Paul et al. (2007 and 2008) (x/d=1.25, 3.35, 5.45 and 7.55).

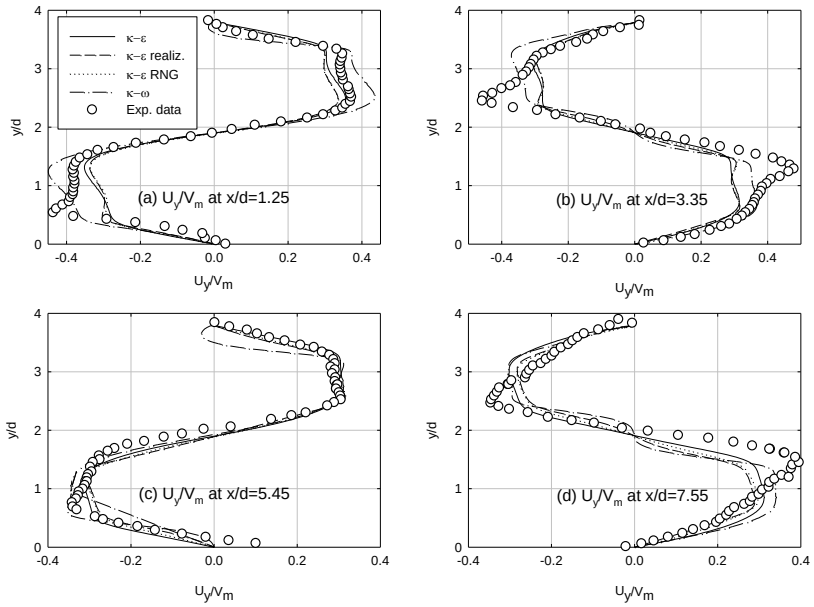

Fig. 11 Comparison of simulated transverse velocity profiles with data of Paul (2006) and Paul et al. (2007 and 2008) (x/d =1.25, 3.35, 5.45 and 7.55).

that all the turbulence models predict better the flow in upstream zones of the cylinders than in the downstream ones. This is difficult to be distinguished from streamwise velocity profiles (Fig. 10), but it may be seen on the transverse velocity profiles (Fig. 11), where any of the turbulence models are able to predict the peaks occurring behind cylinders. This is particularly true for the κ-ω model which admits odd variations near *y/d=2*. If we compare the profiles by pairs, *x/d=1.25* with *x/d=5.45* (upstream) and *x/d=3.35* with *x/d=7.55* (downstream), the results improve when the standard κ-ε and κ-ε RNG models are used, while the opposite occurs for the κ-ω model. Furthermore, if the results of the transverse velocity along the surface *x/d*=5.45 are not considered, the same conclusion as for the other κ-ε models also applies to the κ-ε Realizable one.

From the comparison of the four turbulence models, it can be concluded that for the streamwise velocity (except for the surface at *x/d=1.25*) the standard κ-ε model yields better results than the other κ-ε models while the predictions obtained with the κ-ω model are, in general, not very good. Only along the surface *x/d=1.25* the κ-ω model seems to do a better job. This is also reflected in the transverse velocity along the surface *x/d=1.25* where the κ-ω model seems to be better. Along the surface *x/d=3.35*, κ-ω and κ-ε RNG models are barely better while along surfaces *x/d=5.45* and *x/d=7.55*, the standard κ-ε model seems to produce better predictions than other models while the worst results are obtained with the κ-ω model.

In the flow developing region (i.e., *0.85 < x/d < 3.35*), Paul et al. (2008) have argued that the ω-based model produces results that are in better agreement with the data, while in the spatially periodic region (i.e., *x/d > 5.05*) the ε-based ones are much superior. This conclusion seems also to be true for the present study. It is however quite clear that the κ-ω model predicts the flow through the first row better than κ-ε models, but along the rest of the bundle, the standard κ-ε model gives better predictions. It is also observed that improved κ-ε models do not necessarily yield better results than the standard one.

Along these simulations, isocontours of flow pressures and axial velocities were also obtained. Figs. 12 and 13 illustrate normalized isocontours of pressure and axial velocity obtained with the κ-ε standard model, while Figs. 14 and 15 show similar predictions obtained with the κ-ω model. As stated previously, these figures clearly show that far away from the wall, the κ-ω model tends to overestimate flow eddies. A comparison of static pressure contours for both turbulence models confirms this behavior. In fact, a comparison of pressure contours in impact zones at *x/d=3.35* and *x/d=7.55* indicates that the results of the κ-ω model are smaller than those of the κ-ε.

Furthermore, Fig. 8 shows that at *y/d=2* small swirls are predicted by κ-ω model.
Contrary to the experimental observations, similar lateral accelerations were also predicted with the κ-ω model by Paul et al. (2007 and 2008).

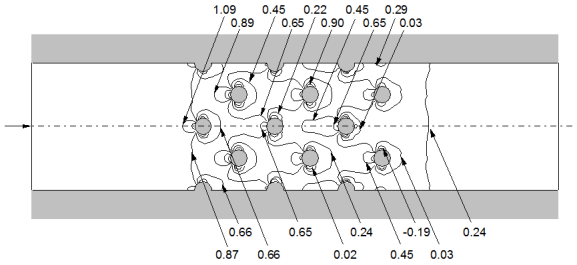

Fig. 12 Contour of normalized pressure using κ-ε turbulence model.

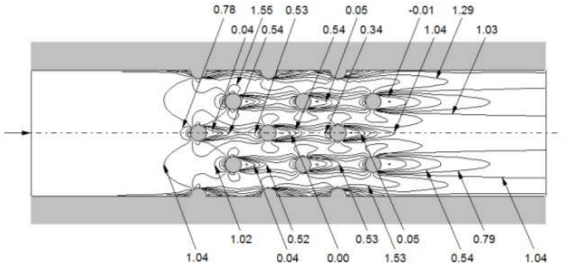

Fig. 13 Contour of normalized axial velocity using κ-ε turbulence model.

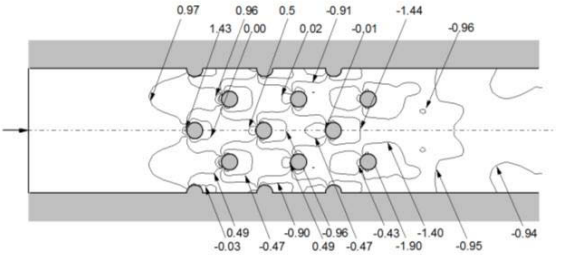

Fig.14 Contour of normalized pressure using κ-ω turbulence model.

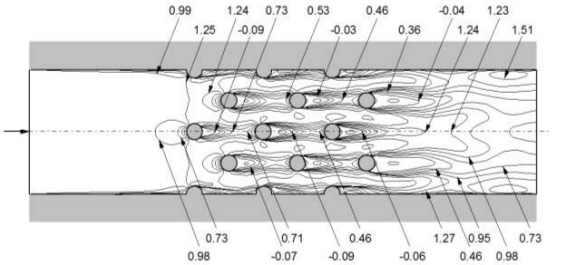

Fig. 15 Contour of normalized axial velocity using κ-ω turbulence model.

Based on this study, which is intended to tackle flow simulations across a staggered bundle of tubes (i.e., having a similar topology to those encountered in the Calandria vessel of CANDU nuclear reactors) Figs. 6 to 11 seem to indicate that the standard κ-ε model should be preferred. In fact, the k-ω option is more sensitive to the mesh structure and requires more calculation time. To determine the flow regime, Reynolds numbers based on both the cylinder diameter and the longitudinal distance between tubes are also calculated for the first row and these values are 9300 and 38345, respectively. For cross-flow around tube bundles, the critical Reynolds number is between 3×10^5 to 4×10^5 (Hoerner, 1965). Even though when several rows are considered, transition and fully turbulent flow could occur at a lower Reynolds number; in the present case its value can never reach a critical value. Consequently, based on either one of the characteristic lengths, the flow is not fully turbulent. Therefore, if the simulation consisted of a unique row of cylinders or a single obstacle, the κ-ω model appears as a better alternative. In turn, for simulating the flow of the moderator in the calandria vessel that contains 380 tubes, the standard κ-ε model, seems to be more precise and viable.

6. COMPARISON OF PRESSURE DIFFERENCE SIMULATIONS WITH DATA

The principal goal of this part of the work consists of validating FLUENT's capability for simulating the flow of the moderator in CANDU-6 nuclear reactors. To this purpose, Hadaller et al. (1996) collected data using in-line and staggered tube-bundle test sections which represent one quarter scale of the central part of a CANDU-6 calandria vessel (see Fig. 1). The locations of the pressure taps used in the staggered and in-line tube bundles are shown in Figs. 16 and 17, respectively. The staggered tube bundle is formed by 33 rows of tubes and the pressure drop was measured between 24 rows (between tap 1 and tap 3). The in-line tube bundle is formed by 24 rows of tubes and the pressure drop was determined between 16 rows. Since the pressure drop per row for both in-line and staggered bundles are considered identical in Hadaller et al. (1996), to compare the predicted pressure drop between 16 rows for in-line and staggered tube bundles, a

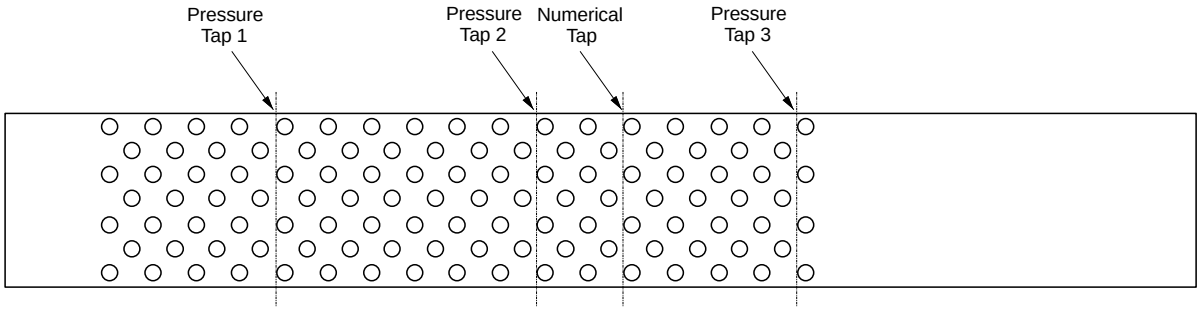

Fig.16 Schematic of staggered tube-bundle test section and location of pressure taps (Hadaller et al., 1996).

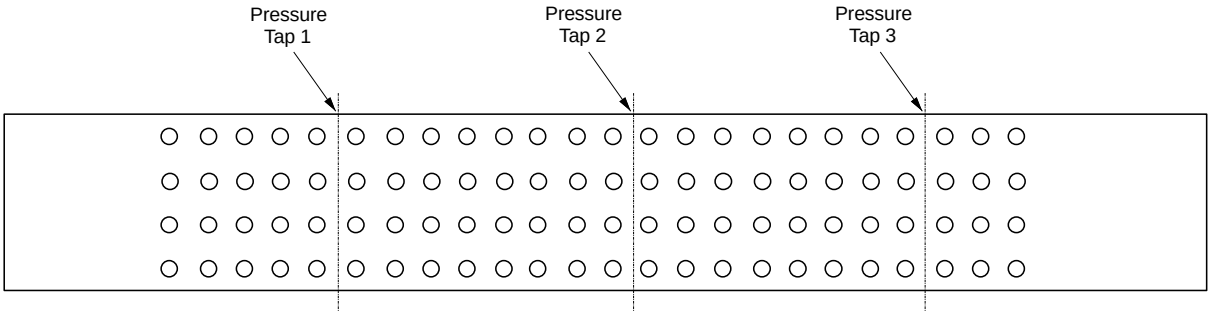

Fig.17 Schematic of in-line test section and location of pressure taps (Hadaller et al., 1996).

numerical tap was also added in the staggered bundle. To obtain the predicted pressure drop, the area-weighted average of the static pressure along lateral surfaces was considered.

Hadaller et al. (1996) have used the experimental data to determine Pressure Loss Coefficients (PLCs) defined as:

$$PLC = \frac{\Delta P}{N \rho \frac{V^2}{2}} \tag{5}$$

where N represents the row number and V the upstream velocity at the tube bank. It is obvious that the PLC calculated with Eq. 5 represents an average value for each row.

Zukauskas (1989) and Hadaller et al. (1996), among others, have observed that in sub-critical incompressible flows, the pressure drop coefficient given by Eq. 5 decreases with increasing Reynolds number. Thus, Hadaller et al. (1996) have proposed correlations for calculating the PLC in different tube bundle configurations as a function of this number, further they have compared the proposed correlations with those previously used in the MODTURC code. These correlations (i.e., MODTURC) are given by Eqs. 6 and 7, respectively.

$$PLC = 4.54 * \mathrm{Re}^{-0.172} \tag{6}$$

$$PLC = 4.56 * \mathrm{Re}^{-0.166} \tag{7}$$

where the Reynolds number is defined based on the upstream flow velocity at the tube bank and cylinder's diameter.

Comparisons between present pressure drop simulations with data estimated by using Hadaller correlations are given in Table 4. The Reynolds numbers as well as the values of the PLC are also included in the table. Absolute values as well as relative error between pressure drop simulations and data estimated from the correlations for in-line and staggered bundles are presented for 16 and 24 rows of tubes. It has been observed that the numerical simulations follow the expected behavior; thus, the static pressure starts increasing upstream the cylinder and reaches a maximum in the stagnation region (zero velocity). The pressure decreases then along the cylinder until a minimum (maximum velocity) is achieved. In the downstream region, a pressure recovery is observed until the flow reaches the next cylinder region where a similar trend repeats while a recirculation zone is present downstream each cylinder.

Table 4 Pressure drop for in-line and staggered tube bundles.

		Reynolds number	PLC	Δp (Pa) 16 rows				Δp (Pa) 24 rows
				I		S		S
					RE (%)		RE (%)	
Stern Lab. T.P. 326	Experiments	2746	1.163	28.2		N/A		N/A
	Correlation			26.92		26.92		40.38
	MODTURC			30.50		N/A		N/A
	κ-ε			16.02	-43	21.36	-20	32.06
	κ-ε R			13.57	-52	21.45	-20	32.25
	κ-ε RNG			14.24	-49	19.83	-26	29.82
	κ-ω			7.28	-74	29.67	+10	44.11
Stern Lab. T.P. 306	Experiments	5237	1.040	41.30		N/A		N/A
	Correlation			41.66		41.66		62.50
	MODTURC			44.90		N/A		N/A
	κ-ε			20.25	-51	30.56	-27	45.94
	κ-ε R			16.52	-60	29.52	-29	44.49
	κ-ε RNG			27.64	-33	26.53	-36	40.04
	κ-ω			12.21	-70	46.65	+12	69.47
Stern Lab. T.P. 299	Experiments	9392	.941	78.70		N/A		N/A
	Correlation			77.61		77.61		116.41
	MODTURC			87.30		N/A		N/A
	κ-ε			36.38	-54	61.96	-20	93.21
	κ-ε R			27.55	-65	55.33	-29	84.69
	κ-ε RNG			30.69	-61	48.45	-37	73.47
	κ-ω			26.49	-66	92.77	+19	137.81

* I = in-line, S = staggered and RE = relative error

Table 4 shows that none of the turbulence models are able to produce satisfactory predictions. It is further observed that for the in-line tube bundle, with the exception of the pressure predicted with the κ-ε RNG model for Test Point (T.P.) 306, the simulations strongly underestimate pressure drops (i.e., they are lower than half the experimental values). Instead, for the staggered tube-bundle, all turbulence models produce more reasonable predictions. In general, κ-ε models underpredict the data while the κ-ω model overpredicts the experimental trends. Nevertheless, this latter model provides the best values with a maximum relative error of about 19%. This error increases with increasing Reynolds number; this observation indicates that this model seems to be more efficient for low velocity flows. For T.P. 326 and T.P. 299 the standard κ-ε model underpredicts the data by about 20% and for T.P. 306 by about 28 %. The κ-ε Realizable model behaves similarly to the standard κ-ε one, however, for high Reynolds the predictions get worse.

In general, within a range of $\pm$ 30%, standard κ-ε, κ-ε Realizable and κ-ω models are able to predict the pressure drop in staggered bundles. However, none of the turbulence models are able to predict Hadaller et al. (1996) in-line tube bundles measurements. Unfortunately, no velocity profiles in in-line tube bundles were provided by these authors which could help to better corroborate numerical results. Since both velocity and pressure fields are linked, some doubts still exit about the capacity of the FLUENT code to correctly simulate the flow in large in-line tube bundle using RANS equations. Furthermore, it is observed that FLUENT, with RANS equations, is not able to correctly simulate the flow in large in-line tube bundles. According to region "A" shown in Fig. 1, it is quite obvious that the central part of the calandria vessel can be considered as an in-line tube bundle; therefore some questions about the ability of FLUENT code to handle this kind of problem still remain open. To this aim, however,

it must be pointed out that the experiments used for carrying out the present work have been obtained with a flow angle of attack to the first row equal to zero, which is not necessarily the case in a CANDU-6 calandria vessel. For this particular case, however, angles of attack different from zero should exist. Thus, the flow must behave similarly to that occurring in staggered bundles of tubes where any angle of attack can occur.

The comparison of FLUENT with MODTURC simulations shows that the results obtained with the latter code, at least for in-line tube bundles, seem to be better. This is not a surprise, because MODTURC uses experimentally determined hydraulic resistance terms that fit the data. In turn, FLUENT handles the complete set of Navier-Stokes equations without requiring any particular empirical adjustment. Even though MODTURC pressure drop calculations for staggered-bundles are mentioned in Hadaller et al. (1996), they do not provide the results of their predictions. Therefore, based on the available data it is not possible to compare simulations performed by using these two codes.

In summary, the κ-ω model overestimates the pressure drop while it predicts quite well the velocity profile only close to the first row of tubes, but it is unable to reproduce the flow patterns along the bundle. The fact that this turbulence model overestimates the pressure drop can be explained by its inability to predict the velocity profiles along the entire channel. In turn, the standard κ-ε model predicts quite well the velocity profiles along the whole bundle but tends to underestimate the pressure drop. Therefore, the standard κ-ε turbulence model seems to be the best option for performing flow simulations along staggered tube bundles. Even though more investigations about the ability of the κ-ω model to handle this kind of flows are still necessary, it must be pointed out that it is quite sensitive to mesh geometry and requires more calculation time, which can bring about additional convergence difficulties.

7. CONCLUSIONS

A series of numerical simulations of cross-flows in both in-line and staggered tube-bundles were performed using FLUENT-14 software. SIMPLE and Coupled algorithms were tested. It was shown that the Coupled pressure-based algorithm is able to handle both staggered and in-line tube-bundle systems, exhibiting asymptotically theoretical convergence rates for all turbulence models. In turn, the SIMPLE algorithm is not able to converge for in-line tube-bundles. Nevertheless, for a staggered bundle, when a large number of cells are used, SIMPLE in conjunction with κ-ε and κ-ε RNG model considerably reduces the computational time. When this criterion is not a constraint and a higher accuracy is required, the use of the Coupled algorithm is strongly recommended. The SIMPLE algorithm can thus be used to provide an initial guess before switching to the Coupled one, which has shown a better convergence behavior.

Furthermore, the present convergence study provides a good estimation of the minimum number of nodes required for a 2D simulation of the calandria of CANDU reactors. In fact, to guarantee a good accuracy, each tube needs a minimum of 9 500 elements; therefore a 2D calandria simulation will necessitate at least of 3.6 millions of elements.

All turbulence models were able to predict experimental flow velocity profiles taken from Paul (2006) and Paul et al. (2007 and 2008). Instead, κ-based two equation models fail to predict pressure drops in in-line tube-bundles. However, they produce reasonable good results for staggered tube-bundles. This particular behavior may be due to the fact that flow mixing is more important in staggered-bundles; thus, the flow achieves its development much faster than in in-line tube-bundles. In general, κ-ε based models tend to under predict the pressure drop, while the κ-ω model over predicts the experimental trends. Even though numerical results obtained from Hadaller et al. (1996) staggered tube bundle experiments are relatively good; it should be interesting to validate the simulations along with velocity profile data. Unfortunately, to the authors' knowledge such information is scarce or does not exist. Further, since the κ-ω model does not necessarily improve the prediction and requires more calculation time, the standard κ-ε should be preferred. Numerical simulations performed within the present framework, should help implementing full moderator flow simulations in CANDU nuclear power reactors by using CFD.

ACKNOWLEDGEMENTS

This work was supported by the Hydro-Québec Chair in Nuclear Engineering, a discovery grant (RGPIN 41929) of the Natural Science and Engineering Research Council of Canada and the Fonds Québécois de la Recherche sur la Nature et

les Technologies (FQRNT-Ph.D. B2) excellence award.

REFERENCES

1. Balabani S, Yianneskis M (1996). An experimental study of the mean flow and turbulence strucutre of cross-flow over tube bundles. Proceedings of the Institution of Mechanical Engineers: Part C *Journal of Mechanical Engineering Science* 210:317-331.
2. Beale SB, Spalding DB (1999). A numerical study of unsteady fluid flow in in-line and staggered tube banks. *Journal of Fluid and Structures* 13:723-754.
3. Hadaller GI, Fortman RA, Szymanski J, Midvidy WI, Train DJ (1996). Frictional pressure drop in aligned and staggered tube banks with large pitch diameter ratio. *17th CNS Conference. Fredericton*, New Brunswick, Canada.
4. Hoerner SF (1965). *Fluid-dynamic Drag: Practical Information on Aerodynamic Drag and Hydrodynamic Resistance.* Sighard F. Hoerner Editor.
5. Huget RG, Szymanski J, Midvidy W (1989). Status of physical and numerical modelling of CANDU moderator circulation. *10th Annual Conference CNS*, Ottawa, Canada.
6. Huget RG, Szymanski J, Galpin PF, Midvidy W (1990). MODTURC_CLAS : An efficient code for analysis of moderator circulation in CANDU reactors. *Third International Conference on Simulation Methods in Nuclear Engineering*, Montreal, Canada.
7. Iwaki C, Cheong KH, Monji H, Matsui G (2004). PIV measurement of the vertical cross-flow if the simulation consists of a unique row of cylinders or an obstacle, the κ-ω model seems to be a better alternative - flow structure over tube bundles. *Experiments in Fluids* 37:350-363.
8. Kim M, Yu S-O, Kim H-J (2006). Analyses on fluid flow and heat transfer inside calandria vessel of CANDU-6 using CFD. *Nuclear Engineering and Design* 236:1155-1164.
9. Launder BE, Spalding DB (1972). Lectures in mathematical models of turbulence. *Academic Press*, London, England.
10. Liang C, Papadakis G (2007). Large eddy simulation of cross-flow through a staggered tube bundle at subcritical Reynolds number. *Journal of Fluid and Structures* 23:1215-1230.
11. Mangoong K, Seon-Oh Y, Hho-Jung K (2006). Analyses on fluid flow and heat transfer inside calandria vessel of CANDU-6 using CFD. Nucl. *Eng. Design* 236(11):1155-1164.
12. Menter FR (1994). Two-equation eddy-viscosity turbulence models for engineering applications. *AIAA Journal* 32:1598-1605.
13. Necciari R, Teyssedou A, Reggio M (2010). Numerical simulation of cross-flow in tube-bundles to model flow circulation of the moderator in CANDU-6. *Proceedings of the CNS Conference*, Montreal, Canada.
14. Paul SS (2006). *Experimental and Numerical Studies of Turbulent Cross-flow in a Staggered Tube Bundle.* PhD Thesis, Department of Mechanical and Manufacturing Engineering, University of Manitoba. Winnipeg, Manitoba, Canada.
15. Paul SS, Tachie MF, Ormiston SJ (2007). Experimental study of turbulent cross-flow in a staggered tube bundle using particle image velocimetry. *International Journal of Heat and Fluid Flow* 28:441-453.
16. Paul SS, Ormiston SJ, Tachie MF (2008). Experimental and numerical investigation of turbulent cross-flow in a staggered tube bundle. *International Journal of Heat and Fluid Flow* 29:387-414.
17. Sarchami A, Ashgriz N, Kwee M (2013). Temperature fluctuations inside the CANDU reactor moderator test. *Annals of Nuclear Energy* 60:157-162.
18. Shih T, Liou W, Shabbir A, Yang Z, Zhu J (1995). A New κ-ε eddy-viscosity model for high Reynolds number trubulent flow - model development and validation. *Computers Fluids* 24:227-238.
19. Simonin O, Barcouda M (1988). Measurement and prediction of turbulent flow entering a staggered tube bundle. *Proceedings of the 4th International Symposium on Applications of Laser Anemometry to Fluid Mechanics*, Lisbon, Portugal. Paper No. 5.23
20. Wilcox DC (1998). *Turbulence Modeling for CFD.* La Cañada, California: DCW Industries Inc.
21. Yakhot V, Orszag SA (1986). Renormalization group analysis of turbulence: I. Basic theory. *Journal of Scientific Computing* 1:1-51.
22. Yoon C, Rhee BW, Min BJ (2004). Development and validation of the 3-D computational fluid dynamics model for CANDU-6 moderator temperature predictions. *Nuclear Technology* 148:259-267.
23. Yoon C, Rhee BW, Bo W, Kim HT, Park J, Min BJ (2006). Moderator analysis of wolsong units 2/3/4 for the 35% reactor inlet header break with a loss of emergency core cooling injection. *Journal of Nuclear Science and Technology* 43:505-513.
24. Yoon C, Park JH (2008). Development of a CFD model for the CANDU-6 moderator analysis using a coupled solver. *Annals of Nuclear Energy* 35:1041-1049.
25. Zukauskas A (1989). *High-performance Single-phase Heat Exchangers.* Hemisphere Publishing Corporation, New York.